UNIVERSITÀ
DEGLI STUDI
DI PADOVA

Head Office: Università degli Studi di Padova

Department Molecular Medicine

Ph.D. COURSE IN: Molecular Medicine
CURRICULUM: Regenerative Medicine
XXXIV SERIES

PERIPHERAL NERVE INJURY AND BIOACTIVE POLYMERS DEVELOPMENT FOR NERVE REGENERATION

Coordinator: Ch.mo Prof. Riccardo Manganelli
Supervisor: Ch.ma Prof.ssa Maria Teresa Conconi
Co-Supervisor: Ch.mo Prof. Andrea Porzionato
Dott.ssa Elena Stocco
Dott.ssa Silvia Barbon

Ph.D. student: Enrico De Rose

INDEX

ABSTRACT

Background. To date, peripheral nerve injuries (PNI) with or without substance loss are considered a significant clinical challenge often resulting in impaired sensory and/or motor function. Nerve injury could provoke a long-lasting neuropathic pain, manifested as allodynia, a decrease in pain threshold and hyperplasia, and an increase in response to noxious stimuli.
Classification of PNI is based on damage severity. In case of sharp injuries *without substance loss*, end-to end nerve repair is the preferred option and nerve wrapping is often used to improve the outcomes; however, to achieve tensionless result with a complete functional recovery is often disappointing. In parallel, in case of *injuries with substance loss*, the bridging of the gap between the proximal and distal nerve stumps is required to guarantee nerve continuity. Autologous nerve graft (gold standard), together with allografts and xenografts are the options currently available; however, these surgical strategies present disadvantages such as donor site co-morbidities for autografts, immunosuppressive therapies and high costs for allografts and xenografts.
Aim of the study. Considering the urgent need for effective devices to use in case of PNIs, thus overcoming the limitations of the currently available solutions/products, the aim of this research study was the fabrication, evaluation and identification of co-morbidities-free, cost-saving and effective alternatives (*wraps* and *nerve conduits* (NCs)) potentially useful in clinical practice for peripheral nerve lesions treatment. Specifically, the new bioresorbable polymer oxidized polyvinyl alcohol (OxPVA) was mainly considered to this purpose. The achievement of satisfactory outcomes in morphological and functional recovery of the injured nerve represents an ambitious challenge to face.
Materials and methods. OxPVA polymers, prepared through the oxidative agents potassium permanganate (OxPVA_$KMnO_4$) or bromine (OxPVA_Br_2), were preliminary synthetized. Thus, the derived scaffolds, fabricated through a chemical free cross-linking strategy (freeze-thawing(F/T)) were compared. Specifically, morphological features (gross appearance and ultrastructure by Scanning Electron Microscopy-(SEM)), physico-chemical characteristics, (swelling ability and porosity, mechanical resistance), biological characteristics (*in vitro* biodegradation study, cytotoxicity assay) and ability to act as a bioactivated platform (ciliary neurotrophic factor (CNTF) covalent binding on tubular scaffolds) were investigated.

Thereafter, two pre-clinical models of disease were considered: i) PNI without substance loss; ii) PNI with substance loss.

As for condition i), after sciatic nerve transection and neurorrhaphy, thirty Sprague-Dawley rats were randomly implanted with a) NeuraWrap^{TM} (commercial wrap, control group); b) OxPVA; c) Leukocyte-Fibrin Platelet membrane (LFPm) wraps. Twelve weeks later, functional recovery tests (Sciatic Functional Index evaluation) were performed; hence, euthanasia occurred, and the explanted nerves were processed for analysis of morphological features by histology (hematoxylin and eosin staining – (H&E); Toluidine-Blue) and immunohistochemistry (anti-CD3, -F4/80, -S100 -β-tubulin staining). Morphometric evaluation (total cross section area, fascicular area, total axons density, total axons number) also was conducted. In parallel, ultrastructural analysis was performed by Transmission Electron Microscopy (TEM) and eventual fibroconnective tissue was evaluated by Second Harmonic Generation (SHG) Microscopy.

Regarding condition ii), different NCs based on OxPVA were implanted in a rat model of sciatic nerve transection (gap=5mm). Briefly, 18 animals were randomized to 6 groups implanted with: Reverse Autograft (RA, control); Reaxon® (commercial device made of chitosan); OxPVA; OxPVA+EAK peptide; OxPVA+EAK-YIGSR peptide; OxPVA+adsorbed NGF. The end point considered was that of 6 weeks. After implantation, wellbeing assessments (weight analysis; autotomy index), functional recovery assessment (i.e., gait analysis, sciatic functional index, von Frey filaments assay for mechanical sensitivity), histological (H&E, toluidine blue staining) and immunohistochemical (CD3, F4/80, S100, β-tubulin) analyses, were conducted on explants; morphometric study was also performed (total cross section area, fascicular area, total axons density and total axons number). Presence of fibroconnective tissue was evaluated by SHG microscopy.

Results. Chemical oxidation improved water uptake capacity of the polymer, with maximum swelling index of 60.5% ± 2.5%, 71.3% ± 3.6% and 19.5% ± 4.0% for OxPVA_Br_2, OxPVA_$KMnO_4$ and PVA, respectively. In accordance, hydrogel porosity increased from 15.27% ± 1.16% (PVA) to 62.71% ± 8.63% (OxPVA_Br_2) and to 77.50% ± 3.39% (OxPVA_$KMnO_4$) after oxidation. Besides proving that OxPVA conduits exhibited mechanical resistance and a suture holding ability, they did not exert a cytotoxic effect on SH-SY5Y and Schwann cells and biodegraded over time when subjected to enzymatic digestion, also successful functionalization with CNTF was performed. Interestingly, higher amounts of CNTF were detected in the lumen of OxPVA_Br_2 (0.22±0.029μg) and OxPVA_$KMnO_4$ (0.29±0.033μg) guides rather than PVA (0.11±0.021μg) tubular scaffolds. As for the

preclinical study on wraps, all devices guaranteed nerve function recovery; at dissection, no scar-tissue/neuromas were visible while, considering re-absorption, only OxPVA and NeuraWrap™ residues were still recognizable. According to histology and immunohistochemistry (CD3 and F4/80), the absence of significant inflammatory infiltrate was observed in all experimental groups, confirming the biocompatibility of the implanted wraps. Then, the process of nerve tissue regeneration was also verified by both immunohistochemistry (S-100 and β-tubulin) and TEM analysis. According to the morphometric study data, wraps showed that total axons density was significantly higher ($p < 0.01$) for NeuraWrap™ ($0.059 \pm 0.007/ \mu m^2$) versus OxPVA wraps ($0.035 \pm 0.005/\mu m^2$) but not versus LFPm wraps ($0.041 \pm 0.004/\mu m^2$) at proximal level; while, considering the distal portion, no differences among the groups aroused (NeuraWrap™, 0.044 ± 0.005; OxPVA wrap, 0.052 ± 0.004; LFPm wrap, 0.047 ± 0.004). Total number of axons was also determined, and a significant difference was encountered only between OxPVA wraps (23,855 ± 3,314) and NeuraWrap™ (14,513 ± 1,416) at distal level ($p < 0.01$); conversely, no significant difference was observed with LFPm group (19,594 ± 2,386). At the proximal stump, there were 23,608 ± 4,628; 21,517 ± 4,106; 19,958 ± 2,487 mean total axons for NeuraWrap™ and the experimental groups OxPVA and LFPm, respectively; statistical analysis of the data revealed no significant difference between the groups. SHG microscopy images supported morphological characterization data: both OxPVA and LFPm derived samples showed an appearance similar to that of NeuraWrap™ implanted nerves at the level of the epineural tissue and in the inner part of each section. All the specimens had characteristics compatible with that of a PNI undergoing to morpho-functional recovery. Regarding the preclinical study on animal model of disease with substance loss, all animals well tolerated surgery as demonstrated by weight analysis. Evaluation of autotomy index revealed that OxPVA devices provided for the better outcomes. Additionally, all NCs sustained nerve regeneration as demonstrated by functional studies: OxPVA+NGF distinguished for better functional outcomes, like RA, in gait analysis; however, no significant differences were detected among groups for both gait and SFI evaluation. Upon explant, all grafts were clearly recognizable without severe formation of fibrous tissue outside the NCs; presence one neuroma was observed in Reaxon®group. Histological/immunohistochemical analyses proved presence of regenerated nerve fibers in the central portion of all grafts (S100, β-tubulin) in absence of lymphomonocytic infiltration (CD3, F4/80). In the center of the NCs, morphometric analysis showed an axon density that was significantly higher for OxPVA+EAK (1118,345± 5,46 axons/mm^2; $p \leq 0.005$) compared to RA (177,31±2,06 axons/mm^2); conversely, no significant difference was found among all other groups. Except for the control group, Reaxon® showed

the lowest values of axon density. Total number of axons was also determined, and a significant difference was encountered between OxPVA (195.83±45.18; $p<0.05$) and OxPVA+EAK (113.4±30.88) and between OxPVA (195.83±45.18; $p\leq0.005$) versus OxPVA+NGF (108.17±21.20); conversely, no significant difference was observed between Reaxon® and all other groups.

SHG Intensity analysis showed OxPVA and OxPVA+EAK-YIGSR groups had statistically higher collagen levels compared to Reaxon® group, which had collagen levels quite comparable with RA group. Coherency analysis, focusing on collagen fibers orientation, showed highly isotropic areas for Reaxon® (0.02 AU); while comparable values for the other groups (range: 0.07-0.10 AU).

Conclusions. Study results highlight OxPVA as a smart and cost-saving biomaterial, acting as a biocompatible and functionalizable platform for tissue engineering purposes. The preclinical study on wraps showed that bioengineered OxPVA and LFPm devices promoted lesion recovery and may be considered an interesting alternative to the commercial NeuraWrap™. As for the preclinical study on NCs, all devices guaranteeded for proximal/distal stumps reconjunction after 6 weeks from surgery; OxPVA, differently from Reaxon®, showed greater mechanical properties, fitting well the injured stumps. According to the morphometric study, OxPVA and OxPVA+EAK-YIGSR NCs displayed the most interesting outcomes in terms of regenerative potential showing the higher total axons number. All OxPVA-based conduits displayed a total axons number comparable to that of RA.

INTRODUCTION

One main difference between the central nervous system (CNS) and the peripheral nervous system (PNS) is the ability of PNS to regenerate after damage through a process of degeneration and regeneration [1–3]. The advancement in neurosurgical equipment and the advent of medical imaging granted better results in terms of nerve repair, however, nowadays the management of PNIs is not able to guarantee to fully satisfactory results in terms of structural and functional recovery [4–8].

1.1 Anatomy of peripheral nervous system

PNS comprehends neurons projecting form spinal cord and brainstem; peripheral nerves involve axons from primary sensory neurons, lower motor neurons (LMNs) and autonomic neurons; the primary sensory axons possess sensorial receptor at their ends, in continuity with their axon segment[9]. The proximal portion of the axon connect with the CNS and ends in secondary sensory nuclei taking connection with cerebellar, lemniscal and reflex channels. LMNs located in the anterior horn of the spinal cord take connections with skeletal muscles via ventral roots, creating the neuromuscular junctions[10]. Autonomic preganglionic axons from the ventral roots connect with autonomic ganglia or end in the adrenal medulla. Autonomic postganglionic axons connect with splanchnic or peripheral nerves creating neuroeffector junctions engaging smooth muscle, cardiac muscle, metabolic cells, immune system cells and secretory glands.

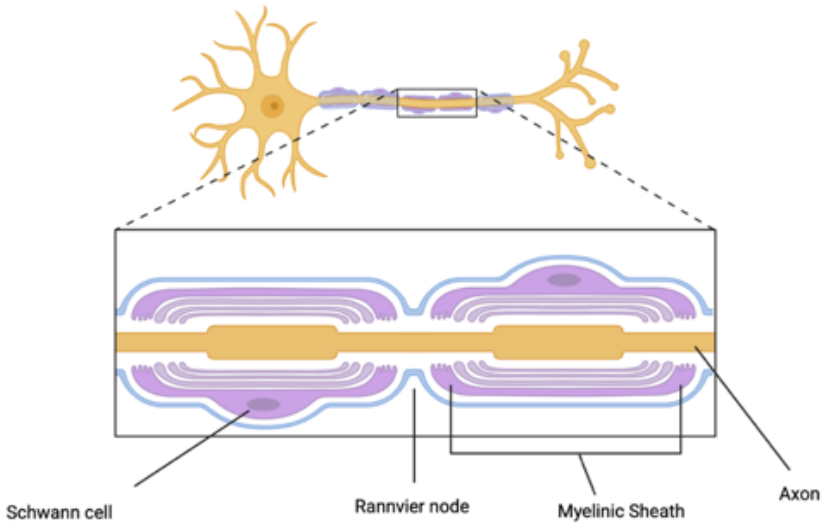

Figure 1 Fundamental elements of myelinated axon.

The main macroscopic elements that identify a peripheral nerve are axons, the sheaths of connective tissue embracing axons and the nearby blood vessels[11]. Axons could be myelinated and unmyelinated; unmyelinated axons are enfolded by Schwann cells sheaths, which constitute the cytoplasm of Schwann cells. Myelinated axons are enveloped by non-continuous segments of myelin sheath of single Schwann cells. Sequential unmyelinated spaces of each axon are called nodes of Ranvier.

Fiber Type	Myelinization	Diameter	Conduction Speed
A	Myelinic	1-20 µm	5-120 m/s
B	Myelinic	1-3 µm	3-15 m/s
C	Amyelinic	0.5-1.5 µm	0.6-1.5 m/s

Table 1 Classification of nerve fibers

Nodes of Ranvier are places where sodium channels are located and where action potentials (APs) propagate in a saltatory way. In unmyelinated axons APs propagates from nearby depolarized axon membrane areas in continuous, but slower way.

The conduction velocity depends on axonal diameter and the presence of myelin sheaths. Neurons with higher axon diameter and myelin sheaths are the ones who conduct APs faster. Peripheral amyelinic nervous fibers, 1-2 µm of diameter, conduct APs slowly (1-2 m/s) since APs needs to be elicited in every nearby axon membrane area through the entire length of the axon. Myelinic peripheral nerve fibers, 2-20 µm of diameter, conduct APs till 120 m/s since saltatory potential propagates from each Ranvier node to another (200-1000 µm length each) (Tab.1-Fig. 2).

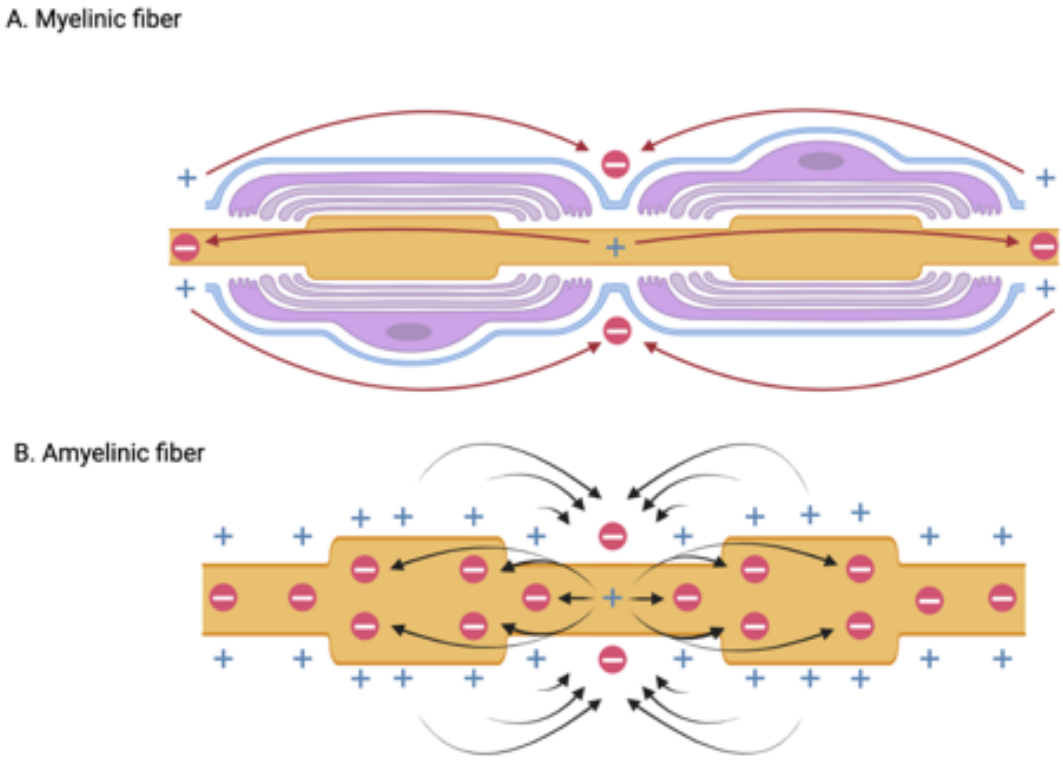

Figure 2 Action potential propagation in myelinic axon fiber (A) and amyelinic fiber (B).

The inner loose connective tissue is called endoneurium; it locates between individual axons within a fascicle. The perineurium instead, circumscribes groups of axon fascicles. It is composed of tight packed flatten cells, kept together by tight junctions. It works as supportive cell sheath and blocks possible damaging substances from nearby environment. The epineurium enwraps the layers of perineurium. Epineurium filling the space between axon bundles is called internal epineurium, when epineurium surrounding the entire nerve is called external, or outer epineurium. The epineural coating provides protection against compression; where peripheral nerves span during joint movement and where compressive forces are engaged, the extent of intern epineural coating is more significant (Fig. 3).

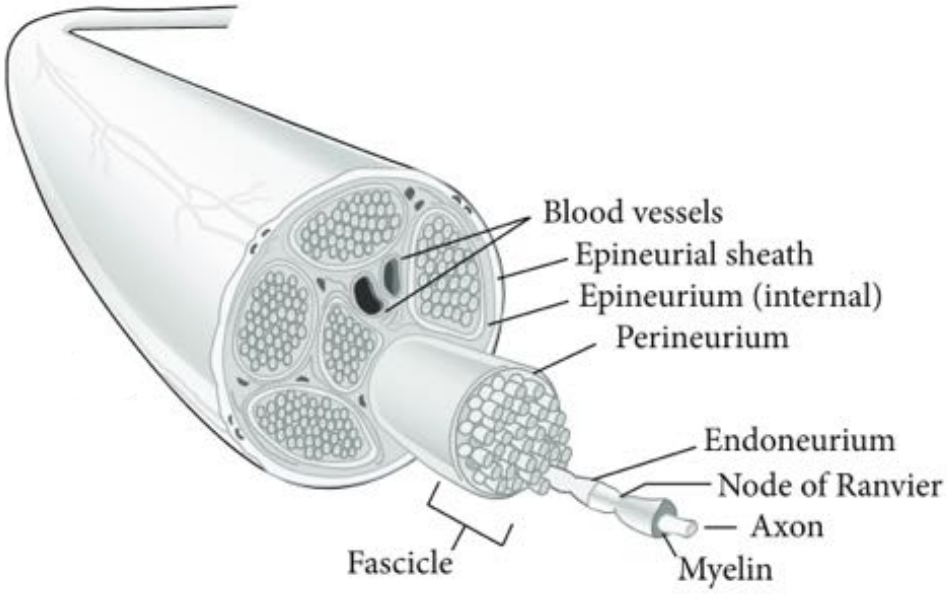

Figure 3 Cross-section anatomy of peripheral nerve. Epineural arterioles make connection through the perineurial sheath and form capillary networks within the endoneurial space. Axons are bundled together by Schwann cells constituting fascicles. Schwan cells distribution around axons determine the nature of the axon fibers. Adapted from [12] .

1.2. Nerve physiopathology

Unlike the CNS, peripheral nerves are able to regenerate spontaneously after damage due to the favorable environment and activation of the intrinsic growth capacity of neurons. A complete regeneration that allows a recovery of functionality requires both the regrowth of the axons and the remyelination of the same by the Schwann cells. Schwann cells play a crucial role in this process, and many factors influence their action, including neurotrophic factors and extracellular matrix proteins [13].

After a lesion of the peripheral nerve, the most relevant pathophysiological alterations occur at the level of the distal stump: Wallerian degeneration causes alteration of the axon's cells responsible of the myelin sheath production [14]. However, this regression of the distal segment has not only a negative implication, because it triggers the development of a microenvironment capable of favoring axonal regeneration, with the participation also macrophages that contribute to the removal of cellular debris[8,15,16].

Schwann cells change their gene expression profile, differentiating into shelter Schwann cells (or Bungner cells), which align in linear structures called Bungner bands, which through their

basement membrane and producing adhesion molecules, act as support to regenerating fibers (Fig. 4).

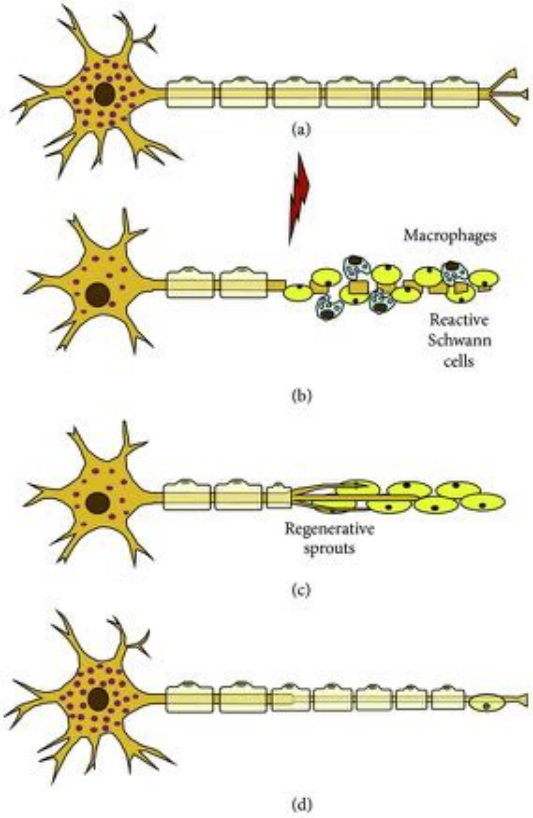

Figure 4 Degeneration and regeneration after peripheral nerve injury (a-d)

1.3 Etiology and classification of peripheral nerve injuries

From 0.013% to 0.023% of population each year is affected from PNIs and despite the low incidence, PNIs lead to heavy drawbacks in patients' life quality, affecting both military and civilian population[17]. Symptoms may range from partial to total impairment of sensory and/or motor functions of affected limb and development of neuropathic pain [18]. Since most of PNIs involves upper or lower limbs, which are areas related to work activities, any damage could be critical for patient's life quality. Main events causing PNIs are excessive pressure and/or stretching, sharp transections and/or poor healing of prior injuries related in example to accidental trauma or medical conditions[19]. Main nerve injury classifications have been made by Seddon in 1943[20] and by Sunderland in 1951[21].

Two classifications are commonly used to classify PNI: Seddon (Fig. 5) and Sunderland (Fig. 6). Seddon classifies PNI into three degrees of severity: neurapraxia, axonotmesis and neurotmesis [20,22]:

Neurotmesis	*Axonotmesis*	*Neurapraxia*
1. OPEN WOUNDS.	1. Open wounds	1. OPEN WOUNDS.
2. Direct blunt injuries	2. DIRECT BLUNT INJURIES (Fractures and dislocations)	2. Direct blunt injuries
3. TRACTION	3. Traction	3. Traction
	4. COMPRESSION sudden or prolonged	4. COMPRESSION
4. Local chemical poisoning (sulphapyridine)	5. Local chemical poisoning	5. Certain drugs
	6. Freezing	6. Freezing
	7. Experimental crushing	7. Experimental compression

Figure 5 Seddon classification of peripheral nerve injuries: Neurapraxia, Axonotmesis and Neurotmesis. From Seddon 1943.

Neurapraxia (transient blockage): it is the mildest lesion, where compression or stretching cause axonal and myelin damage, without affecting the integrity of the endoneurium. In this type of damage, the injury is minimal, and the electrical response of the muscle remains unchanged, there may be minimal objectivist sensory disturbances, loss of postural sensitivity and sense of vibration is common, rarely there is loss of sweating. The recovery is very good because the continuity of the axon and the endoneurium is preserved and Wallerian degeneration does not occur.

Axonotmesis (continuous injury): in this type of damage there is interruption of axonal continuity without alterations of the connective sheaths of the nerve. Axonotmesis is indicative of the importance of connective sheaths in the process of nerve regeneration, in fact in this type of lesion the prognosis is very good precisely because the intact connective tissue is the guide for the axons in regeneration.

Neurotmesis (division of the nerve): the nerve is completely divided into two stumps, resulting in complete loss of both sensory and motor function. Spontaneous regeneration is impossible and it is necessary to surgically restore the continuity of the nerve.

The Sunderland classification includes five degrees of injury and compared to the Seddon classification it also considers the level of damage to the connective sheaths, that is, whether there is damage to the endoneurium, perineurium or epineurium [21]:

- Stage 1: conduction blockade, corresponding to neurapraxia of Seddon;
- Stage 2: axonal damage, corresponding to Seddon's axonotmesis;
- Stage 3: axonal damage with destruction of the endoneurium;
- Stage 4: axonal damage with destruction of endoneurium and perineurium, with structural damage to the nerve fascicles;
- Stage 5: axonal damage with destruction of endoneurium, perineurium and epineurium, with the nerve that can be severed.

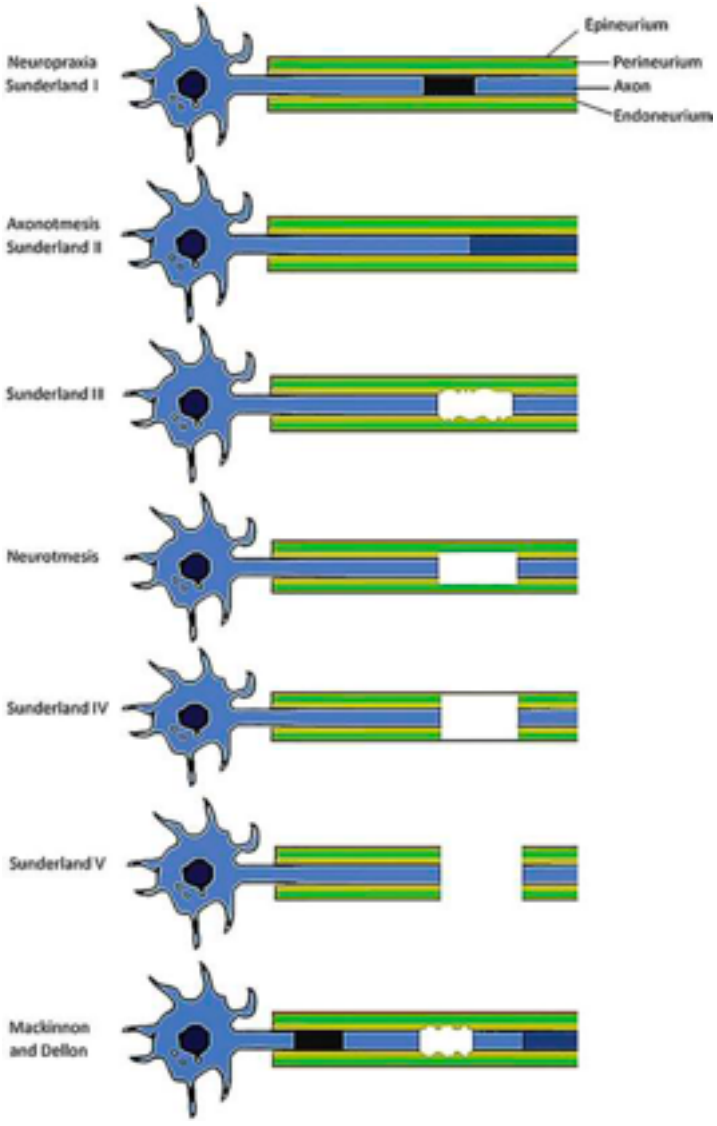

Figure 6 Schematic representation of Sunderland classification of PNIs. From Alvites et al., 2017

Mackinnon and Dellon later proposed adding a stage 6, indicating nerve damage in continuity with a mixed degree of injury that requires specific microsurgical techniques[23] (Fig 6).

1.4 The management of peripheral nerve injuries: from bases to tissue engineering approaches

1.4.1 General surgical principles

Progress in diagnostic capabilities would remain unsatisfactory if it were not accompanied by a parallel advancement in surgical techniques of peripheral nerve repair. The goal of nerve repair surgery is to obtain the greatest correspondence between the proximal stump fascicles and those of the distal stump, to facilitate nerve regeneration effectively possible. The principles and objectives that underlie the repair surgery of peripheral nerves are:

- minimize the handling of the stumps to reduce the risk of fibrosis;
- regularize and orient the stumps as accurately as possible;
- avoid tension at the site of anastomosis between the proximal segment and the distal one;
- place the suture in a soft and above all well vascularized;
- perform a primary repair when the conditions allow, otherwise postpone treatment to three weeks;
- ensure specialist assistance in the follow-up and during sensory and motor re-education.

To adequately perform a microsurgical intervention to repair a PNI it is mandatory to equip oneself with magnifying optics and use appropriate suture materials, in particular inert threads (polypropylene, nylon) measuring 7-0, 8-0, 9-0, 10-0. The points must be detached from each other and not particularly narrow, and sometimes fibrin glues can be added, the main purpose of which is to make the suture site impermeable to the scar tissue outside the nerve.
As mentioned above, it is very important to ensure optimal orientation of the nerve stumps, and to do this it is necessary to identify the epineural vessels of the two stumps and try to make them match. Another fundamental point is the regularization of the extremities of the lesioned segments, also called *trimming*: it is necessary to dissect the neuromas formed on the lesioned stomps, obtaining ends of healthy and valid nervous material for the purposes of nerve regeneration.

Finally, the absence of tension is essential: it has been shown that a 15% increase in the tension of a nerve causes an 80% drop in blood flow, with dramatic consequences on the regenerative capacity of axons [24]. To verify the absence of tension, it is advisable to give a first epineural point with a 9-0 thread: if it yields or is not able to approach the stumps then this indicates there is too high tension and that direct suture is impossible, it is therefore necessary to use grafts or other techniques[25]

1.4.2 Microsurgical techniques

Depending on the type of injury, the length of the gap between the proximal and distal segments, and the site of the damage, various repair techniques can be used (Tab 2): end to end neurorrhaphy, end to side neurorrhaphy, autograft nerves, vascularized grafts, nerve allograft, nerve xenograft, nerve transfer, nerve tubules.

Microsurgical Technique	Material
Neurorrhaphy	End to end suture
End to side neurorrhapy	End to side suture
Nerve Autograft	Autologus nerve
Vascular graft	Nerve graft with vascular bed
Nerve Allograft	Nerve graft from corpse
Nerve Xenograft	Animal nerve graft
Nerve Transfer	Nerve from other district
Nerve conduit	Synthetic/Natural

Table 2 Classification of surgical treatments and combined materials used in PNIs

It is very important to choose the most appropriate surgical technique because, together with the age and general state of health of the patient, the mechanism of damage and the involvement of the surrounding tissues, it represents the most important predictor of healing [26]. In particular, the algorithms, as represented in Figure 7, suggest using direct suture for lesions with a gap of up to a maximum of 0.5 cm, nerve tubules for gaps between 0.5 and 1.5 – 3 cm, allografts for injuries with a gap between the two stumps up to 5 cm and autografts for extended lesions even beyond 5 cm [27].

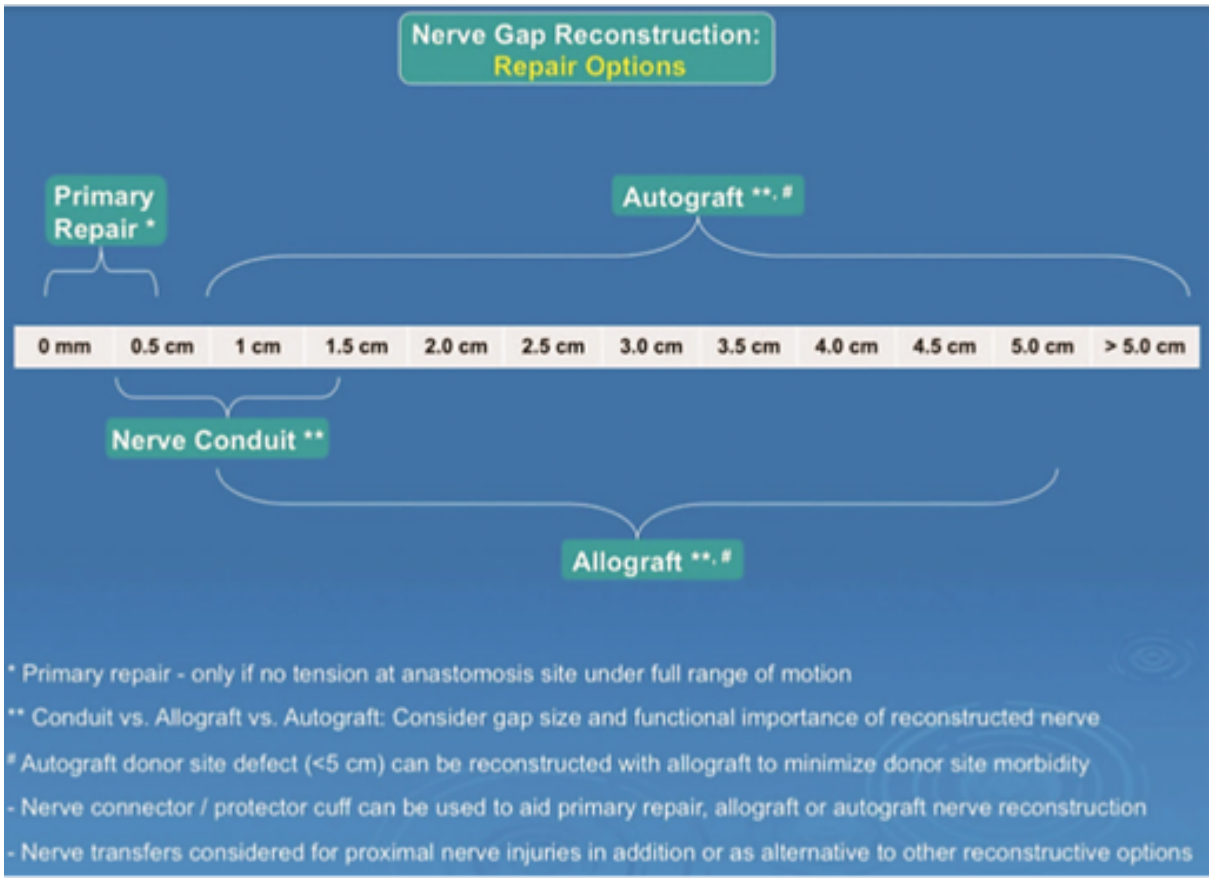

Figure 7 Clinical indication for peripheral nerve injuries based on the gap between nerve ends

1.4.3 Neurorrhaphy

The *termino-terminal* (end-to-end) neurorrhaphy consists of the direct suture of the two lesioned stomps and is possible only when the two ends can be juxtaposed without the presence of tension, deleterious for the purpose of healing.

Over the years, different techniques of nervous suture have been described, all based on the principle of manipulating the nerve as little as possible, giving the least number of points needed to ensure the correct orientation of the fibers. The most used techniques are epineural, fascicular and epineural sutures:

- Epineural suture: to correctly align the fascicles of the two stumps, the epineural vessels are used as a guide, and then the sutures are passed, only crossing the epineurium of the two segments. The advantages of this strategy are the ease of execution and poor manipulation of the nerve; the disadvantages are represented by the ease of misalignment of the regenerating fibers;
- Fascicular suture: it is based on the idea of directly juxtaposing the fascicles of the two stumps in order to facilitate the correct alignment of the fibers in regeneration;

technically a dissection of the epineurium (epinerectomy) is performed and the perineurium of the individual fascicles is sutured; the main advantage consists in the better correspondence between proximal and distal axons, while the disadvantages are the technical difficulty, the long operating time and the greater degree of manipulation of the fibers, which leads to a greater probability of fibrosis.

- Epi-perineural suture: it is a hybrid between the two previous techniques, in which the epineurium and the perineurium of the most peripheral fascicles are sutured; the aim of this approach is to combine the advantages of epineural and fascicular sutures while sparing the most central fascicles from surgical manipulation [26].

Some surgeons use suture site protectors to promote directional growth of axons and to prevent axonal sprouting in uninvited directions; on the market there are nerve wraps of various kinds that can be used for this purpose (e.g., NeuraWrap™).
Sometimes it is difficult to locate the proximal stump of the injured nerve, and in these cases the distal segment to the lesion is sutured to a donor nerve through a termino-lateral suture, preceded by the creation of a fenestrations on the epineurium of the donor nerve itself, so as to favor the invasion of the damaged nerve by the axons coming from the donor nerve. In the use of this technique is very important to anastomose "compatible" nerves with each other, therefore innervate adjacent districts or synergistic muscle groups. Several studies have shown that sensory regeneration occurs even without performing a section of the axons of the nerve donor; otherwise, to obtain a colonization of the damaged nerve by motor fibers, it is necessary to act more invasively on the donor nerve by performing an axotomy. The advantage of this technique is the possibility of recovering the sensory function when it is not possible to recover the proximal portion of a damaged nerve, while the prevailing disadvantage is the poor outcome with regard to motor function [28].

1.4.4 Nerve autografts

In many cases, when there is too much tension or the two ends cannot be re-conjunct, it is not possible to perform a direct end to end suture. In this condition, the current therapeutic gold standard corresponds to the nerve autograft implantation, which consists in the withdrawal of a segment of another nerve of the same individual, who is interposed between the two extremes of the gap previously trimmed. The implanted segment undergoes Wallerian degeneration, thus providing a valid support for the regeneration of the fibers of the damaged nerve. Usually, the

nerves taken in autografting interventions are sensory nerves that are expendable without causing major deficits, such as the sural nerve (Fig. 8) or the skin nerves of the forearm. In this procedure, the grafts can be interposed individually between the two ends of the gap, or they can be placed side by side, and in this case, the aim is to try to interpose each graft between the stumps of the same fascicle, after fascicular mapping; to facilitate the stability of this multiple implants, the different segments side by side can be stabilized through a packaging with fibrin glue. The advantages of nerve autograft are non-immunogenicity (the implanted segment comes from the patient himself) and the possibility of covering gaps also of considerable length; the disadvantages are the loss of sensory function at the donor site, the need for a second incision for graft sampling, the risk of neuromas formation, and lower outcomes compared to a tension-free end to end neurorrhaphy [28,29].

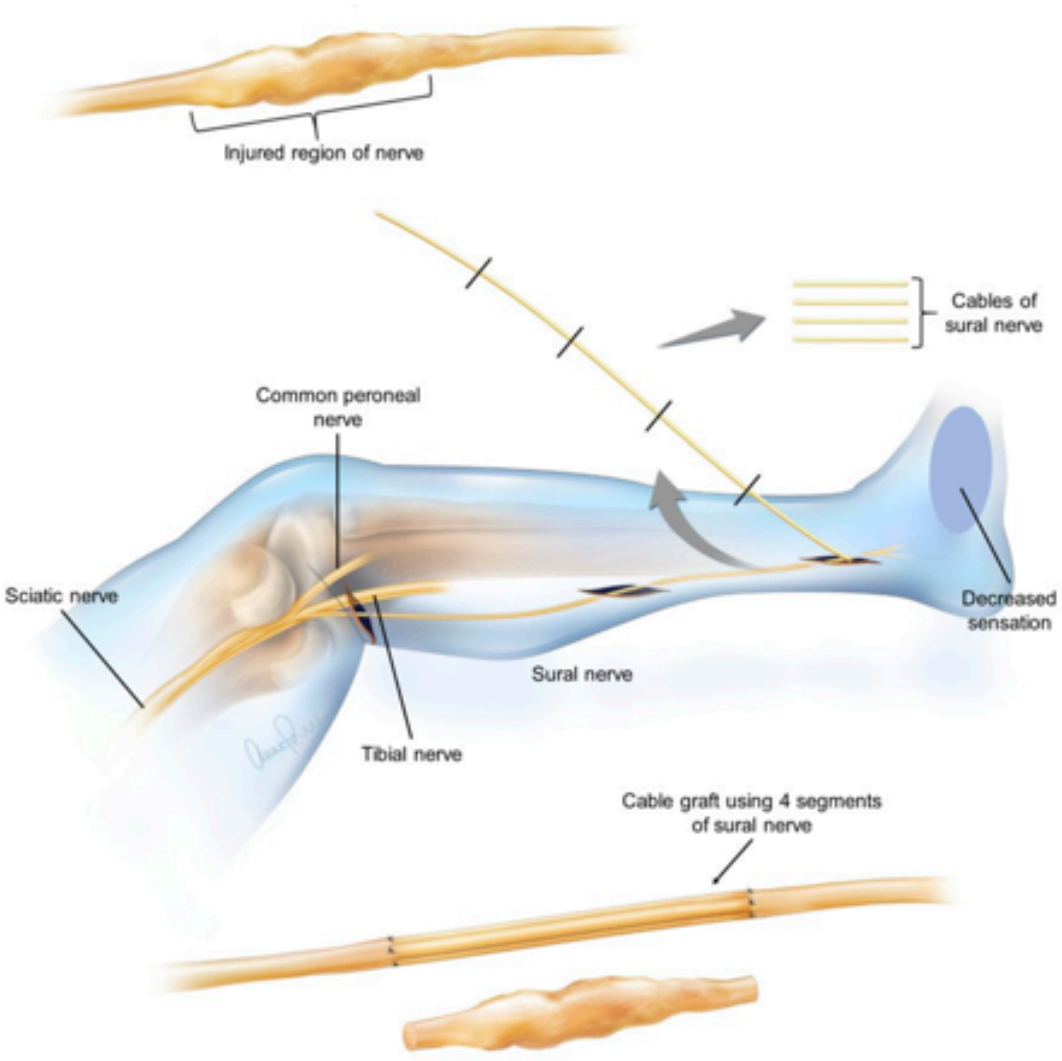

Figure 8 Autograft from sural nerve (adapted from Nerve Graft- Paralysis center) [30].

1.4.5 Vascular nerve graft

Nerve grafts need the recipient district to adhere to have an adequate vascular bed, which is not always possible, especially in the event of major scarring outcomes.
In this case, the use of nerve segments including a proper vascular peduncle has been proposed. The advantages are the possibility of use even for very long grafts and in poorly vascularized and / or scar tissues; the disadvantages are the technical difficulty of the intervention and the lack of comparative studies able to demonstrate its real effectiveness [29].

1.4.6 Nerve allograft

Allografts are based on the same principle as autografts, providing support for the regeneration of the fibers of the damaged nerve. Unlike autografts, allografts are not taken from the same subject but from a donor, usually a corpse. Allografts are preferentially used in the event of particularly severe nerve damage. Clearly, coming from another individual, allografts induce an immune response from the host, which determines the need for long-term immunosuppressive therapy until the completion of nerve regeneration; to manage this critical issue, different graft preparation techniques have been proposed to make it less immunogenic, such as cryopreservation, irradiation and decellularization; however, it should be noted that excessive treatment before implantation is not entirely optimal, as Schwann cells of the donor present in the graft perform the important function of providing guidance to the regeneration of the axons of the recipient's nerve; that explains how a complete removal of donor cells is not possible and explains the need to maintain systemic immunosuppressive therapy, usually with Tacrolimus. The advantages of allografts are the fact that there is no need for a second surgical site in the patient, the possibility of covering high range of defects, ready and abundant availability; the disadvantages are the need for long-term immunosuppressive therapy and the potentials side effects of the same [28,31].

1.4.7 Nerve xenograft

A nerve xenograft is a nerve graft obtained from an organism of a species other than the human one. Inter-species experiments in rodents have brought conflicting results, but the use of these grafts is burdened with the risk of cross-species diseases transmission [32,33].

1.4.8 Nerve transfer and neurotization

Nerve transfer is applied when the injury does not allow the use of grafts, for example in the case of a radicular avulsion or a tearing that interrupts communication between the peripheral nerve and the spinal cord. The purpose of nerve transfer is to convert a proximal lesion into peripheral, sacrificing a less important nerve or with redundant function to rebuild a more important nerve that has been damaged [34].

The surgical procedure of nerve transferring consists in dissecting a healthy nerve, whose function can be vicariated by branches of other healthy nerves, and going to anastomize it to the distal stump of a nerve that has been damaged in a proximal portion (Figure 9); clearly the donor nerve must be chosen carefully: after the procedure there must be no functional deficits and the function of the donor and recipient nerve must be similar, both as regards the area from which they collect the sensitivity and for the innervated muscle groups, which must be synergistic [35].

Muscle neurotization is used when the nerve has been torn from the muscle that was responsible for innervating. In this case, a nerve trunk is implanted directly into the muscle. Since in muscle cells there is a considerable amount of laminin (fundamental for axonal regeneration) the regenerating fibers find a favorable microenvironment, easily managing to reconnect with the muscle, reforming the neuromuscular junctions [13].

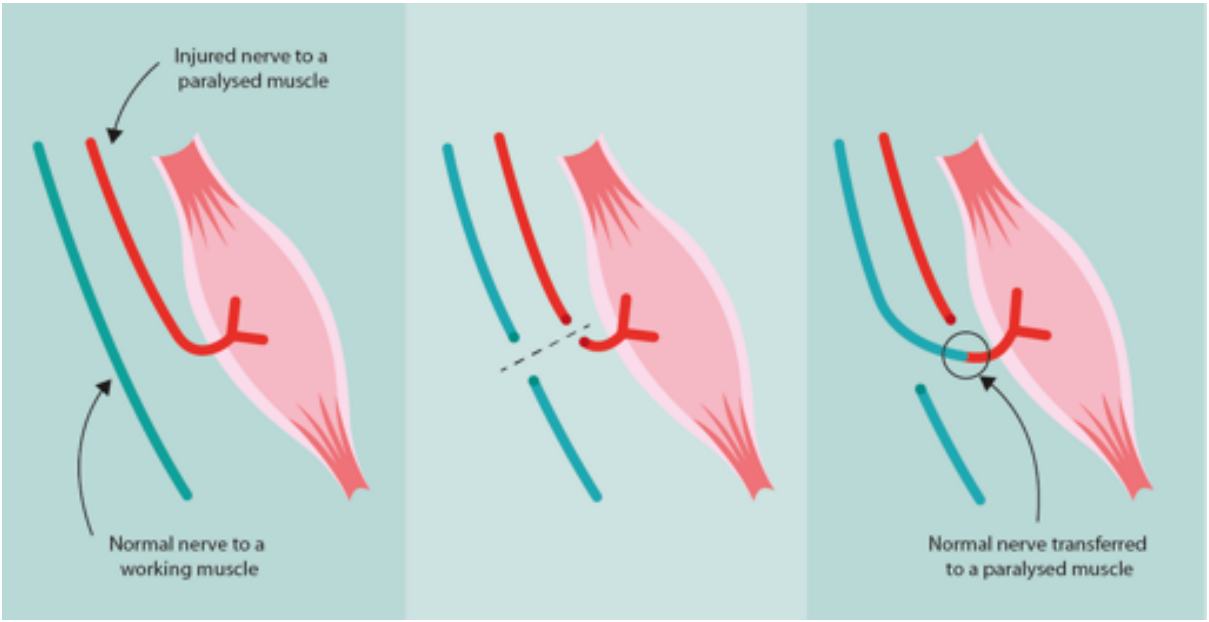

Figure 9 Nerve transfer principles from Melbourne TetraHand [36].

1.4.9 Nerve conduits

Due to the described disadvantages of nerve autografts, allografts and xenografts, there has been in recent decades a deep research towards the identification of alternative methods for the repair of nerve lesions with loss of substance. This lead to the concept of regeneration chamber. This expression refers specifically to tubules or neuroguides that once interposed between two stumps of a damaged nerve will behave as a guide for regeneration itself [13] (Figure 10).

The ideal characteristics that a nervous tubule (or conduct) should possess are:

• biocompatibility and biodegradability, with a degradation rate appropriate to maintain a valid support structure for the time necessary for regeneration;

• flexibility and softness;

• transparency;

• absence of immunogenicity;

• ease of manufacture and possibility to customize the tubule for the specific lesion;

• low cost and ready availability;

• easy implantation technique;

• semi-permeability, to promote the influx of oxygen and nutrients for the purpose of regeneration, but at the same time prevent the entry of fibrous scar tissue from the outside [37,38] (Fig 10).

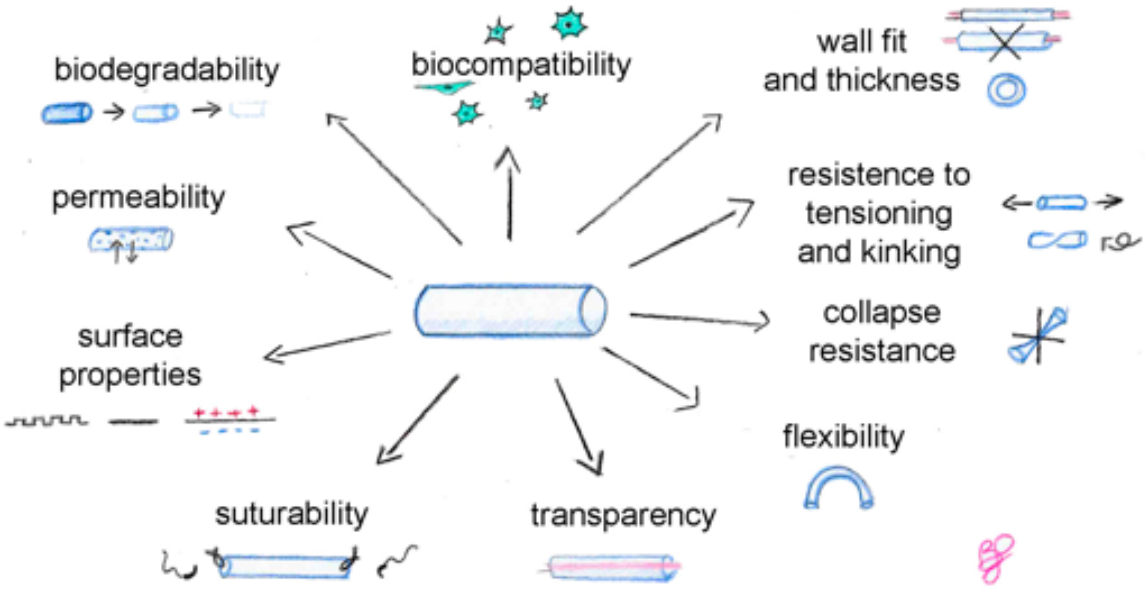

Figure 10 Ideal nerve conduits characteristics. From Ferreira-Duarte et al., 2020.

Since their introduction in clinical practice, the nerve conducts have undergone a remarkable evolution and numerous types of conduits can be distinguished (Fig. 11). Specifically, it is possible to distinguish between: biological tubules, obtained from autologous tissues, and synthetic tubules. Synthetic tubules can in turn be made of non-absorbable or resorbable materials, of natural or artificial origin.

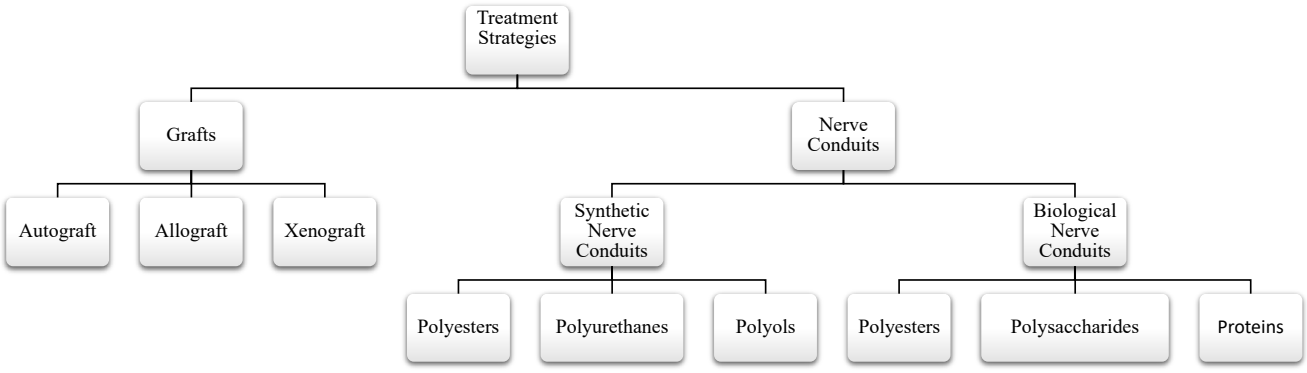

Figure 11 Natural and synthetic materials for peripheral nerve injury-based nerve conduits.

The creation of this vanguard type of devices is today an important area of interest within a multidisciplinary science known as Tissue Engineering (T.E.).

The T.E., first described by Langer and Vacanti in 1993 [39] applies the knowledge of engineering, biology and chemistry to the end to build functionally active tissue substitutes in the laboratory that allow the regeneration of the patient's own tissues, thus obviating the problems of immuno-compatibility that weigh on current transplantation techniques. The 3 pillars on which T.E. is based are scaffolds, cells and growth factors (Figure 12). Scaffolds are scaffolds that have the function of mimicking the extracellular matrix, assisting adhesion, proliferation and biosynthesis cellular. Cells, depending on their origin, can be autologous, allogenic or xenogenic, and can result from different stages of differentiation; the role of the cells is to colonize the scaffold producing extracellular matrix until the tissue regenerates. Growth factors are proteins that induce cell proliferation and differentiation, ensuring the adequate development of the bio-engineered material that is going to be implanted [40].

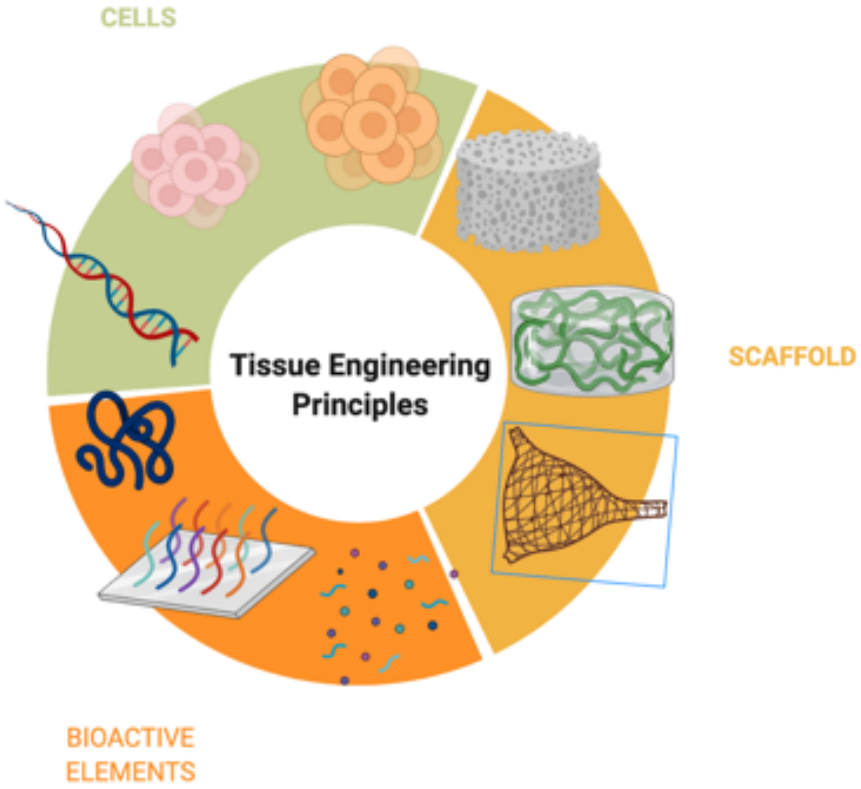

Figure 12 Tissue Engineering Principles

1.4.9.1 Natural conduits

Among the various types of biological tubules, those consisting of vessels (arteries and veins), and muscles [41] aroused the greatest interest from surgeons and researchers.

Arteries

The use of arteries as a conduit for nerve regeneration has been known for a long time but has been abandoned in favor of other techniques because in most cases it is impossible to obtain an artery segment of adequate size without incurring serious consequences for the individual himself[42].

Veins

The veins are an excellent biological tissue for nerve tubulization, so much so that they have been used since the early '900. In the 90s Tang et al. [43] highlighted the efficacy of vein segments filled with autologous nerve tissue for the repair of gaps between 2 and 4.5 cm in digital sensory nerves. However, this type of tubule still remains inferior to nerve autograft due to the ease with which the venous wall collides, causing difficulties in the progression and orientation of the regenerating fibers[44–47].

Muscles

The characteristics of muscle tissue that suggest its use as a regenerative conduct are the presence of a basal lamina and connective tissue that acts as a support to the regenerating nerve fibers, in addition to the longitudinal orientation of these components. An advantage in using muscle tissue for the realization of nerve conduits is the presence of numerous possible donor sites; however, the sampling implies the creation of an additional surgical site. The risk of nerve fibers lying outside the muscle tissue during regeneration remains[48–50].

Muscle in vein

To overcome the specific limits of vein and muscle as a graft for the recovery of PNI (i.e. ease of vein collapse, risk of unidirectional neuronal growth for the muscle) while exploiting its advantages, one can resort to the muscle-in-vein tubule (MIV) which consists of a venous tubule in which a segment of muscle tissue is inserted[51].

1.4.9.2 Synthetic conduits

Scientific improvements and the discovery of new materials has allowed the creation of artificial nerve conduits that, thanks to progress in chemistry and engineering, today possess characteristics increasingly close to those of the "ideal tubule". Synthetic tubules can be divided into: non resorbable and resorbable categories.

The manufacture of these devices can take place through different methodological approaches:

a) immersion molding technique: it involves the immersion of a guide inside a polymer solution, with consequent evaporation of the solvent that results in a solid tube;

b) electrospinning: produces nanofibers aligned longitudinally or randomly through the use of an electric field;

c) additive manufacturing techniques: include methodologies that allow the 3D printing of polymers based on models previously designed with CAD (Computer Aided Design).

The characteristic aspect of these approaches is to allow the manufacture of hollow tubules even of very small caliber (few millimeters), overcoming the dimensional limits of other techniques and allowing the production of custom-made devices;

d) 3D-bioprinting: it is a recent 3D bio fabrication technique, with which biomaterials (especially hydrogels) and cellular components can be combined, making it possible to manufacture devices that mimic nerve tissue [52].

NON-ABSORBABLE TUBULES

Among the materials initially considered for the fabrication of non-absorbable tubules conduits, silicone, Gore-Tex®, tetrafluoroethylene and polyvinyl alcohol were considered. Silicone was the first material used for this purpose, thanks to its flexibility, biocompatibility and transparency (useful in studies in vivo for a macroscopic evaluation of the progress of regeneration). Various studies showed it effectiveness in the repair of very small nerve gaps (less than 5 mm), with results comparable to end to end neurorrhaphies [53–55].

Gore-Tex® tubules were used for the repair of lesions of the inferior alveolar nerve, but results were poor [56].

Polytetrafluoroethylene was successfully used as a regeneration conduit in gaps of up to 4 cm at the level of the nerves of the forearm [57].

Polyvinyl alcohol (PVA) is a non-biodegradable water-soluble synthetic polymer, already used in the biomedical field in the treatment of cartilage lesions; there is currently a PVA-based conduit marketed usedin clinical practice and named Salutunnel™ [33].

The limits of the non-absorbable conducts are the induction of a remarkable fibrotic response, with possible compression of the nerve, and the need for a second surgical operation to remove the device after the time necessary for the regeneration process [58].

RESORBABLE TUBULES

Resorbable synthetic tubules are made of biodegradable polymers of both natural or artificial origin. The big advantage associated with them is the fact that they degrade over time, thus limiting the reaction from a foreign body resulting in fibrosis and the need for a second surgical intervention to remove the device [6,59,60].
Ideally, degradation should occur in a progressive manner, from the proximal stump to the distal end [52,61–63].

1.4.9.3 Natural polymers

Among the materials of natural origin, the most interesting for the fabrication of useful devices in PNI include:collagen, chitosan, silk fibroin, gelatin, hyaluronic acid and submucosa intestinal porcine.
Collagen is a natural component of the extracellular matrix and is widely used in T.E. After proper purification, collagen is only weakly immunogenic; its adhesive properties increase cell proliferation and survival. Several collagen-based conduits are now marketed (Neuragen®, Neuroflex™, Neuromatrix™, Neuromend™). The advantages of collagen-based tubules are ease of production, adhesion to various cell types, high level of biocompatibility; among the disadvantages emerges the slow biodegradation profile (from 8 to 48 months) entailing the risk of compression of the neo-regenerated nerve [64].
Chitosan is a polysaccharide obtained by the deacetylation of chitin, a constituent of the exoskeleton of arthropods. Chitosan has a good affinity for nerve cells and in vitro studies show its ability to support the survival and growth of axons [37]. There is currently a nervous conduit based on chitosan and used in clinical practice known as Reaxon®. The advantages of chitosan conduits are the scarcity of inflammatory response and protection from infections (antibacterial properties of chitosan are also described); the disadvantages are represented mainly from the high rigidity of this type of ducts and the high cost of devices on the market.

Silk fibroin is a protein produced by spiders and other insects and constitutes one of the main components of silk; it is an excellent candidate for the creation of nerve ducts by virtue of its high biocompatibility, degradation profile and adequate mechanical characteristics. A disadvantage of silk fibroin is its fragility with the consequent possibility of rupture at the surgical site: consequently, a solution to this problem could be the combination of fibroin with other materials, enhancing its advantages and minimizing its defects [65].

Gelatin is another water-soluble and biodegradable natural polymer, but in its native form it does not have sufficient resistance for application to nerve ducts: cross-linking can remedy this defect increasing its mechanical strength; however, high attention must be paid to how this treatment can alter the rate of degradation [65].

Hyaluronic acid is a natural polymer with very favorable characteristics, such as non-adhesiveness, support for axonal growth and the absence of immunogenicity. A major limitation of hyaluronic acid is its structural weakness, which remains even after cross-linking: a solution was found using esterified derivatives of hyaluronic acid, which, however, proved to have a too rapid degradation rate [65].

The porcine intestinal submucosa is a resistant, flexible and acellular matrix: after treatment with hypotonic solution, the matrix is composed of collagen, fibronectin, growth factors, glycosaminoglycans, proteoglycans and glycoproteins. A nerve conduct based on porcine intestinal submucosa is marketed under the name Axoguard™. It shows excellent potential in promoting tissue regeneration, also thanks to the abundant stimulation of local neo-angiogenesis.

The advantages of the porcine intestinal submucosa as a constituent of the nerve tubules are the absence of immunogenicity (guaranteed by the processes to which it is subjected), the excellent biomechanical support, the creation of a pro-regenerative microenvironment; the disadvantages are represented by: the high cost, the variability of the physicochemical properties and degradative (by virtue of its biological origin), the risk of disease transmission given the xenogenic origin of the material [38].

1.4.9.4 Synthetic polymers

There are many artificial and biocompatible materials used to manufacture bio-absorbable nerve guides, characterized by adequate mechanical characteristics. Some of the polymers used are polyesters, polyurethanes, caprolactones, carbon compounds, electroconductive polymers.

Polyesters include polylactic acid (PLA) and polyglycolic acid (PGA); these materials are thermoplastic and can be shaped easily through various manufacturing techniques and biodegrade through the hydrolysis of ester groups in the polymer chain [11,65–67].

Polylactic acid (PLA) has higher hydrophobicity and longer degradation time than polyglycolic acid (PGA), characteristics that make it more suitable for use for nerve regeneration [68].

Polyglycolic acid (PGA) takes 2-3 months to fully degrade, but already after a short period of time it begins to lose some of its strength; although there is a commercial PGA (Neurotube®) product, its use is limited by the excessive speed of degradation, the production of acidic substances during its hydrolysis and low solubility [64].

Polyurethane is a good candidate as a component of nerve conduits due to its biocompatibility and mechanical properties, among which flexibility is preeminent [65].

Polycaprolactone, in the form of Poly-D,L-lactic-co-ε-caprolactone (PCL) has aroused considerable interest in the field of nerve tubules because the its production is relatively simple and low cost; the degradation of polycaprolactone occurs by hydrolysis and its copolymerization with Poly-D, L-lactic acid accelerates the time of this process; compared to other compounds, it has the advantage that its degradation compounds are absolutely non-toxic and do not cause any inflammatory response. On the market there is a conduct based on caprolactone with the name of Neurolac®, which has shown excellent effectiveness in repairing gaps up to 2 cm in length, but which has the main limit in its excessive rigidity [69].

Recently, the neuro-regenerative capabilities of electroconductive polymers, smart materials that increase axonal regeneration through electrical stimulation, have been studied.

Another interesting material is carbon, in the form of nanotubes and nanofibers, which exhibit excellent electrical and mechanical properties; in particular, nanofibers assemble into structures similar to those of tissue proteins and have superior biocompatibility characteristics compared to carbon nanotubes[70–74] .

1.5 Actual limits and future perspectives towards nerve conduits

The current nerve guides have not yet reached the ideal characteristics necessary to fully meet the needs of the surgeon as well as the patient, in terms of morpho-functional recovery of the injured nerve. As a result, research is moving towards the identification of bioengineered materials capable of overcoming the limitations of currently available devices. Researchers at the University of Padua have recently developed a new bioresorbable polymer, derived from polyvinyl alcohol, which is called oxidized polyvinyl alcohol (OxPVA). OxPVA, in addition

to a biodegradation profile that can be modulated according to the degree of oxidation itself, also acts as a tunable platform thanks to the presence in the backbone of the molecule of carbonyl groups capable of giving rise to interactions or chemical bonds with proteins or peptides of interest [75–78]. To date, some preclinical studies [75,79] have already suggested the efficacy of OxPVA for neuro regenerative purposes, proving that it can be adequately used as a biomaterial for the realization of wraps and neuro guides. However, the great intrinsic potential of the polymer leaves space for new evaluations and comparisons both in terms of timing of the pro-regenerative response and functional recovery. In addition, the peculiar presence of the carbonyl group introduced through oxidation, encourages the development of approaches aimed at further optimizing the characteristics of the devices that can be obtained from OxPVA. The goal is to develop neuro-guides capable of recreating within them an optimal neurotrophic environment for regeneration; specifically, the incorporation of bioactive molecules such as peptides, growth factors and cells seems to be the most promising strategy.

THE AIM OF THE STUDY

Peripheral nerve injuries (PNI) are a critical clinical condition as, despite microsurgical advances, their treatment is often a challenge in terms of structural and functional recovery of the affected nerve, thus resulting in impaired sensory and/or motor function.

Classification and current treatment of PNI is based on damage severity. In case of sharp injuries *without substance loss*, end-to end nerve repair is the preferred option and nerve wrapping is often used to improve the outcomes; however, to achieve tensionless result with a complete functional recovery is often a challenge. In parallel, in case of *injuries with substance loss*, the bridging of the gap between the proximal and distal nerve stumps is required to guarantee nerve continuity. Autologous nerve graft (gold standard), together with allografts and xenografts are the options currently available; however, these surgical strategies present disadvantages such as donor site co-morbidities for autografts, immunosuppressive therapies and high costs for allografts and xenografts.

Considering the urgent need for effective devices to use in case of PNI, this experimental work will focus on fabrication, characterization and pre-clinical evaluation of new wraps and nerve conduits based on the synthetic bioresorbable polymer *oxidized polyvinyl alcohol* (OxPVA), recently developed by our group.

The aim of this study recognizes 3 objectives:

i) in vitro characterization studies on OxPVA-based scaffolds

Different oxidative strategies will be compared for the identification of the best OxPVA-derived hydrogel: two distinct oxidative agents will be assayed, potassium permanganate ($KMnO_4$) and bromine (Br_2). Thus, after scaffolds preparation by physical crosslinking, the specific characteristics (morphology, ultrastructure, swelling ability and porosity, mechanical features, in vitro cytotoxicity, in vitro biodegradation, protein binding ability by UHPLC-MS) will be investigated and compared to that of the non-oxidized PVA.

ii) Evaluation of OxPVA-based devices in an animal model of disease: sharp transection of the sciatic nerve without substance loss

Wraps made of OxPVA (oxidative agent: $KMnO_4$) will be evaluated for preclinical outcomes after nerve transection and neurorrhaphy (animal model: Sprague-Dawley rats; implant site: sciatic nerve). The experimental groups will include: NeuraWrap™ (commercial wrap, control group), OxPVA, Leukocyte-Fibrin Platelet membrane (LFPm) wraps; end point: twelve weeks. The analysis that will be performed for outcomes evaluation will include: functional recovery tests (Sciatic Functional Index evaluation), histological (hematoxylin and eosin staining –

(H&E); Toluidine-Blue staining) and immunohistochemical (anti-CD3, -F4/80, -S100, β-tubulin staining) studies, morphometric evaluation (total cross section area, fascicular area, total axons density, total axons number), ultrastructural analysis by Transmission Electron Microscopy (TEM), evaluation of the eventual fibroconnective infiltrate by Second Harmonic Generation (SHG) microscopy.

iii) Evaluation of OxPVA-based devices in an animal model of disease: sharp transection of the sciatic nerve with substance loss

Different nerve conduits based on OxPVA will be implanted in an animal model (Sprague Dawley rats) of sciatic nerve transection with substance loss (gap=5mm). Briefly, 6 groups will be considered: Reverse Autograft (mimicking autograft), Reaxon® (commercial device made of chitosan), OxPVA based conduits; OxPVA+EAK peptide conduits; OxPVA+EAK-YIGSR peptide conduits; OxPVA+adsorbed NGF conduits. The end point considered will be that of 6 weeks. After implantation, the effectiveness of the devices will be assayed considering animals wellbeing (weight analysis; autotomy index), functional recovery (gait analysis, sciatic functional index, von Frey filaments assay for mechanical sensitivity), evaluation of the surgical site after euthanasia, histological (H&E, toluidine blue staining) and immunohistochemical (CD3, F4/80, S100, β-tubulin) analyses on explants which will also undergo to morphometric study (total cross section area, fascicular area, total axons density and total axons number) and evaluation of fibroconnective infiltrate by SHG microscopy.

MATERIALS AND METHODS

3.1 Reagents and instruments

Polyvinyl alcohol (PVA), molecular weight (MW) 146,000–184,000 Da, 70% hydrochloric acid, bromine (Br_2), acetonitrile, perchloric acid ($HClO_4$), collagenase B, calcium gluconate, sodium bicarbonate ($NaHCO_3$), bovine pancreatic trypsin, poly-L-lysine, Dulbecco's Modified Eagle Medium/Nutrient Mixture F-12 (DMEM-F12), Dulbecco's Modified Eagle Medium (DMEM), fetal bovine serum (FBS), phosphate buffer saline (PBS), penicillin/streptomycin (PEN/STREP) solution, gentamicin solution, Heregulin β1, Forskolin, ethylenediaminetetraacetic acid (EDTA), [3-(4,5-dimethylthiazol-2-yl)-2,5-dimethyltetrazolium bromide] (MTT) and dialysis membranes (cut-off 8000 Da) were purchased from Sigma-Aldrich (S. Louis, Missouri, USA). Potassium permanganate ($KMnO_4$), acetic acid, 2-propanol, 100% ethanol, sodium cyanoborohydride ($NaBH_3CN$) and dimethyl sulfoxide (DMSO)were purchased from Carlo Erba (Milan, Italy). Ciliary neurotrophic factor was purchased from Peprotech, (London, UK). Reaxon® nerve guides were purchased from KeriMedical, Friedrich-Koenig-Str. 355129 Mainz, Germany). Scanning electron microscope JSM-6490 (Jeol USA, Peabody, MA, USA), analytical balance (mod.E/50 macro/semi-micro, Gibertini, Milan, Italy), vacuum evaporator (Speed Vac Concentrator Savant, Instruments Inc. Farmingdale, NJ, USA), Microplate Auto Reader VICTOR3. (Perkin Elmer, Waltham, MA, USA), Ultra-high performance liquid chromatograph-coupled with mass spectrometer (UHPLC-MS, Waters Acuity H Class, Milford, Massachusetts, USA). Confocal microscope (Zeiss 800, Leica Microsystems, Wetzlar, Germany).

3.2 Synthesis of oxidized polyvinyl alcohol solutions

Oxidation of PVA by $KMnO_4$

For the preparation of a 16% neat PVA solution, a pre-weighed quantity of polymer powder was suspended into MilliQ water and heated for 48 h at 100°C under stirring until complete dissolution. Partial oxidation of PVA was performed by using potassium permanganate as oxidizing agent: potassium permanganate ($KMnO_4$) in dilute perchloric acid ($HClO_4$). The polymer solution was treated with the stoichiometric quantity of the oxidative agent enough to

oxidize the 1% of secondary alcoholic groups to carbonyl groups. Oxidized PVA by means of potassium permanganate (OxPVA_$KMnO_4$) was prepared as follows: 10 g of PVA powder was suspended in 200 ml of MilliQ water; the solution was then heated till complete polymer solubilization occurred (60 min). After cooling at 36-37 °C, to this solution were added 156,5 mg $KMnO_4$ dissolved into 10 ml of MilliQ water and 1,60 g 70 % $HClO_4$. After this oxidation step, the resulting solution was dialyzed extensively against water using a membrane with 8000 Da cut-off. If not used immediately, oxidized PVA solutions were frozen at - 20°C and lyophilized by an under-vacuum evaporator (Speed Vac Concentrator Savant, Instruments Inc. Farmingdale, NJ, USA).

Oxidation of PVA by Br_2

Oxidized PVA by means of bromine (OxPVA_Br_2) was obtained as follows: 10 g of PVA powder was suspended in 200 ml of MilliQ water; the solution was then heated till complete polymer solubilization occurred (60 min). After cooling at 15 °C 528 mg of sodium bicarbonate ($NaHCO_3$) were suspended, then 20 ml of MilliQ water at 15°C containing 116,30 µl of bromine (Br_2) were added to the solution. Oxidation was conducted for 4 h at 15-18°C till complete discoloration was observed. Dialysis and lyophilization process occurred as same as PVA oxidized with $KMnO_4$.

3.3 Fabrication of OxPVA-derived scaffolds

Different scaffold types (discoidal scaffolds, wraps and conduits) were prepared for future in vitro characterization studies. OxPVA_$KMnO_4$ and OxPVA_Br_2 solutions were used.
OxPVA-based discoidal scaffolds (diameter:7mm; thickness:2 mm) /wraps (10 mm length; 1 mm thickness) were manufactured pouring the polymers solutions into a mold consisting of two glass sheets separated by a 3 mm thick steel spacer. Cross-linking was performed by F/T process consisting of seven cycles of cooling at -20°C for 24 h and thawing at -2.5°C for 24 h. After removal from the molder, scaffolds were kept at -20°C until use.
Tubular scaffolds were prepared through the injection molding-technique82. Each tubular scaffold was then assembled by aspiring the hot solution in a stainless-steel cylinder having an internal diameter of 2.1 mm and length of 5 cm, followed by coaxial introduction of a stainless-steel plunger with external diameter of 1 mm and length of 10 cm. Cross-linking of the polymer was performed by F/T process consisting of seven cycles of cooling at -20°C for 24 h and

thawing at -2.5°C for 24 h. After removal from the molder, the nerve guides were kept at -20°C until use (Fig 13).
Neat PVA-derived scaffolds were used as control group.

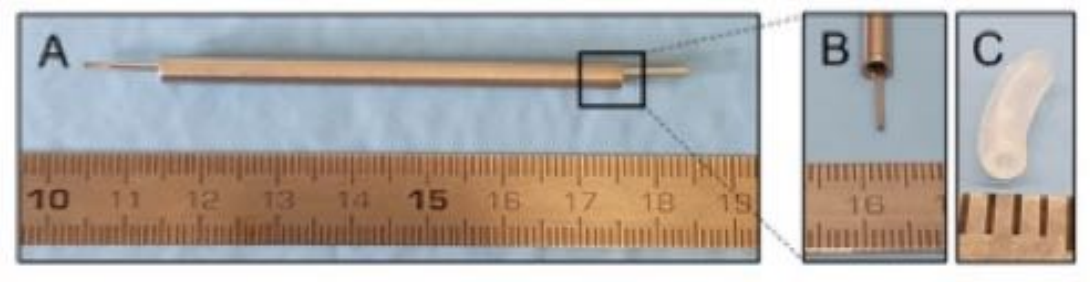

Figure 13 Cylinder used to fabricate nerve conduits with mandrel inside (A-B). Nerve conduit lumen (C).

3.4 In vitro characterization studies

3.4.1 Swelling behavior of nerve conduits

Neat PVA (control group) and OxPVA (OxPVA_$KMnO_4$ and OxPVA_Br_2) nerve conduits (diameter: 1 mm; length: 10 mm) were placed separately on a 24-well plate (Corning), immersed in 1 mL phosphate buffer solution (PBS) and kept at room temperature (RT) for a total time of 600 h. Thus, samples were weighed every 48 h after the removal of PBS excess by wiping with filter paper. The following equation was used to obtain the swelling ratio:

$$\frac{W_s - W_d}{W_d} \cdot 100$$

Ws is the weight of the swollen scaffold and Wd is the weight of the dry scaffold.

3.4.2 Porosity measures

PVA and OxPVA (OxPVA_$KMnO_4$ and OxPVA_Br_2) porosity was evaluated by the solvent replacement method 83. Briefly, pre-weighted dried discoidal scaffolds were immersed in PBS for 48 h and then weighed again, after removing the excess of PBS on their surface. The porosity was calculated from the following equation:

$$\frac{W_s - W_d}{\rho V} \cdot 100$$

Wd and Ws are the weight of hydrogel before and after the immersion in PBS, respectively; ρ is the density of PBS and V is the volume of the hydrogel.

3.4.3 Morphological characterization

Ultrastructural analysis of PVA-based scaffolds was performed by scanning electron microscopy (SEM). Samples were dehydrated through a series of graded ethanols, exposed to critical point drying and gold sputtering and finally observed. Images were taken using a JSM-6490 scanning electron microscope.

3.4.4 Preliminary mechanical and suture tests

A preliminary demonstration of flexibility, elasticity, and mechanical strength of PVA and OxPVA-based nerve guides was performed by means of suture tests using Nylon 8–0 sutures. A microsurgeon specialized in peripheral nerve reconstruction performed suture tests by passing the needle perpendicular to the surface of the conduit wall and exerting some tensile force to evaluate the mechanical resistance to the suture. Furthermore, a microsurgical anastomosis between two conduits was performed to test the material capacity to hold the suture knots.

3.5 In vitro cytoxicity assay

3.5.1 Cell cultures, extract test and viability assessment

Neat and OxPVA cytotoxic effects were evaluated using a) the human neuroblastoma cell line SH-SY5Y (ATCC, Manassas, VA, USA) and b) primary cultures of Schwann cells isolated from a rat sciatic nerve according to a published protocol 84,85.

SH-SY5Y cells were cultured in 25 cm^2 flasks (Corning, NY, USA) using DMEM/F-12 supplemented with 15% FBS and 1% penicillin (10,000 U/mL)/streptomycin (10 mg/mL) solution. In parallel, Schwann cells were cultured in 25 cm^2 flasks on poly-L-lysine coating, using DMEM supplemented with 10% FBS, 50 µg/mL gentamicin solution, 1 nM Heregulin β1 and 1 nM Forskolin. Cultures were maintained at 37°C, 95% relative humidity and 5% CO_2 changing medium every other day until the time of use. SH-SY5Y cells of passage 35 and Schwann cells of passage 3 were used in the extract cytotoxicity test.

For the cytotoxicity assay, neat PVA and OxPVA (OxPVA_$KMnO_4$ and OxPVA_Br_2) was assessed by the following described extract test. Briefly, the tubes were incubated for 24 h into SH-SY5Y or Schwann cell culture medium (100 mg/mL), at 37°C. In parallel, cells at 80–90% confluence were harvested by treatment with 0.025% EDTA and 0.25% trypsin in PBS and seeded at high density (60,000 cells/cm^2) on 96-well culture plates (Corning). After 24 h from seeding, the cell culture medium was removed and replaced with the extract medium. As

positive (cytotoxic) control, cells were incubated in culture medium added with 50% DMSO, whereas the negative control was represented by untreated cultures. Treated and control samples were incubated for 24 h at 37°C, 95% relative humidity and 5% CO_2 and the effect of extract medium on cell survival was then evaluated by the 3-(4,5-dimethylthiazol-2-yl)-2,5-dimethyltetrazolium bromide (MTT) assay. According to routine protocols, the adherent cells were incubated with 0.5 mg/mL MTT for 4 h and then with 2-propanol acid (0.04 M HCl in 2-propanol) for 15 min to dissolve formazan precipitates. Finally, the optical density was measured at 570 nm by using a Microplate auto reader VICTOR3. Results were expressed as relative cell viability measured in treated samples in comparison with the untreated control (100%).

3.5.2 In vitro biodegradation

Enzymatic degradation of neat and OxPVA (OxPVA_$KMnO_4$ and OxPVA_Br_2) nerve conduits was investigated by incubating samples in a 5 mg/mL collagenase B solution and monitoring the weight loss over time, up to 14 days. To mimic physiological conditions, collagenase was dissolved in human plasma and samples were incubated at 37°C. Nerve conduits were weighed at well-defined time points (1, 3, 5, 8 and 14 d), after being extracted from the collagenase solution and dried to remove solvent excess. At each time point (t), weight loss was calculated according to the following formula:

$$\frac{W_\mathrm{i} - W_\mathrm{t}}{W_\mathrm{t}} \cdot 100$$

Wi represents the initial weight and Wt represents the weight of the sample after the time point 86.

3.6 Evaluation of OxPVA bioactive potential

3.6.1 Coupling of CNTF to the nerve guides and UHPLC-MS evaluation

Nerve guides made of native PVA and OxPVA (OxPVA_$KMnO_4$ and OxPVA_Br_2) were rinsed with PBS and filled with a 0.16 mg/mL CNTF solution in PBS pH 7.4 containing 3 mg/mL sodium cyanoborohydride. The adopted CNTF concentration for functionalization was chosen to prevent the precipitation of the growth factor in the solution, in accordance with our previous studies. After 2 h at 16°C the initial solution was discarded and substituted with a fresh one, continuing the coupling for further 4 h at 16°C. After that, the tubes were rinsed internally five times with PBS, for 5 min each time. Hence, to recover absorbed CNTF, nerve

guides were filled with few microliters of a solution containing 0.40 mg/mL trypsin in PBS and kept at 16°C for 15 min. Thereafter scaffolds were squeezed to collect all the inside solution enriched with the digested protein, which was subsequently lyophilized for the analyses of the tryptic peptides by UHPLC-MS. The solutions extracted from neat PVA scaffolds were also tested as a negative control (low binding ability). The tryptic peptides derived from digestion of 0.30 μg of CNTF were also evaluated by UHPLC-MS as a reference for quantification of the neurotrophic factor.

3.7 Peptides synthesis

In the perspective of in vivo preclinical study, the synthesis of two different peptides with ability in promoting neural regeneration was here considered. Specifically, two bioactive sequences were prepared and purified thanks to the collaboration established with the Research Laboratory Group of Prof. Monica Dettin, Department of Chemical and Material Engineering of Padova University 87.

EAK

The self-assembling peptide EAK (sequence: H-Ala-Glu-Ala-Glu-Ala-Lys-Ala-Lys-Ala-Glu-Ala-Glu-Ala-Lys-Ala-Lys-NH2) was produced by solid phase peptide synthesis using a Syro I automatic synthesizer and Fmoc chemistry. Rink Amide mBHA resin (substitution 0,52 mmol/g) was used as solid support. The side-chain protections were OtBu for Glu and Boc for Lys. Each coupling was carried out with 5 equivalents of Fmoc-protected amino acid, 5 eq. HBTU and 10 eq. DIPEA. Each single coupling lasted 45 minutes. All amino acids were introduced with double couplings. Finally, the peptide was cleaved from resin and all side chain protections were removed through a treatment with the following solution: 0.125 mL MilliQ water, 0.125 mL TES and 4.725 mL TFA for 90 min at room temperature. The crude peptide was purified in RP-HPLC. The homogeneity grade (about 100%) and the identity of the purified peptide were ascertained by analytical HPLC and MALDI mass analysis. The reaction with 5(6)-carboxytetramethylrhodamine of side chain-protected EAK peptide on resin produced the EAK analogue used for SAP distribution evaluation assay. For the coupling reaction 4 equivalents of 5(6)-carboxytetramethylrhodamine, 4 equivalents of HBTU and 8 equivalents of DIPEA were used.

EAK-YIGSR

The peptide EAK-YIGSR (sequence: H-Ala-Glu-Ala-Glu-Ala-Lys-Ala-Lys-Ala-Glu-Ala-Glu-Ala-Lys-Ala-Lys-Tyr-Ile-Gly-Ser-Arg-NH2) was produced by solid phase peptide synthesis using a Syro I automatic synthesizer and Fmoc chemistry. Rink Amide mBHA resin (substitution 0,52 mmol/g) was used as solid support. The side-chain protections were OtBu for Glu and Boc for Lys and tBu for Tyr and Ser and Pbf for Arg. Each coupling was carried out with 8 equivalents of Fmoc-protected amino acid, 8 eq. PyOxim and 16 eq. DIPEA. Each single coupling lasted 45 minutes. All amino acids were introduced with double couplings. Finally, the peptide was cleaved from resin and all side chain protections were removed through a treatment with the following solution: 0.125 mL MilliQ water, 0.125 mL TES and 4.725 mL TFA for 90 minutes (min) at room temperature. The crude peptide was purified in RP-HPLC. The identity of the purified peptide was ascertained by analytical HPLC and MALDI mass analysis.

3.8 Validation of OxPVA scaffolds bioactivation through EAK mechanical incorporation

The model peptide EAK+ Rhodamine (Rh) was resuspended in MilliQ water to a final concentration of 1 mg/mL; in parallel, 3 g of OxPVA hydrogel were poured onto a glass slide. Hence, the EAK-Rh solution was added drop by drop, to reach 0.2 % w/w in OxPVA: a stainless laboratory spatula was used for their homogeneous distribution within the OxPVA hydrogel. The solution of OxPVA+EAK-Rh was poured into tubular mold for nerve conduits fabrication and underwent to F/T as described above (paragraph 3.3). The derived scaffolds were observed under a confocal microscope (Zeiss800) (wavelength excitation: 561 nm; Emission signal: 580-620 nm). A non-functionalized OxPVA conduit was used as a negative control.

3.9 Manufacture of conditioned nerve conduits

3.9.1 Bioactivation of OxPVA nerve conduits by EAK and EAK-YIGSR mechanical incorporation

Two different tubular scaffolds were prepared through mechanical incorporation of the peptides EAK and EAK-YIGSR in OxPVA solution. The protocol for conduits fabrication was the same reported in paragraph 3.8.

3.9.2 Bioactivation of OxPVA nerve conduits by NGF adsorption

OxPVA solution was poured into a tubular mold which underwent F-T for nerve conduits fabrication. Hence, each conduit was incubated for 24h at 37°C in 0.5 ml of PBS solution containing 0.1 % BSA and 125 μg/ml NGF.

4. Preclinical studies in animal models of PNIs

All animal procedures were approved by the ethical committee of Padua University (D.M. n.162/2013-B), according to the Italian Department of Health Guidelines.

4.1 PNI without substance loss

Three different wraps were compared for effectiveness in this preclinical study on an animal model of PNI without substance loss. Specifically the experimental groups considered where: the commercial NeuraWrap™, OxPVA (oxidative agent $KMnO_4$) wraps and leukocyte-fibrin-platelet membrane derived wraps (LFPm) (provided S.Martino hospital, Belluno, Italy [86]).
Prior to use OxPVA wraps were disinfected with 70% alcohol solution and carefully washed with PBS (0.1M pH 7.4).

4.2 Surgery

The sciatic nerve was exposed trough a gluteal-splitting method and transected with microsurgical scissors. To connect the epineuria of the proximal and distal stumps were performed Nylon 8-0 sutures and the nerve protectors were trimmed and wrapped around the site of repair. Each wrap specimen was 1centimeter in length and 1 millimeter in thickness; for assuring better grip with the operated nerve, wraps were secured along their length uninterruptedly with Nylon 8-0 sutures. The incision was closed in layers using 4-0 silk sutures. After surgery, adequate anti-inflammatory (Rimadyl, 5 mg/kg) and antibiotic (Baytril, 5 mg/kg) therapies were administered for 5 days, and the rats recovered in the cage being housed in a temperature-controlled facility and fed with laboratory rodent diet and water ad libitum. The final endpoint was set-up at 12 weeks after surgery; euthanasia by carbon dioxide asphyxiation was performed.

4.3 Functional tests

At 2 and 12 weeks after surgery, animals were subjected to sciatic functional test to evaluate the functional status of the operated sciatic nerve. A gangway 100 cm long and 10 cm wide

covered with white paper was created. Rats with their feet stained with black ink were placed at the beginning of the walk track and allowed to walk up thereby. For each rat, five measurable footprints were taken for the calculation of the sciatic functional index (SFI) according to the formula of Bain et al. [87]

$$SFI = -38.3\frac{EPL - NPL}{NPL} + 109.5\frac{ETS - NTS}{NTS} + 13.3\frac{EIT - NIT}{NIT} - 8.8$$

Print length (PL) stands for the distance from the heel to the top of the third toe, toe spread (TS) corresponds to the distance from the first to the fifth toe and intermediary toe spread (IT) represents the distance between the second and the fourth toe. EPL, ETS and EIT match PL, TS and IT values for the operated groups, respectively. NPL, NTS and NIT match PL, TS and IT values for non-operated group, respectively.

4.4 Macroscopic evaluation of wraps explants

At 12 weeks after surgery dissection was performed. A surgeon submitted a blind evaluation of the macroscopic aspect of the neurolysis site. Quality of wound healing, presence of inflammation signs and perineural adhesion were the parameters considered.

4.5 Histological and immunohistochemical analysis

Explants corresponding to repaired nerves were fixed with 10% formalin in phosphate buffer saline soon after removal. Subsequently they were crosscut in the middle portion (corresponding to the coaptation site) and retrogradely cut into 4 μm thick serial sections after paraffin embedding. Sections were dewaxed with xylene and hydrated with graded alcohol series (from absolute to 75%) and then stained with H&E.

Immunohistochemical characterization was performed with the following antibodies diluted in phosphate buffer saline. Anti-CD3 (polyclonal rabbit anti-human CD3, diluted 1:500); anti-F4/80 (polyclonal rabbit anti-mouse anti-F4/80), diluted 1:800; anti S-100 (polyclonal rabbit anti-S100), diluted 1:5000; anti-β-tubulin (polyclonal rabbit neuronal class III β-tubulin). Antigen unmasking was performed with 10 mM sodium citrate buffer, pH 6.0, at 90 °C for 10 minutes, except for S-100. The sections were then incubated for 30 minutes in blocking serum [0.04% bovine serum albumin (BSA) and 0.5% normal goat serum] to eliminate unspecific binding, and then incubated for 1 hour at room temperature with the above primary antibodies.

Primary antibody binding was revealed by incubation with anti-rabbit/mouse serum diluted 1:100 in blocking serum for 30 minutes at room temperature and developed in 3,3′-diaminobenzidine for 3 minutes at room temperature. Lastly, the sections were counterstained with hematoxylin. As a negative control, sections were incubated without primary antibodies.

4.6 Ultrastructure analysis

To investigate the contribute of wraps in tissue healing effectiveness, ultrastructural details (as tissue quality and axon distribution) of operated sciatic nerves were analyzed at 12 weeks after surgery. Explant samples were fixed in 2.5% glutaraldehyde in 0.1 M phosphate buffer saline. Subsequently, each nerve was sectioned 8 mm distal and proximal from the coaptation site. Sections, post-fixed in 1% osmium tetroxide in 0.1 M phosphate buffer, were dehydrated in a graded alcohol series and embedded in Epoxy resin. Semi-thin sections (0.5 μm) were cut with an ultramicrotome before staining with 1% Toluidine Blue. A Leica DMR microscope (Leica Microsystems Wetzlar, Germany) was used to acquire images; further images analysis was performed using ImageJ image processing software (National Institutes of Health, Bethesda, MD) for blinded analysis. Ultrathin sections, 60 nm, were collected on 300-mesh copper grids, counterstained with 2% uranyl acetate and then with Sato's lead. Specimens were observed by a Hitachi H-300 TEM.

4.7 Morphometric analysis

Morphometric investigation was carried on semithin Toluidine Blue stained section of proximal and distal portions of each sample. Two areas of each proximal and distal stump were analyzed with TEM. Total cross section area, fascicular area of each portion was measured. Subsequentially five random quadrants in the fascicular area were identified. Then, searching for myelinated and unmyelinated axon, 3 high power fields (100x) of equal area from each quadrant were investigated. Average axon density was determined dividing total axon number by the area sampled.

4.8 Second harmonic generation microscopy (SHG) analysis

Neural collagen distribution was imagined 12 weeks after surgery. SGH label free microscopy was performed for a qualitative comparison with data from histology, immunohistochemistry, and TEM. Specimens were processed as previously described for histology and

immunohistochemistry. 4 μm-thick serial sections were fixated in 10% formalin in PBS and embedded in paraffin. Then sections were cut and deparaffinized. SHG imaging was performed using a custom developed multiphoton microscope. An incident wavelength of 800 nm (~40 mW average laser power measured under the microscope objective) was used in order to detect the collagen's SHG signal at 400 nm, while simultaneously excite the two-photon autofluorescence signal from the elastin and the intrinsic fluorophores within the nerves (collected by a PMT inside the operative wavelength range of 505–545 nm). The images were acquired at a fixed resolution of 1024 × 1024 pixels, averaged over 120 consecutive frames, with a pixel dwell time of 0.14 μs.

5. PNI with substance loss

Six different nerve conduits were compared for effectiveness in this preclinical study on an animal model of PNI with substance loss. Specifically, the experimental groups here considered were based on: Reverse Autograft (RA), Reaxon® (commercial product based on chitosan), OxPVA (oxidative agent $KMnO_4$) conduits, OxPVA+EAK conduits, OxPVA+EAK-YIGSR conduits, OxPVA+NGF (adsorbed) conduits.

Prior to use, the OxPVA-based devices were disinfected with 70% alcohol solution and carefully washed with PBS (0.1M pH 7.4).

The end point considered was that of 6 weeks. A second end point, evaluating outcomes at 12 weeks is currently ongoing.

5.1 Surgery

All animal protocols were approved by the ethical committee of Padua University, in agreement with the Italian Department of Health guidelines. Eighteen Sprague-Dawley rats were randomly divided into six experimental groups (n=3/each): RA, Reaxon®, OxPVA, OxPVA+EAK, OxPVA+EAK-YIGSR and OxPVA+NGF group and anaesthetized using a binary gas mixture of isoflurane/oxygen. Prior to perform a 2.5 cm incision on the left thigh, the area was shaved and disinfected. After separating the fascia and muscle groups by blunt dissection, the left sciatic nerve was exposed and transected creating a nerve gap of 5 mm between the proximal and distal stumps.

As regards the reverse-autograft group, a segment of sciatic nerve (5 mm in length) was excised, inverted and reimplanted using Nylon 8–0 sutures. Concerning the conduits (10 mm

in length), these were coaxially interposed between the stumps and then sutured to the epineurium using Nylon 8–0 sutures. The incision was closed in layers using 4–0 silk sutures. After surgery, the animals recovered in the cage, and they were treated with anti-inflammatory (Rimadyl®, 5mg/kg) and antibiotic (Baytril, 5mg/kg) therapy for 5 days. In the following period, they were housed in a temperature-controlled facility and were given laboratory rodent diet and water ad libitum.

After 6 weeks, the rats were euthanized by carbon dioxide asphyxiation and the implants were excised and preliminarily analyzed for their size/integrity. Thereafter, samples were properly fixed for histological/immunohistochemical analyses.

5.2 Animal wellbeing assessment and functional tests

5.2.1 Weight analysis

At 1,3 and 6 weeks after surgery animal weight was monitored to assure for animal healthcare. Evident variations in animals weight suggest poor toleration of the surgical procedure.

5.2.2 Autotomy index

At 1, 3 and 6 weeks after surgery animal tendency to autotomy was measured. Parameters were considered according with Wall et al [88]. At each observation a score was assigned to indicate the extent of autotomy. A score of 1 was given for the removal of 1 or more nails. A score of 1 was added for each distal half digit attacked. A further score of 1 was added for each proximal half digit attacked. If all nails and all parts of all toes were attacked a score of 11 was achieved.

5.2.3 Von Frey hair test

Animals were subjected to Von Frey Hair Test to evaluate the sensitivity threshold through the stimulation of the plant of operated paw. Briefly, animals were placed in a setup consisting of a net raised from the worktop of about 20 cm, with side walls of plexiglass and polystyrene roof. The structure was built for the purpose of this study based on the indications reported in the literature [89–91]. Before proceeding with the test, animals were left exploring for 15 minutes to acclimatize in the new environment. Then animals were then stimulated in the plantar region using a series of monofilaments able to exert increasing strength/weight (1 g, 1.4 g, 2 g, 4 g, 6 g, 8 g, 10 g, 15 g, 26 g, 60 g and 100g). For each monofilament, 3 attempts were made to stimulate the treated paw, and the response was indicated as response percentage. The

retraction of the paw by the animal was considered as positive response. As a control, the behavior of an untreated healthy animal was taken into account.

5.2.4 Gait analysis

At 6 weeks after surgery, and before the sacrifices, the animals were made to walk on a transparent plexiglass lane (50 cm long and 10 cm wide). Below this lane it was placed one 45° inclined mirror mounted on a support created through 3D printing. This placement allowed the simultaneous monitoring of the side profile of the rat and the support of the sole of the paws on the lane. The walk of each rat was videotaped for groups comparisons. Specifically, the parameters that were compared, as introduced by Ijkema-Paassen et al. [92], were:

• preservation of the opening between the first and fifth toes;
• extent of the support with the sole of the paw;
• absence of entrainment of the paw;
• quality of the swing phase;
• fluidity of the walk;
• absence of eversion and exorotation of the paw;
• alternation of the steps with the two legs;
• point of support with respect to the shape of the body;
• level of contracture of the phalanx joints.

For each parameter a score was assigned: 0 points if not assessable, 1 point if assessable but abnormal, 2 points if normal. A mean total score was attributed to each animal and groups were then compared.

5.2.5 Sciatic functional index

At 6 weeks after surgery, animals were subjected to sciatic functional test (see 4.2 paragraph) to evaluate the functional status of the operated sciatic nerve.

5.3 Ex vivo macroscopic evaluations

5.4 Explant evaluation

After 6 weeks, the rats were euthanized by carbon dioxide asphyxiation and the implants were excised and preliminarily analyzed for their size/integrity. After dissection, the surgeon performed a blind evaluation of the macroscopic aspect of the neurolysis site. Quality of wound

healing, presence of inflammation signs and perineural adhesion were the parameters considered.

Specifically, adherences were classified as described by Petersen et al. [93]:

• Lv1: minimal adhesion that did not require dissection or that required minimal dissection;

• Lv 2: moderate adhesions that required vigorous dissection but without sharp tools;

• Lv 3: significant adhesions that required a dissection with sharp tools.

5.4.1 Histological and immunohistochemical analysis

Histological and immunohistochemical investigations referring to the central sections of nerve conduits were carried on same as described in paragraph 4.5. Briefly, histological (Toluidine Blue) and immunohistochemical characterization (CD3, F4/80, S100, β-tubulin) were performed.

5.4.2 Morphometric analysis

Axonal regeneration was assessed by examining the ultrastructural features of the explants. Briefly, explanted samples were fixed in 2.5% in glutaraldehyde in 0.1M PBS. Thereafter, each sample was divided in different portions to allow the evaluation of axonal regeneration at different levels; thus, central sections were considered. Sections, post-fixed in 1% osmium tetroxide (Agar Scientific Elektron Technology - UK) in 0.1M phosphate buffer, were dehydrated in a graded alcohol series and embedded in Epoxy resin. Semi-thin sections (0.5μm) were cut with an ultramicrotome RMC-PTX PowerTome (Boeckeler Instruments, Arizona-USA) and stained with 1% Toluidine Blue. Images were acquired by using Leica DMR microscope (Leica Microsystems Wetzlar- Germany). Morphometric investigation was carried on semithin Toluidine Blue stained section of central portions of each sample. Total cross section area, fascicular area of each portion was measured. Subsequentially five random quadrants in the fascicular area were identified. Then, searching for myelinated axon, 3 high power fields (100x) of equal area from each quadrant were investigated. Average axon density was determined dividing total axon number by the area sampled. All measurements were performed using ImageJ software.

5.4.3 Second harmonic generation microscopy (SHG) analysis

Neural collagen distribution was imagined 6 weeks after surgery by Second Harmonic Generation Microscopy (SGH). SGH label free microscopy was performed for a qualitative comparison with data from histology, immunohistochemistry. Specimens were processed as previously described for histology and immunohistochemistry.

6. Statistical analysis

For animal weight monitoring statistical analyses were performed using 2way ANOVA and Tukey's multiple comparison test. The results were expressed as mean± standard deviation. P values < 0.05 were considered as statistically significant. For morphometrical analysis statistical analyses were performed using Kruskall-Wallis and Dunn's multiple comparison test. The results were expressed as mean± standard deviation. P values < 0.05 were considered as statistically significant. Statistical calculations were made using Prism 9 software (GraphPad Software, San Diego, CA).

RESULTS

7 In vitro characterization study

7.1 Gross appearance and ultrastructural morphology of OxPVA-derived scaffolds

The OxPVA-based conduits (OxPVA_KMnO4 e OxPVA_Br2) were obtained with the injection molding-technique and cross-linked by FT. After manufacture, gross appearance and ultrastructural morphology were considered and compared to that of native PVA (Fig. 14). An augmented transparency of the material was detectable after oxidation, OxPVA_$KMnO_4$ conduits appeared more transparent than OxPVA_Br_2 guides. The lumen was clearly recognizable in all conduits. No tendency to collapse was found.

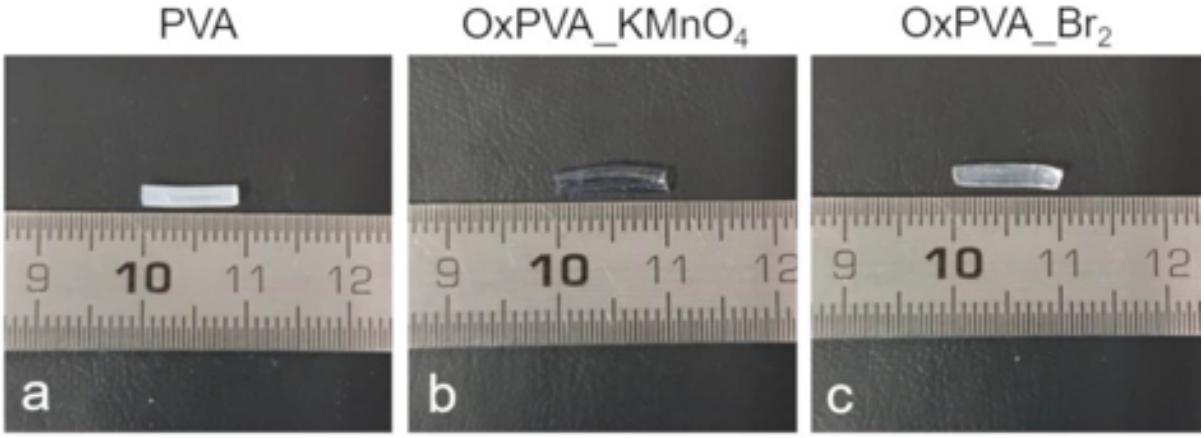

Figure 14 Tubular scaffold morphology. Gross appearance of cross-linked PVA (a), OxPVA_KMnO4 (b) and OxPVA_Br2 (c) nerve guide conduits prepared according to the injection-molding technique.

As for ultrastructural characterization (Fig.16), native PVA conduits exhibited a smoother surface compared to that of OxPVA-based samples, with an increased rugosity detectable in OxPVA_Br_2 nerve guides. Transverse cross-section of tubular scaffolds demonstrated a certain regularity of the conduit's walls.

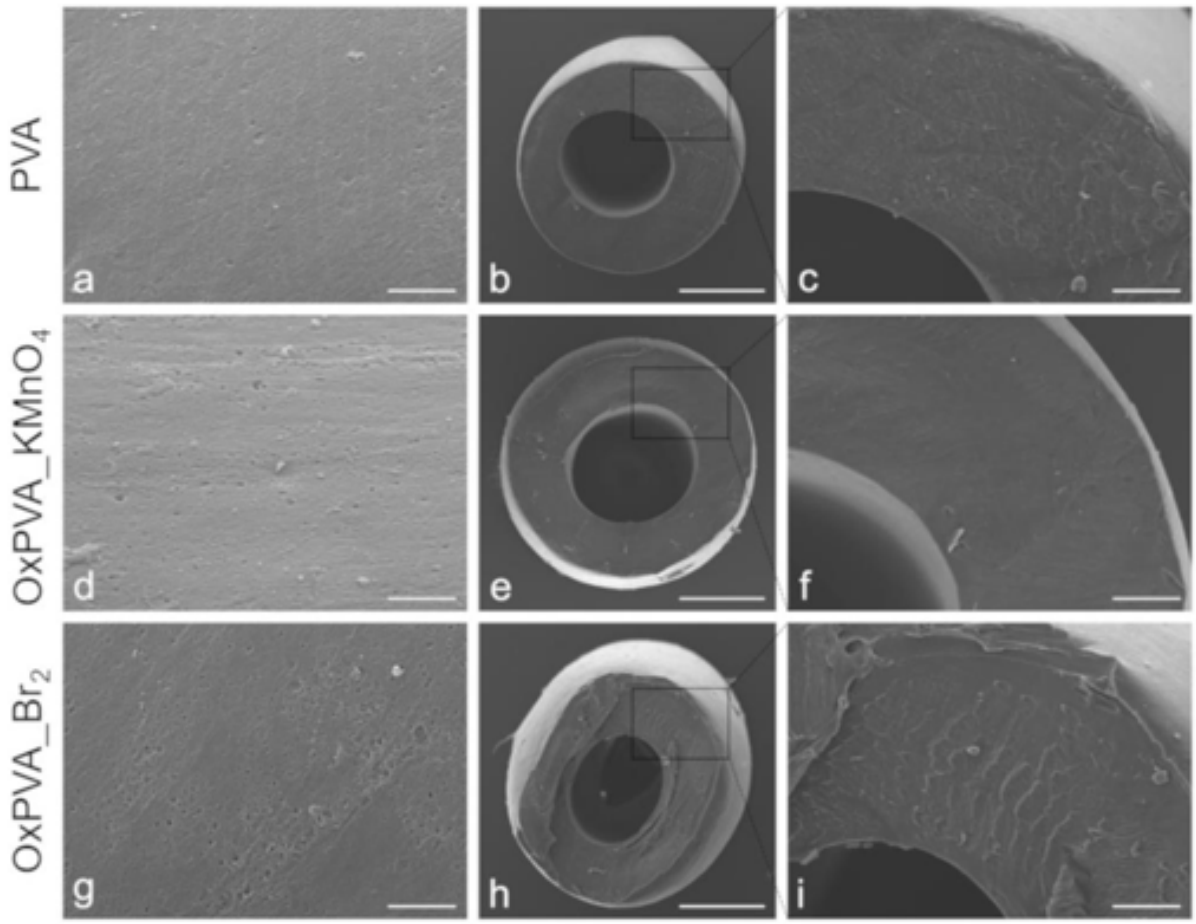

Figure 15 Ultrastructural analysis. SEM micrographs of crosslinked PVA-based nerve guidance conduits. (a,d,g) Side view and (b,c,e,f,h,i) transversal cross-sections of tubular scaffolds. Scale bars: (a,d,g) 10 μm; (b,e,h) 500 μm; (c,f,i) 100 μm.

7.2 Swelling index and porosity

The impact of $KMnO_4$ and Br_2 mediated oxidation on polymer swelling properties was assessed through the comparison with neat PVA. Maximum water retention capability for OxPVA_Br_2 was 60.5% ± 2.5% of the dried weight, at 96 h incubation; 71,3% ± 3,6% for OxPVA_$KMnO_4$, at 48 h; 19,5% ± 4,0% for neat PVA, at 96 h (Fig.19).

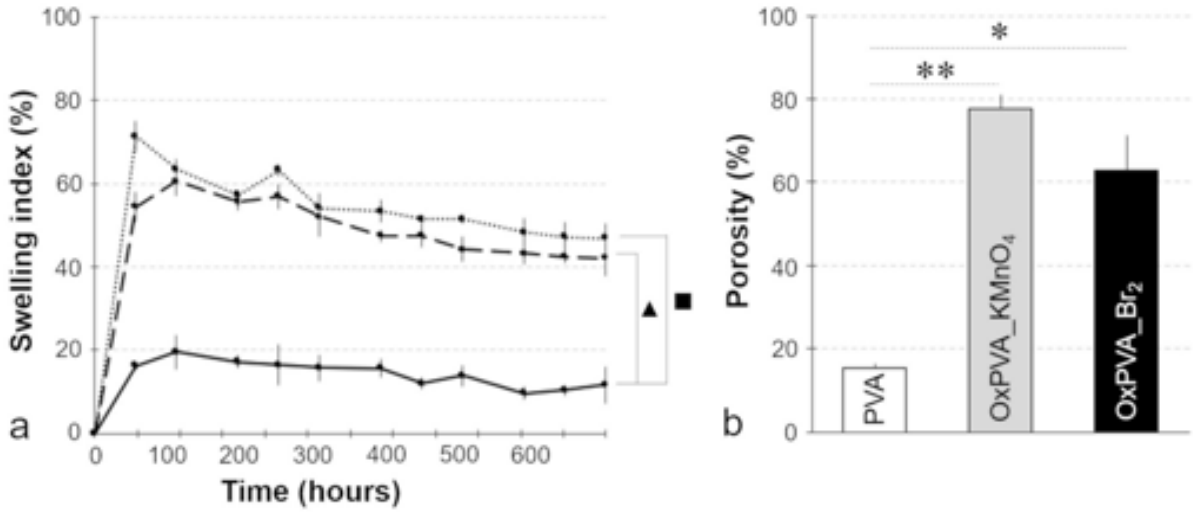

Figure 16 Swelling behavior and porosity of PVA-based hydrogels. Effect of chemical oxidation on PVA swelling kinetics (a) and porosity (b). The experiments were repeated on three samples of each hydrogel at all time points. Response is the average swelling/porosity of replicates ± standard deviation. (_: $p < 0.05$, OxPVA_KMnO4 vs. PVA; N: $p < 0.05$, OxPVA_Br2 vs. PVA; **: $p < 0.01$, OxPVA_KMnO4 vs. PVA; *: $p < 0.05$, OxPVA_Br2 vs. PVA.

Porosity of neat and OxPVA was also measured and compared: PVA porosity (15.27% ± 1.16%) increased after oxidation treatment 77.50% ± 3.39% (OxPVA_$KMnO_4$) and 62.71% ±8.63 (OxPVA_Br_2).

7.3 Mechanical and suture tests

The conduits were easy to handle and exhibited adequate consistency to be sutured. They also showed to be mechanically strong, with excellent properties of elasticity/flexibility. Neuro guides did not collapse with the needle passage, held sutures well during microsurgical anastomosis and could be stretched without ruptures of the conduit wall.

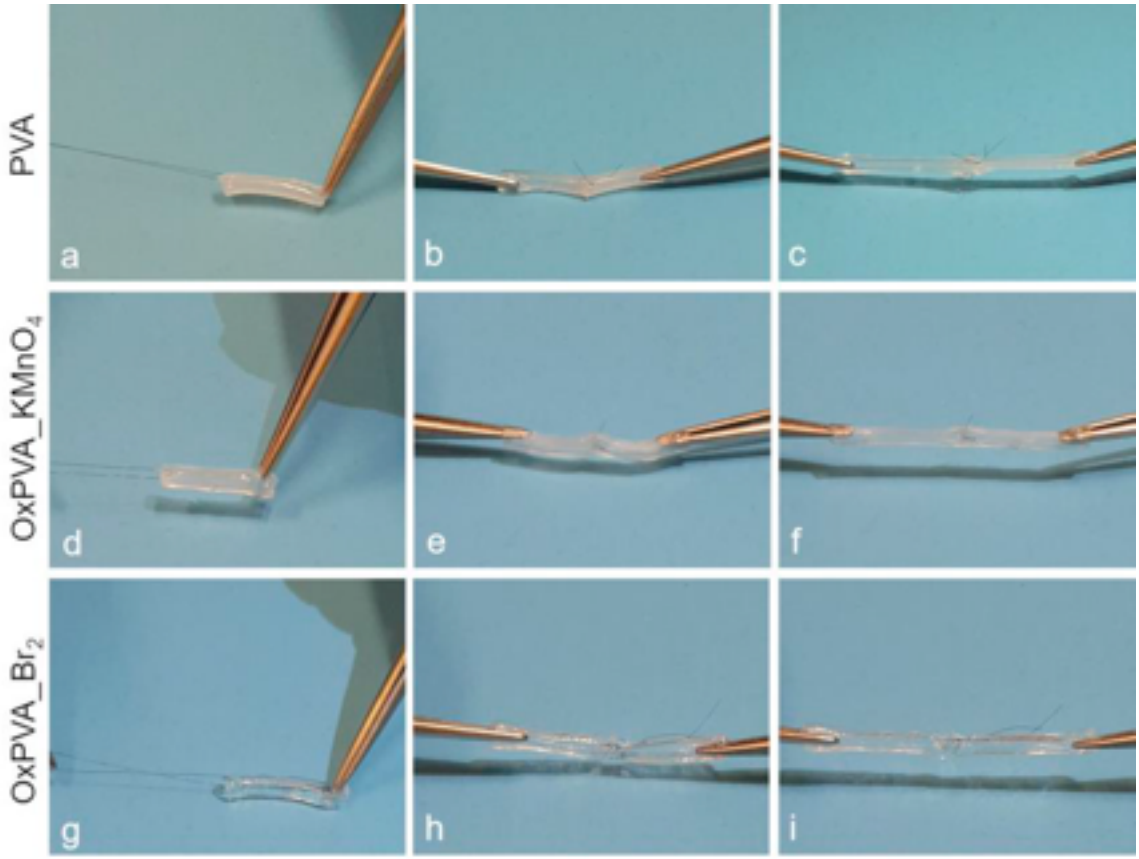

Figure 15 Suture test. Neat and OxPVA tubular scaffolds were tested for suture holding ability by passing the needle perpendicular to the surface of the conduit wall and exerting some tensile force (a,d,g). Furthermore, a microsurgical anastomosis between two conduits was performed (b,e,h) and the material capacity to hold the suture knots was assessed by stretching the sutured conduits (c,f,i).

7.4 Cell cultures, extract test and viability assessment

As for MTT assay results, considering adherent cells treatment with scaffolds-conditioned solutions, a significant preservation of cell viability and proliferation was observed in treated samples compared to the cytotoxic control, 50% DMSO. Setting to 100% the viability of untreated cells, the relative cell viability was 95.2% ±7.7% (PVA), 96.6% ± 4.1% (OxPVA_KMnO4), 95.3 ±6.6 (OxPVA_Br2) and 5.0% ±0.5% (DMSO) for SH-SY5Y cells. In parallel, the relative cell viability of Schwann cell cultures was 97.2 ±3.2% (PVA), 94.2% ±5.4% (OxPVA_KMnO4), 94.5% ±6.2% (OxPVA_Br2) and 10,8% ±0,7% (DMSO) (Fig.18)

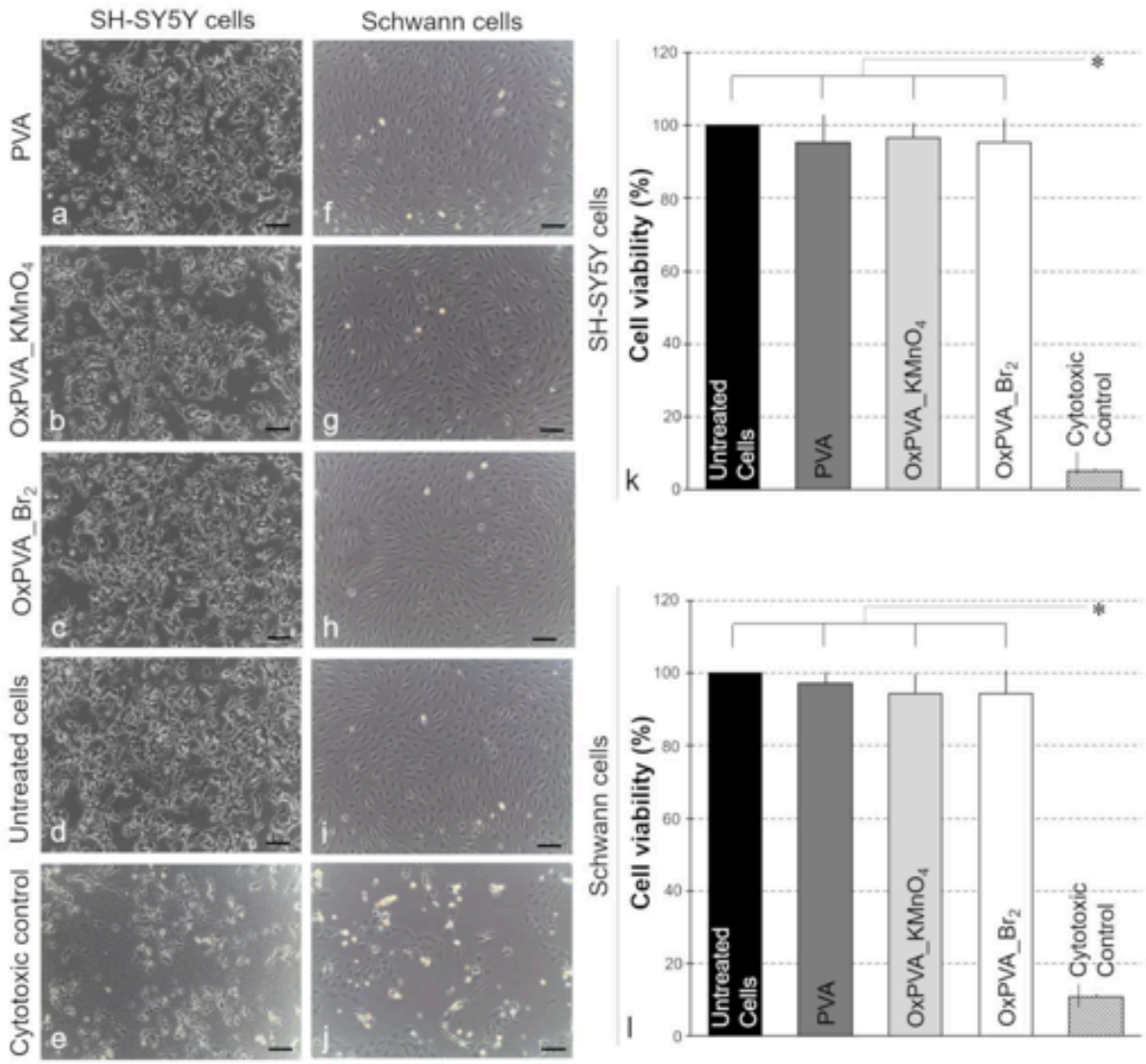

Figure 16 Cytotoxicity test. (a–j) Morphological analysis by optical microscopy of SH-SY5Y (a–e) and Schwann cell (f–j) cultures after treatment with native and OxPVA-conditioned media. (k,l) Cell viability of SH-SY5Y (k) and Schwann cell (l) cultures after treatment with native and OxPVA-conditioned media. Data are the average of three different experiments±standard deviation and results are presented as percentage of living cells compared to the untreated control (*:$p<0.01$).Scale bars: 100μm.

No statistical difference was observed in the cell viability of SH-SY5Y and Schwann cell populations cultured with neat and OxPVA-conditioned media and the blank culture medium.

7.5 In vitro biodegradation assay

The oxidation introduced an important property for polymeric scaffolds intended for PNI applications: biodegradability; this parameter was assessed by enzymatic degradation (up to 14 days); all oxidized nerve conduits showed increasing weight loss over time, suggesting sample

progressive degradation (Fig.19). Higher weight loss rates were registered for OxPVA_$KMnO_4$ (from 14.8% at day 1 to 34.4% at day 14) and OxPVA_Br_2 (from 21.2% to 41.25%) in comparison with PVA-based scaffolds (from 14.6% to 28.9%).

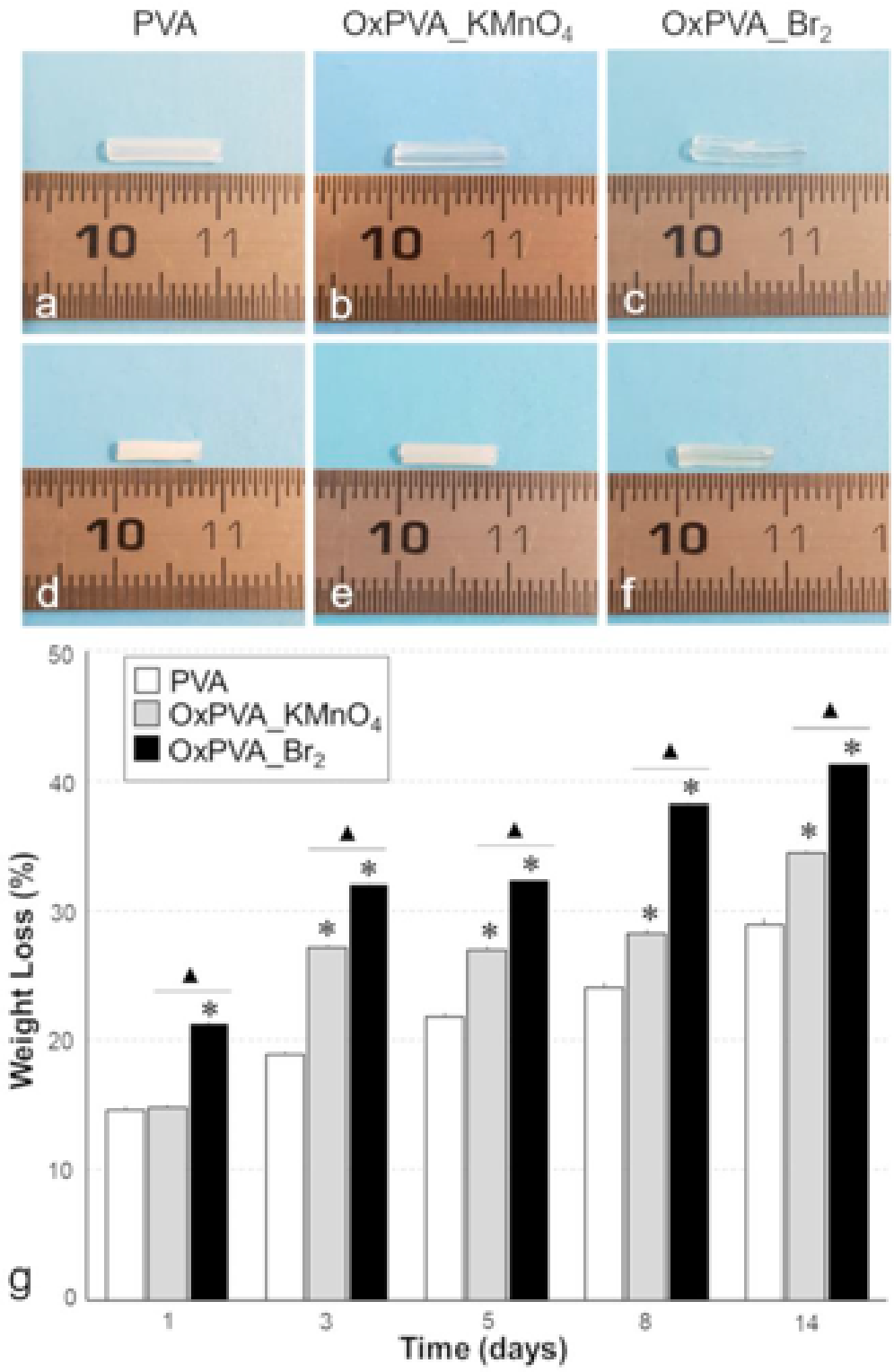

Figure 17 Enzymatic degradation. (a–f) Gross appearance of neat and OxPVA nerve conduits soon after manufacture (a,b,c) and after 14 days of incubation in human plasma + collagenase B solution (d,e,f). (g) Sample weight loss measured at 1, 3, 5, 8 and 14 d

7.6 Nerve conduits functionalization by CNTF covalent binding

Functionalization of PVA and OxPVA with CNTF was performed using the mild reducing agent sodium cyanoborohydride allowing for covalent binding of the molecule to the polymeric surface.

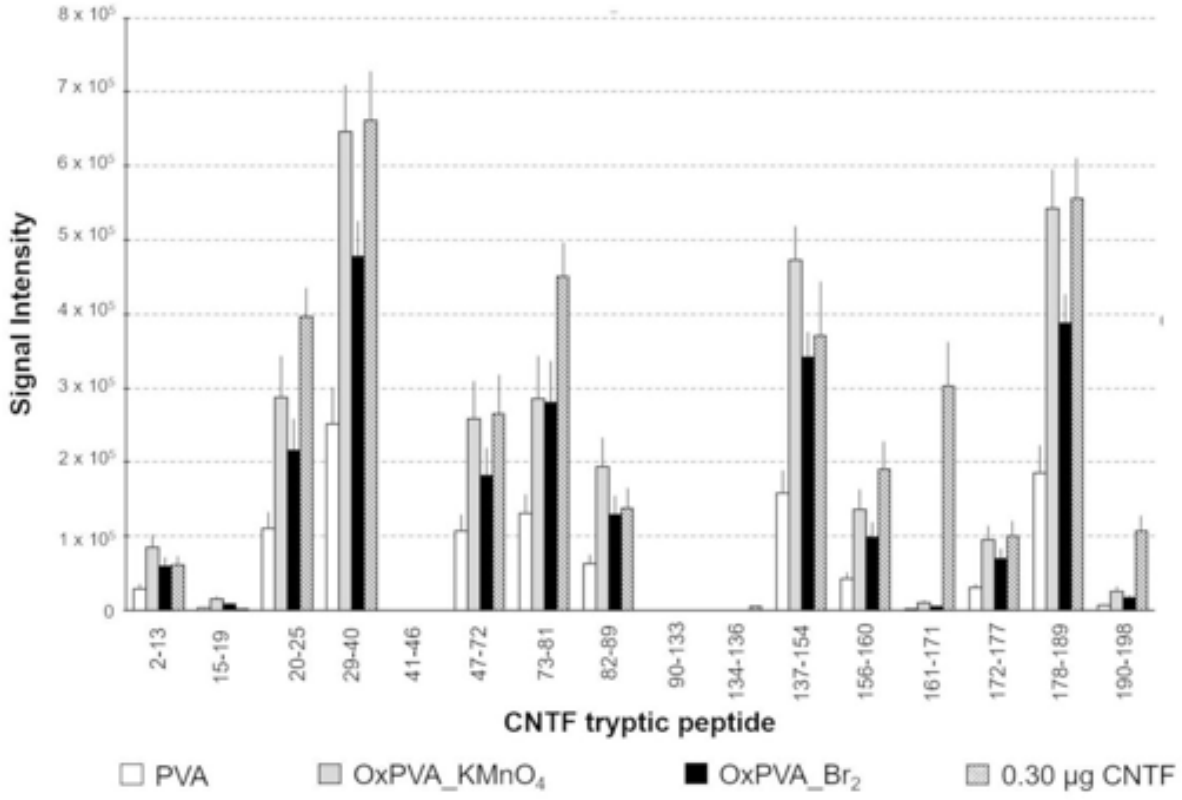

Figure 18 Neuroguide functionalization. Ultra-high-performance liquid chromatography-mass spectrometry (UHPLC-MS) analysis of tryptic peptides derived from digestion of the ciliary neurotrophic factor (CNTF) bound in the luminal side of tubular scaffolds. The y-axis reports the peak area referred to the ion extracted by total ionic profile.

After factor binding, the tubes were flushed with PBS and then filled with trypsin solution allowing the proteolysis of the small quantity of protein (Fig. 20). Estimated amount of CNTF bound in the luminal surface of PVA was 0.11± 0.021 µg and for the OxPVA was 0.29± 0.033 µg (OxPVA_$KMnO_4$) and 0.22 ±0.029 µg (OxPVA_Br_2). UHPLC-MS analysis of tryptic peptides showed implemented loading ability of OxPVA in comparison with neat PVA.

7.7 Validation of OxPVA scaffolds bioactivation through EAK mechanical incorporation

Once incorporated within the hydrogel the EAK-Rh conferred a typical pink colour to the polymer, maintained even after F-T. Efficacy of the mechanical incorporation was preliminarily desumed once the conduit was separated from the mold; in fact, the colour appeared homogeneously distributed. Subsequently, these gross-appearance features were confirmed by confocal microscopy. The analysis showed a uniform fluorescent red-colour signal once the EAK-Rh was excited. In contrast, OxPVA conduits did not emit signal in the same experimental conditions, as expected (Fig. 21).

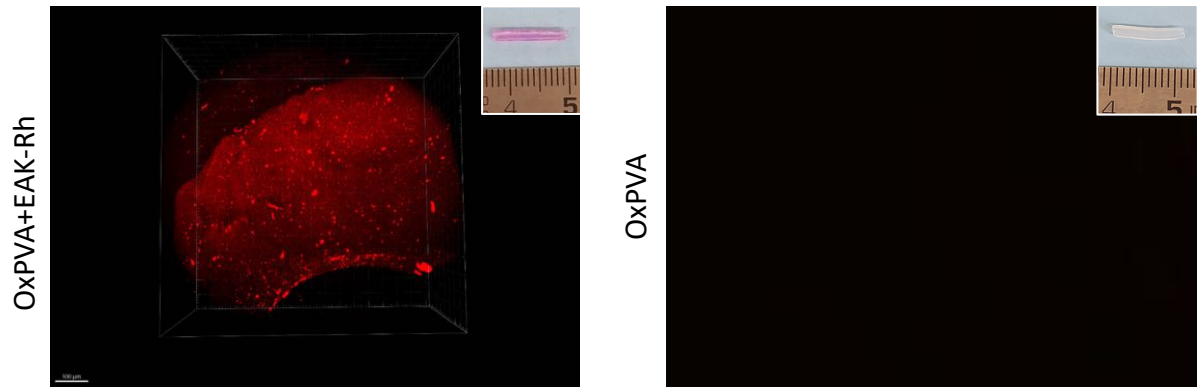

Figure 21 Assessment of efficacy in SAPs mechanical incorporation. The rhodamine labelled peptide (EAK-Rh) emits a fluorescent signal (orange) collected between 580 and 620 nm when laser-excitated at 561 nm wavelength. No signal was detected in the peptide-free scaffold (PF-OxPVA) (a) compared to EAK-Rh OxPVA (b). Scale bar: 30μm.

7.8 Preclinical study results: PNI without substance loss

7.8.1 Surgery

Surgical procedure is showed in Fig. 22. Animals were randomly implanted with NeuraWrap™, OxPVA_$KMnO_4$ and LFPm functioning like nerve protectors.

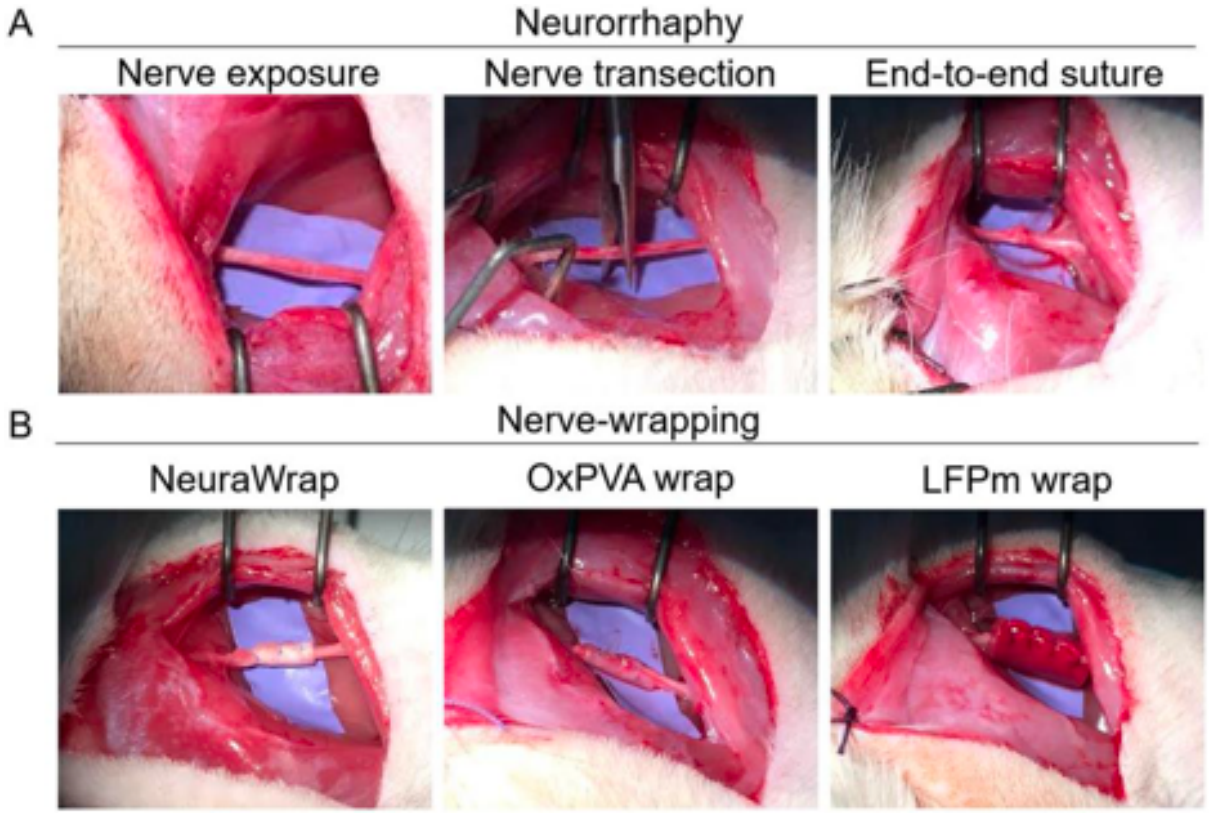

Figure 22 Animal model of peripheral nerve injury and wraps implantation. Neurorrhaphy (A) and nerve protectors implantation (B); in particular, NeuraWrap™ and wraps based on OxPVA and LFPm were used.

Similar to the commercial control both OxPVA_$KMnO_4$ and LFP-based wraps showed good handling properties during surgery. Hence, materials were suturable and did not give rise to tears. Surgery was well tolerated by rats of each group.

7.8.2 Functional tests

All animals showed adequate recovery after end-to-end neurorrhaphy and wraps implantation. After 2 and 12 weeks from surgery, Sciatic Function Index was acquired. SFI data showed a recovery in nerve function for all animals. At 2 weeks, the recorded values were 3.15 ± 0.52, 82.45 ± 1.55, 81.18 ± 2.25, 81.55 ± 2.15 for the non-operated foot, NeuraWrap™ group, OxPVA_$KMnO_4$-wrap group and LFPm-wrap group, respectively. While, at 12 weeks, the recorded values were 2.25 ± 0.15, 52.14 ± 1.18, 46.5 ± 2.55, 49.46 ± 3.24 for the non-operated foot, NeuraWrap ^{TM}group, OxPVA_$KMnO_4$-wrap group and LFPm-wrap group, respectively. No significant differences were present between NeuraWrap^{TM} group, OxPVA_KMnO4-wrap group and LFPm-wrap group at both endpoints.

7.8.3 Macroscopic evaluation of explants

Soon after euthanasia and before sample excision, the surgery site was observed to preliminary assess implants adequacy.

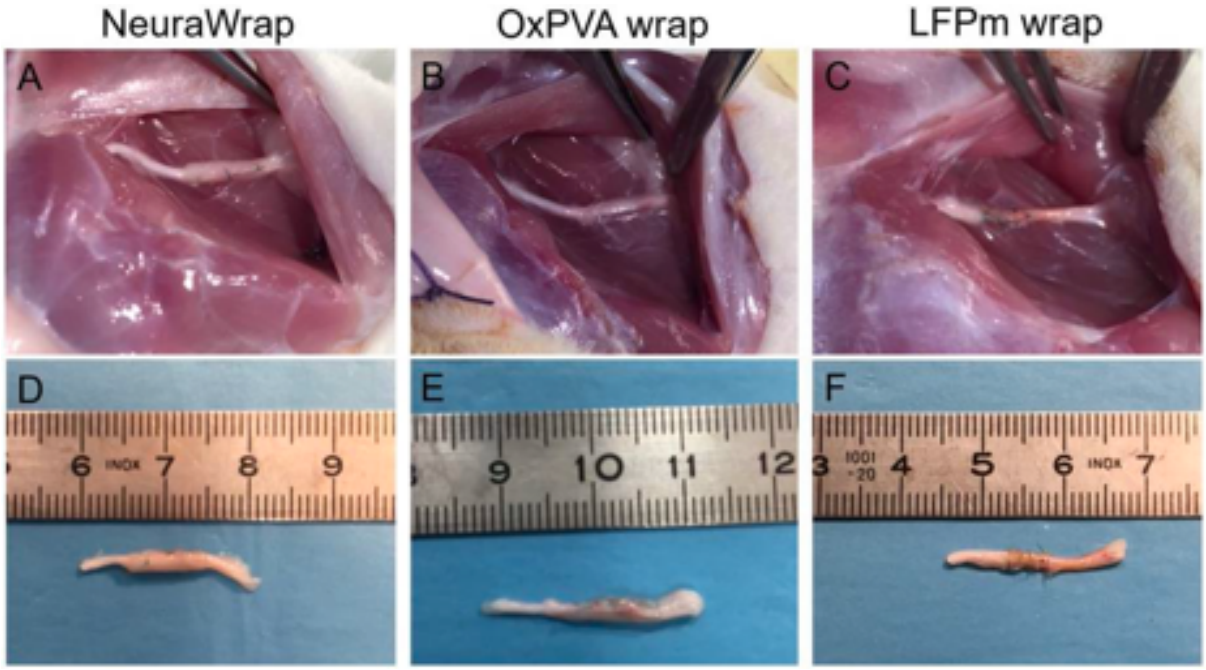

Figure 23 Gross appearance of surgical Gross appearance of surgical field and operated nerves explants at 12 weeks from surgery. In situ implant (A–C) and appearance after excision (D–F), of wraps based on NeuraWrap™ (A, D), OxPVA (B,E) and LFPm (C,F). After 12 weeks, no inflammation, scar tissue or neuromas were observed. Wrap residues were identified only for NeuraWrap™ and OxPVA while LFPm was resorbed.

No subcutaneous or facial edema were identified. Moreover, no signs of severe inflammation or scar tissue or neuromas were visible. Similarly to NeuraWrap™, sciatic nerves implanted with OxPVA_$KMnO_4$ showed the presence of wraps residues. Conversely, LFPm wraps were completely resorbed (Fig. 23).

7.8.4 Histological and immunohistochemical results

For each experimental group, the Hematoxylin and Eosin staining allowed to discriminate the morphology of the area of interest, also confirming previous evaluations according to gross appearance. NeuraWrap™ and OxPVA_$KMnO_4$ wraps were both recognizable after 12 weeks from surgery. In transversal section, NeuraWrap™ appeared like a thick layer with fibrillar organization due to collagenous nature; adipose tissue was in the area between the nerve protector and the epineurium. OxPVA_$KMnO_4$ presented itself as a transparent, dense layer surrounding the repaired nerve; structurally, the nerve showed the presence of a regular and

homogeneous epineurium and regular fascicles organization. A thin fibrous capsule accountable to adherences was recognized around the OxPVA_$KMnO_4$ wraps. Accounting for LFPm wraps, the nerve protector was completely resorbed, and a thick and poorly organized epineurium was observed around the sectioned sciatic nerve. Differently from NeuraWrap™ group, adipose tissue was recognized in the space between the epineurium and the fascicles, which showed artefactual ruptures in the mid area.

According to H&E staining, no significant inflammatory infiltrate was visible in all experimental groups, also confirmed by anti-CD3 and anti-F4/80 immunohistochemical specific staining. Thus, only few CD3 positive and F4/80 positive cells were detected in all sample groups, suggesting the absence of infiltrating lymphocytes and macrophages. In addition, the repaired tissues were positive to β-tubulin and S100 stains, specifics for axons and Schwann cells, respectively, proving the nervous nature of tissues (Fig. 24).

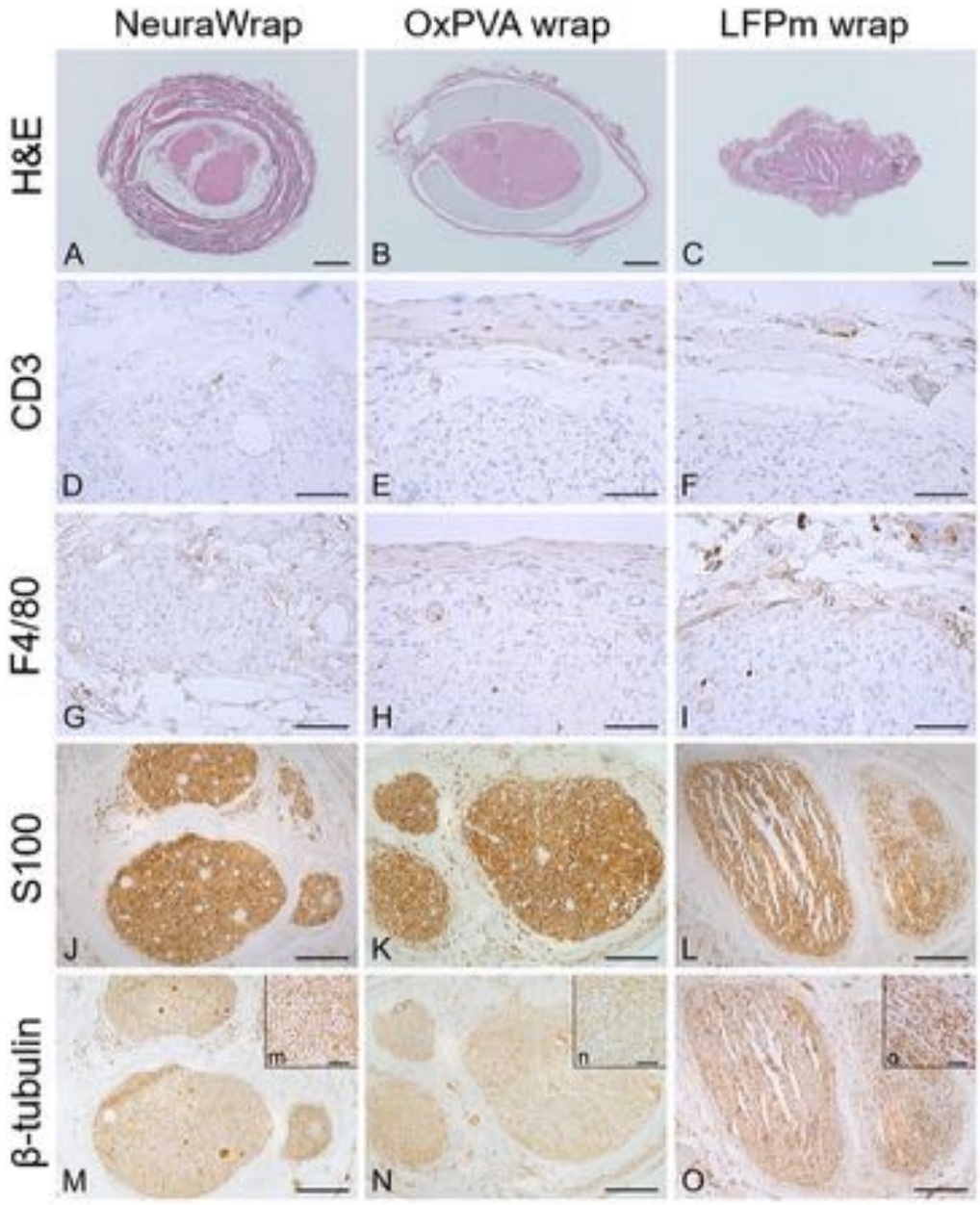

Figure 24 Histological and immunohistochemical analysis. Hematoxylin and eosin staining (H&E), anti-CD3, anti-F4/80, anti-S100 and anti-β-tubulin reactions performed on the coaptation site of Sprague-Dawley sciatic nerves implanted with NeuraWrap™, OxPVA wraps and LFPm wraps. Analysis occurred at 12 weeks from surgery (Scale bars: (A–C), 400 μm; (D–I), 50 μm; (J–O), 200 μm; scale bar in upper right insert (m–o) = 40 μm).

7.8.5 Morphometric and ultrastructure findings

Morphometric analysis was carried on semithin Toluidine Blue stained section of proximal and distal portions of each sample (Fig.25). Total cross-sections and fascicular areas, axons density and number of axons/fasci data were acquired.

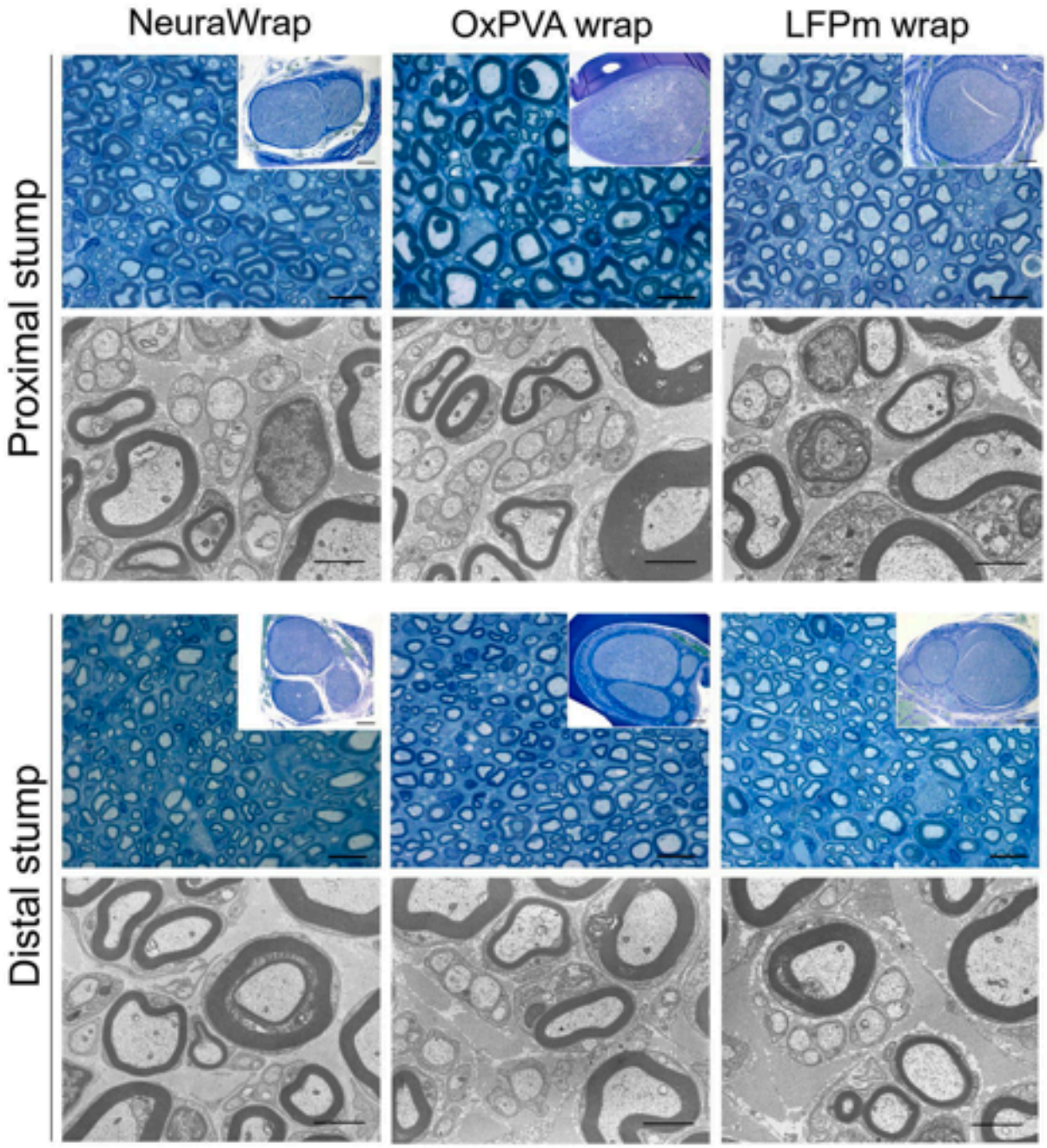

Figure 25 Characterization of Sprague-Dawley sciatic nerve explants at 12 weeks after surgery. Cross-sections of the proximal and distal portions of explants evaluated with Toluidine Blue staining (scale bars: 10 μm; scale bars in upper right insert: 200 μm) and Transmission Electron Microscopy (TEM) (scale bars: 2 μm).

Transmission Electron Microscopy (TEM) was used to qualitatively explore the ultrastructure of the explanted tissues at proximal and distal level. In all specimens, both myelinic and unmyelinic axons were recognized (Fig.25).

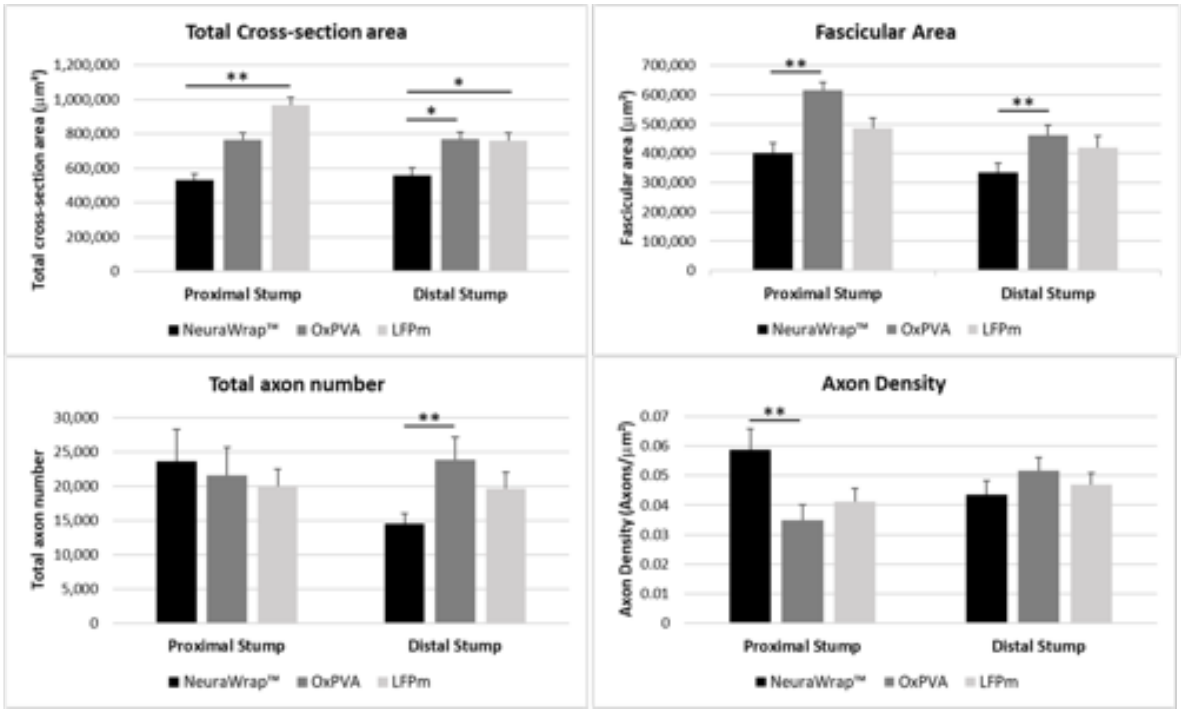

Figure 26 Morphometric assessment of repaired sciatic nerves at 12-weeks after surgery. Histograms show mean total cross-section nerve area (µm2), fascicular area (µm2), axon density (axons/ µm2) and total axons number of the proximal and distal portions of sciatic nerves implanted with NeuraWrap™ (control group) and wraps based on OxPVA and LFPm. Statistical analyses were performed by the Kruskal-Wallis test and Dunn's multiple comparison test. Results are expressed as mean values ± SD (*$p < 0.05$; **$p < 0.01$).

Morphometric data of the repaired sciatic nerves are presented in Fig. 26 being expressed as mean value ± SD. The measurements of the total cross-section areas at the proximal stump showed significant difference between the LFPm-wrap group (967,318 ± 44,334 µm^2) and NeuraWrap™ (533,176 ± 34,139 µm^2; $p < 0.01$) but not compared to OxPVA_$KMnO_4$ (764,625 ± 42,364 µm^2); while at distal level, both experimental groups had significantly higher ($p < 0.05$) values of mean total cross-section area (OxPVA_$KMnO_4$ wrap, 768,058 ± 41,555 µm^2; and LFPm wrap, 762,634 ± 44,627 µm^2) versus the commercial product NeuraWrap™ (558,021 ± 46,056 µm^2). Considering fascicular area (i.e. only fasci, without the connective tissue sheath around), OxPVA_$KMnO_4$ guaranteed significantly higher ($p < 0.01$) mean values compared to NeuraWrap™ at both proximal stump (615,080 ± 26,736 µm^2 versus 400,061 ± 35,526 µm^2) and distal level (461,577 ± 36,035 µm^2 versus 334,427 ± 33,006 µm^2); conversely, no significant differences were recorded for LFPm wraps at the two levels (proximal stump, 484,806 ± 34,325 µm^2; distal stump, 418,437 ± 41,483 µm^2). Total axons density was significantly higher ($p < 0.01$) for NeuraWrap™ (0.059 ± 0.007/ µm^2) versus OxPVA_KMnO4 wraps (0.035 ± 0.005/µm^2) but not versus LFPm wraps (0.041 ± 0.004/µm^2) at proximal level; while, considering the distal portion, no differences among the groups aroused (NeuraWrap™, 0.044 ± 0.005; OxPVA_$KMnO_4$ wrap, 0.052 ± 0.004; LFPm wrap, 0.047 ± 0.004). Total

number of axons was also determined, and a significant difference was encountered only between OxPVA_$KMnO_4$ wraps (23,855 ± 3,314) and NeuraWrap™ (14,513 ± 1,416) at distal level ($p < 0.01$); conversely, no significant difference was observed with LFPm group (19,594 ± 2,386). At the proximal stump, there were 23,608 ± 4,628; 21,517 ± 4,106; 19,958 ± 2,487 mean total axons for NeuraWrap™ and the experimental groups OxPVA_$KMnO_4$ and LFPm, respectively; statistical analysis of the data revealed no significant difference between the groups.

7.8.6 Second Harmonic Generation analysis

Second Harmonic Generation Microscopy investigation was performed at proximal stump, coaptation site and distal stump to detect structural and inflammatory response after neurorrhaphy and wraps implantation (Fig. 27). Taking into account the proximal stump, a thin collagenous epineural tissue was confirmed in all the samples; for NeuraWrap™ and OxPVA_$KMnO_4$ wraps, collagen was also maintained among the fasci. Considering the coaptation site, a thicker epineural tissue was observed for both NeuraWrap™ and OxPVA_$KMnO_4$ wraps; regarding LFPm wrap epineural tissue appeared less organized and compact than other specimens. However, all distal stumps showed a well-recognizable epineural tissue which had more filamentous appearance in OxPVA_$KMnO_4$ and LFPm wraps than in NeuraWrap™. SHG microscopy images correlated with morphological characterization data [12,94]. All specimens showed a scenario compatible with that of PNI experiencing morpho-functional recovery with more collagen at epineural layer and traces of connective tissue inside the fascicular area.

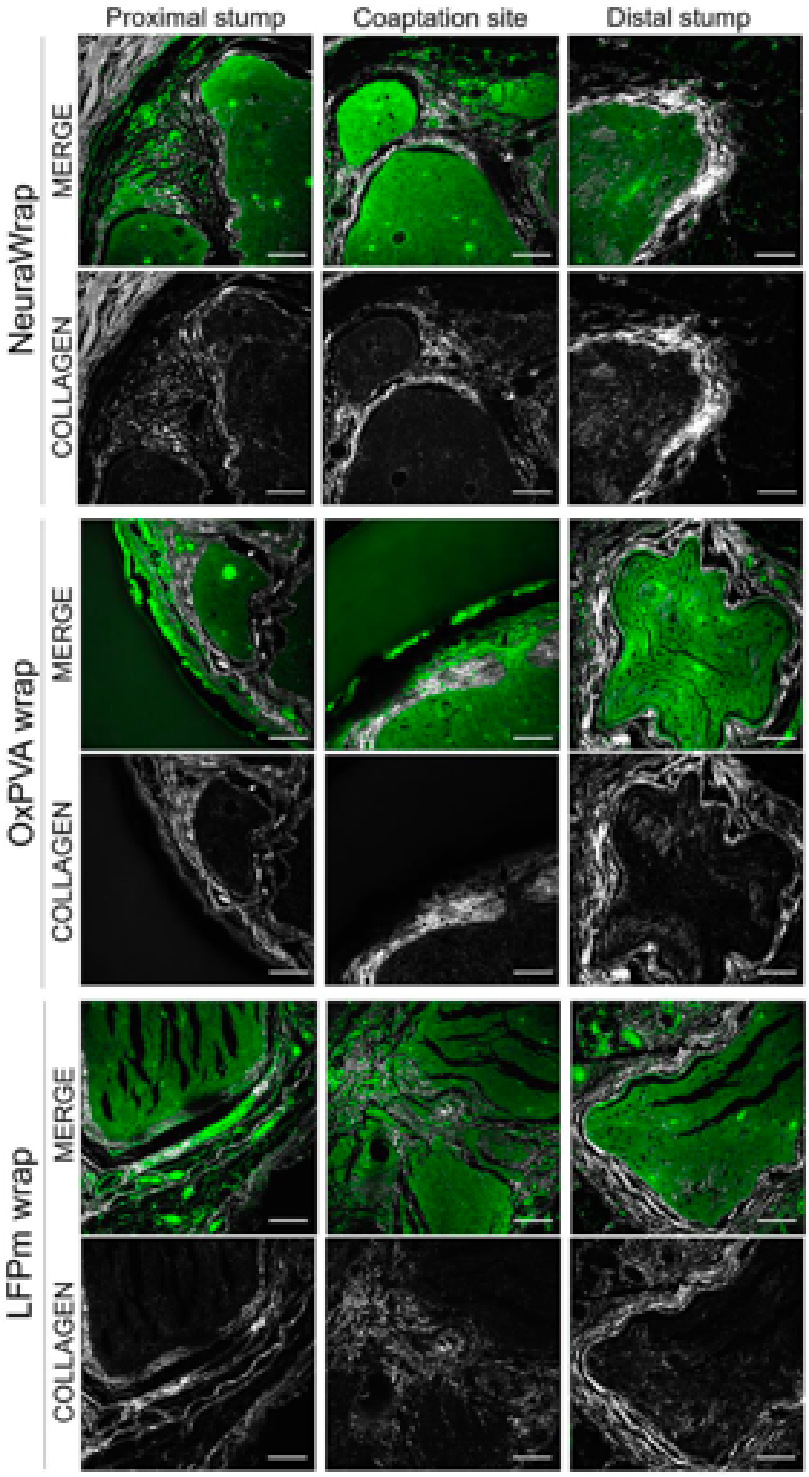

Figure 27 Second Harmonic Generation Microscopy of repaired sciatic nerves at 12 weeks after surgery. Cross-sections of the proximal portion, coaptation site and distal portion of NeuraWrap™, OxPVA wraps and LFPm wraps explants, qualitatively evaluated by Second Harmonic Generation (SHG) microscopy (scale bars: 100 μm).

7.9 Preclinical study results: PNI with substance loss

7.19.1 Surgery

Surgical procedure is showed in Figure 28. Animals were randomly implanted with RA, Reaxon®, OxPVA, OxPVA+EAK, OxPVA+EAK-YIGSR, OxPVA+NGF nerve conduits. While OxPVA, OxPVA+EAK, OxPVA+EAK-YIGSR, OxPVA+NGF groups showed good handling properties during surgery, Reaxon® nerve conduits proved to be more rigid than OxPVA ones.

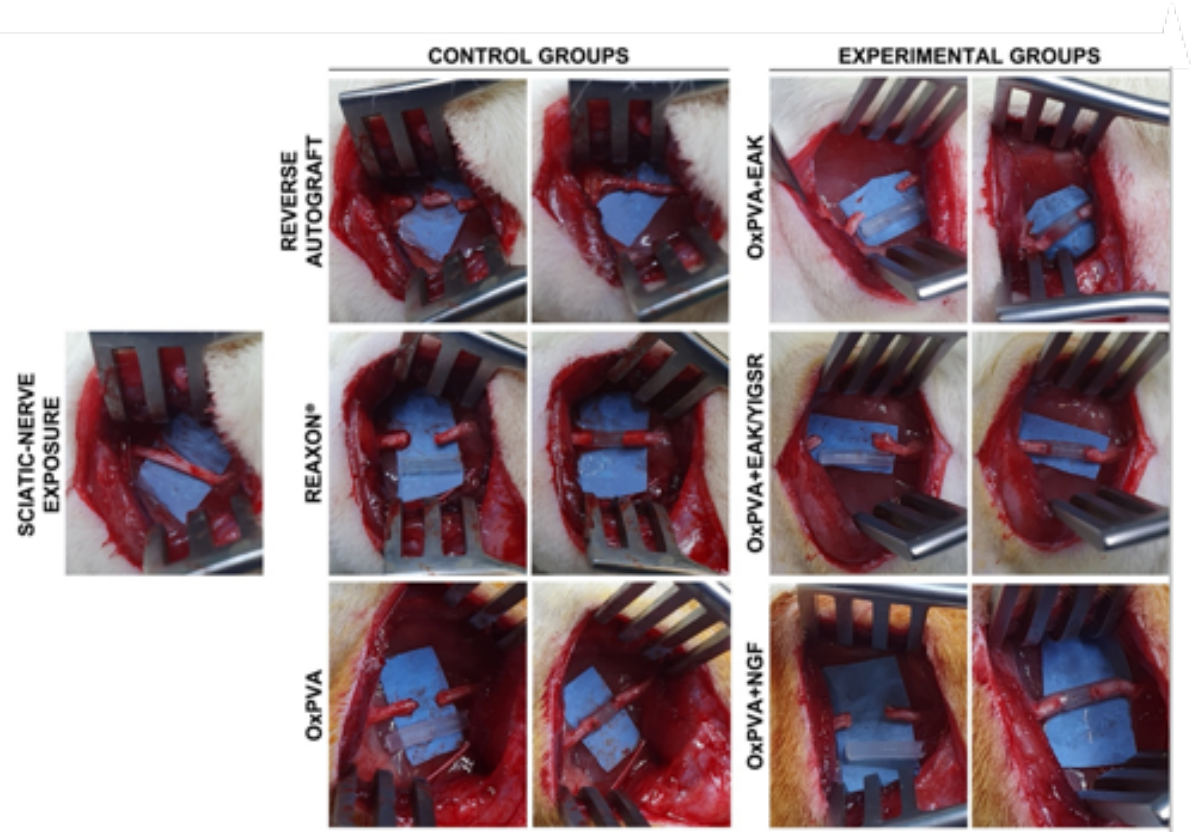

Figure 28 Animal model of peripheral nerve injury and nerve conduit implantation. In particular, nerve conduit insertion between the two nerve stomp ends.

Hence, OxPVA hydrogel-based nerve conduits were softer and easier to suture compared to the commercial product. Stiffness and absence of noticeable elasticity of the commercial could be ascribed to the chitin origin of the material. However, none of materials used give rise to tears. Surgery was well tolerated by rats of each group. All animals showed adequate recovery after nerve conduit application, also showed by weight analysis.

7.9.2 Animal wellbeing assessment and functional tests results

7.9.2.1 Animal weight monitoring

Animal weight was effectively tracked at week 1, 3 and 6 after surgery. No significant weight loss was detected within each experimental group neither comparing groups, thus suggesting that the animal well tolerated the surgical procedure (Fig. 29).

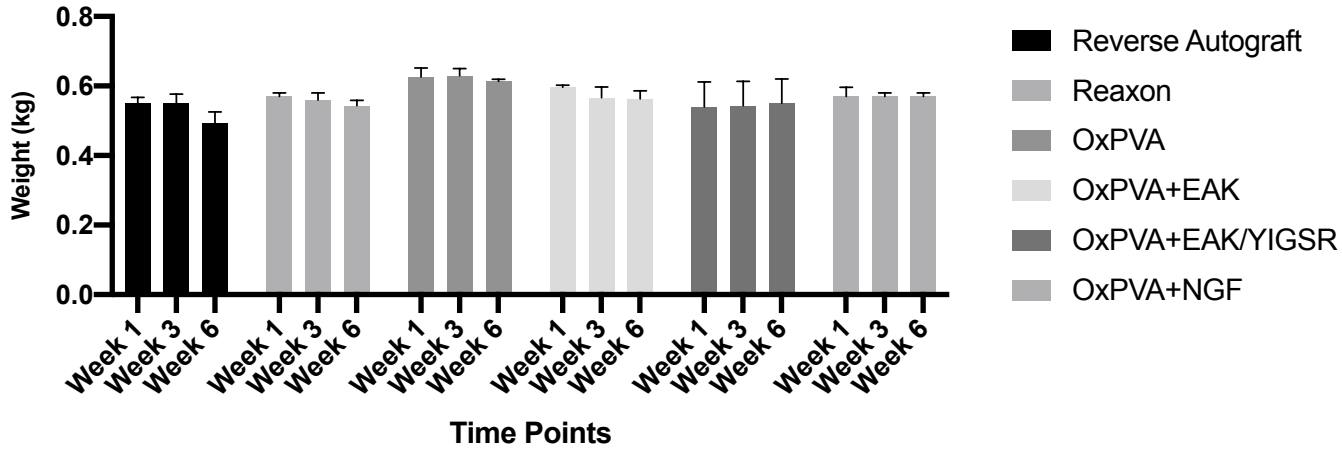

Figure 29 Animal weight chart after nerve conduit application in rat model of sciatic nerve transection.

7.9.2.2 Autotomy index

Autotomy index was also tracked at the 1st, 3rd and 6th week after surgery. Tendency to autotomy appeared to be more consistent after 3rd week from surgery. However, OxPVA was able to guarantee for less automutilation than other groups (Fig 30.), with an outcome comparable to that of RA. Despite the debate on the significance of autotomy (pain or loss in sensitivity), our evidence, considering a broad spectrum of wellbeing/functional tests, suggest that this event (common in case of PNI) is related to a reduced sensitivity. This assumption is also corroborated by the fact that the endpoint considered here is of 6 weeks only.

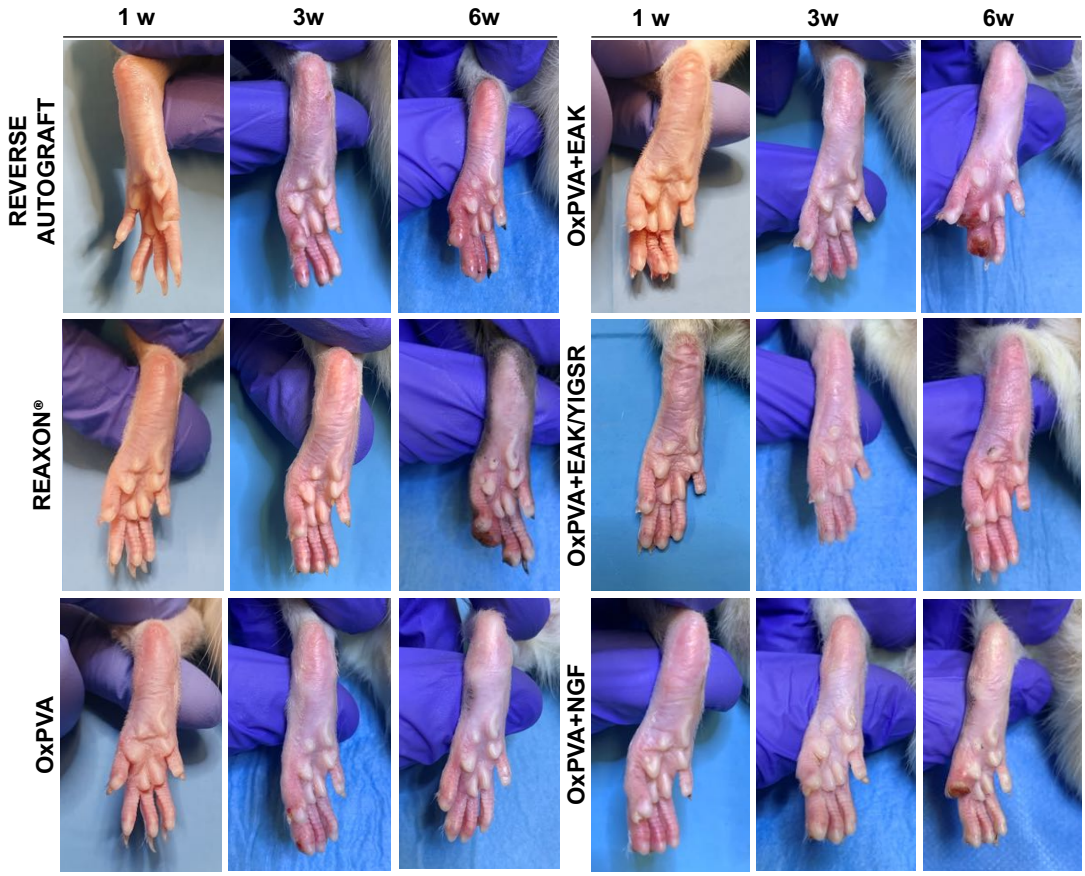

AUTOTOMY INDEX			
	1 WEEK	3 WEEKS	6 WEEKS
Reverse Autograft	0,00 ± 0,00	2,33 ± 4,04	3,00 ± 3,46
Reaxon®	2,33 ± 4,04	3,33 ± 3,51	4,67 ± 2,52
OxPVA	0,00 ± 0,00	0,33 ± 0,58	0,33 ± 0,58
OxPVA+EAK	0,00 ± 0,00	2,00 ± 3,46	6,00 ± 1,73
OxPVA+EAK/YIGSR	2,33 ± 4,04	2,33 ± 4,04	4,67 ± 4,04
OxPVA+NGF	0,00 ± 0,00	0,33 ± 0,58	5,67 ± 2,31

Figure 30 Animal operated paws after 1,3 and 6 weeks after surgery of all experimental groups (upper panel). Autotomy index charted in accordance with Wall et al. protocols (lower panel).

7.9.2.3 Von Frey test

At 3 and 6 weeks after surgery, animals were subjected to Von Frey Hair Test to evaluate the sensitivity threshold of the animal through the stimulation of the plant of operated paw. Given the highly operator-dependent procedure and the presence of false negative reaction due to repeated stimulus on the operated limbs, data were not considered reliable.

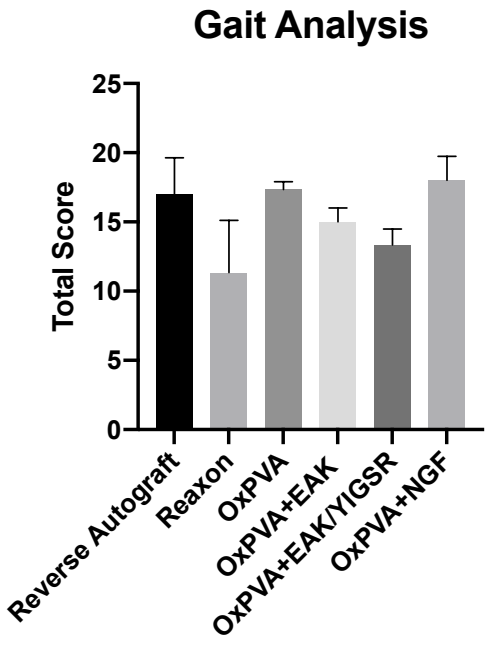

Figure 31 Gait analysis outcomes at 6 weeks after surgery in accordance with IJkema-Paassen et.al [92]

Gait analysis at 6 weeks after nerve conduit application allowed for qualitative analysis of walking of animals (Fig 31-32). No statistical difference was found between the groups. However, OxPVA+NGF group showed higher total marks followed by OxPVA group. OxPVA-based nerve conduits granted better results compared to the commercial product and analogous results compared with RA.

Groups		A	B	C	D	E	F	G	H	I	J
Reverse Autograft	Rat 1	2	2	2	2	2	2	2	2	2	2
	Rat 2	0	1	2	2	2	1	2	2	2	1
	Rat 3	1	2	2	1	1	2	2	2	1	2
Reaxon	Rat 1	0	1	1	1	1	0	0	1	1	1
	Rat 2	0	2	2	1	1	2	2	2	1	1
	Rat 3	0	1	2	2	2	1	2	2	1	0
OxPVA	Rat 1	1	2	2	2	2	2	2	2	1	2
	Rat 2	1	2	2	1	1	2	2	2	2	2
	Rat 3	1	2	2	2	2	2	1	2	1	2
OxPVA+ EAK	Rat 1	0	2	2	2	2	1	2	2	1	2
	Rat 2	0	2	2	2	2	2	1	2	1	0
	Rat 3	0	2	2	2	2	1	2	2	2	0
OxPVA+EAK-YIGSR	Rat 1	0	2	1	2	2	1	1	2	2	1
	Rat 2	0	2	2	2	2	2	1	2	1	0
	Rat 3	1	2	1	1	1	2	1	1	1	1
OxPVA+NGF	Rat 1	1	2	2	2	2	2	2	2	2	2
	Rat 2	1	2	2	2	2	2	2	2	2	2
	Rat 3	0	2	2	2	2	2	2	2	2	0

A: TOE SPREAD
B: WALKING ON PLANTAR SIDE
C: ABSENCE OF DRAGGING
D: NORMAL SWING PHASE
E: FLUENT WALKING
F: ABSENCE OF EVERSION
G: ABSENCE OF EXROTATION
H: ALTERNATING STEPS
I: HINDFOOT WITHIN BODY PERIMETER
J: JOINT CONTRACTION

Figure 32 Gait chart. For each animal 10 parameters were considered for qualitative walk analysis.

7.9.2.4 Sciatic Functional Index (SFI)

After 6 weeks from surgery, SFI was acquired. SFI data showed a mild recovery in nerve function for all animals, compatible with the end point considered.

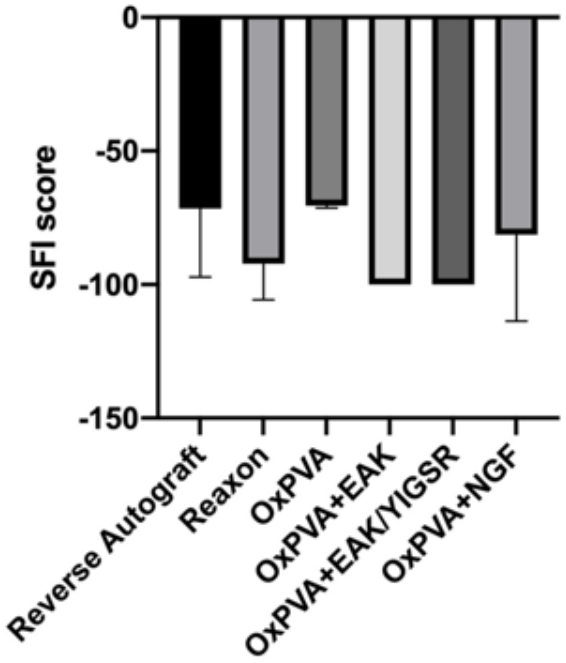

Figure 33 Sciatic Functional Index (SFI) at 6 weeks after surgery. SFI scores ranged from -100 (total impairment) to 0 (complete recovery).

At 6 weeks, the recorded values were - 71.542± 25,674, -92.178±13,547, -70.492±0,816, -100±0,00, -100±0,00 and -81.349±32,304 for RA group, Reaxon® group, OxPVA group, OxPVA+EAK group, OxPVA+EAK-YIGSR group and OxPVA+NGF group, respectively. No significant differences were present between all groups at the endpoint. Despite that, OxPVA group showed better results compared to Reaxon® group and similar results compared to the RA (gold standard) (Fig 33).

7.9.3 Macroscopic explant evaluation

Soon after euthanasia and before samples excision, the surgery site was observed to preliminary assess implants adequacy (Fig.34). All nerve conduits were recognizable, and tissue was clearly

visible inside the lumen of the scaffolds; no subcutaneous or facial edema were identified. Moreover, no signs of inflammation or scar tissue were visible. One neuroma was identified in the Reaxon® group at explant site on the proximal stomp (Fig. 35) Mild level of adhesion of surrounding tissues was detected in all groups[93], compatible with the nerve conduit surgical implantation. No dislocation of the implant was detected in all groups (Fig. 34).

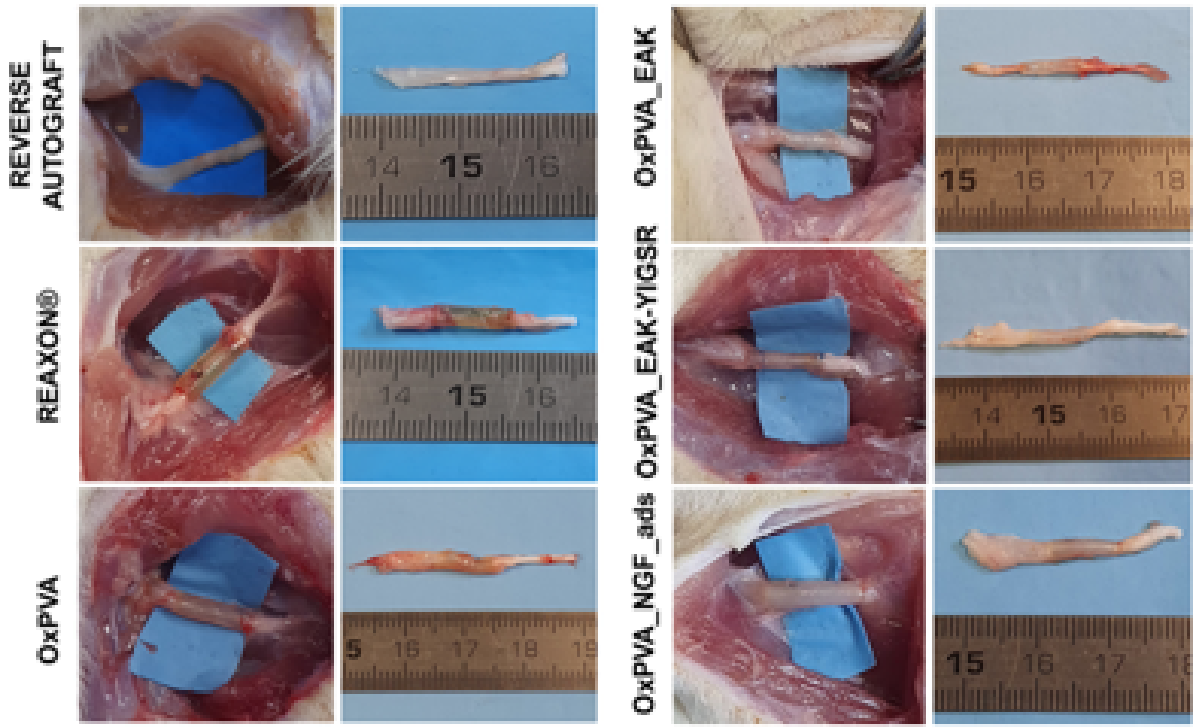

Figure 34 Gross appearance of surgical field and operated nerves explants at 6 weeks from surgery. In situ implant (left columns) and appearance after excision (right columns), of nerve conduits based on RA, Reaxon®, OxPVA, OxPVA+EAK, OxPVA+EAK-YIGSR and OxPVA+NGF. After 6 weeks, no inflammation, scar tissue was observed. One neuroma was observed on the proximal extremity of the commercial product Reaxon®.

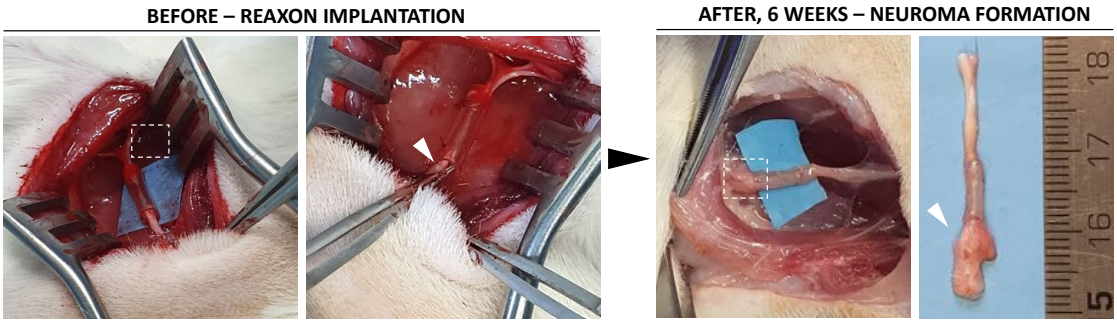

Figure 35 Sciatic nerve exposure before explantation (Left Side). Neuroma identification on Reaxon® nerve conduit (Right Side)

7.9.4 Histological and immunohistochemical results

For each experimental group, no significant inflammatory infiltrate was visible, also confirmed by anti-CD3 and anti-F4/80 immunohistochemical specific staining. Thus, only few CD3 positive and F4/80 positive cells were detected in all sample groups, suggesting the absence of infiltrating elements (Fig.36).

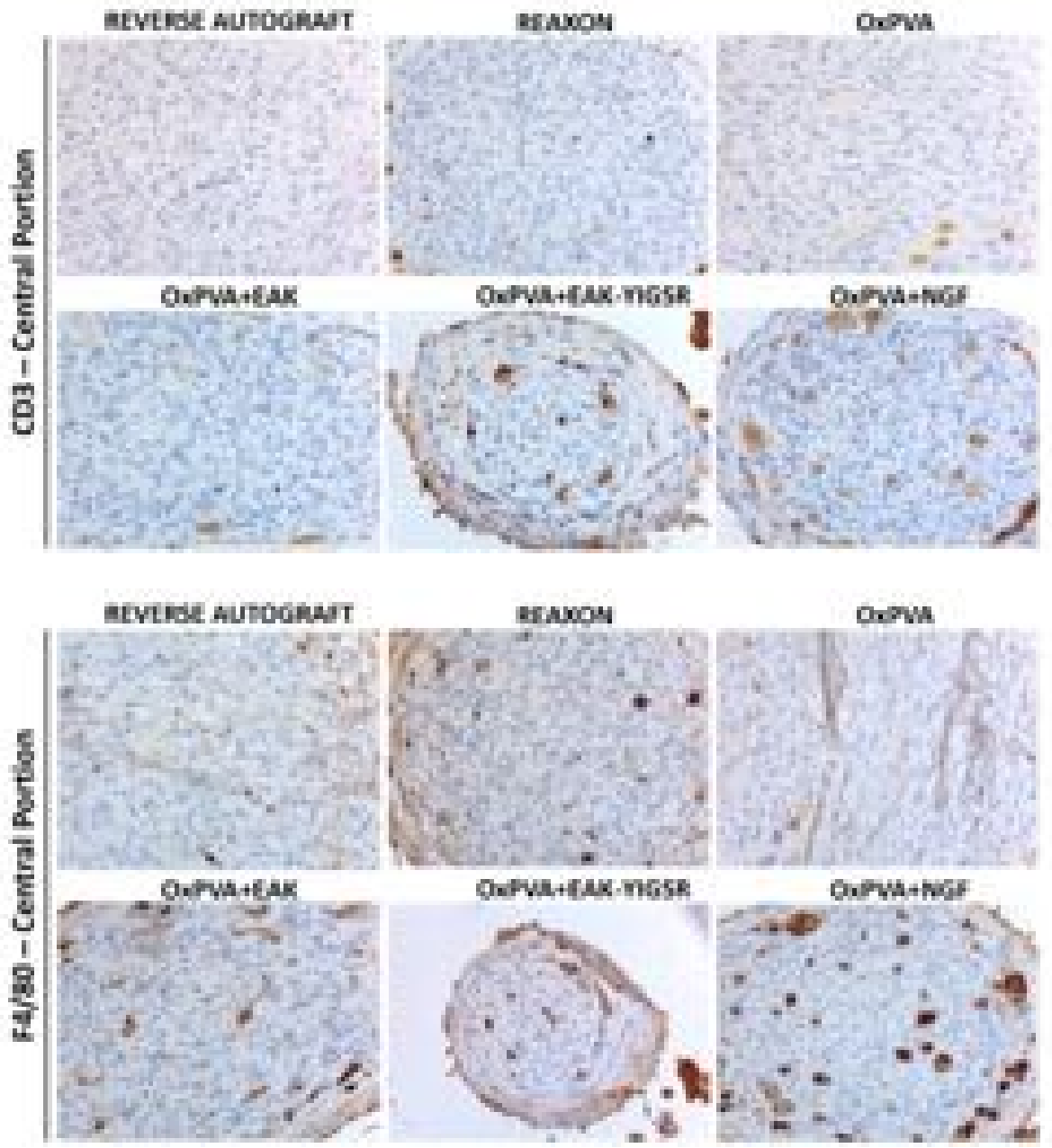

Figure 36 Immunohistochemical analysis. Anti-CD3, anti-F4/80 reactions performed on the central portion of Sprague-Dawley sciatic nerves implanted with RA, Reaxon®, OxPVA, OxPVA+EAK, OxPVA+EAK-YIGSR and OxPVA+NGF. Analysis occurred 6 weeks from surgery (40x magnification).

In addition, the central portion of each conduit showed a strongly positive immunoreaction towards S100 and β-tubulin markers, thus proving the specific nervous nature of the regenerated tissues in all experimental groups (Fig. 37).

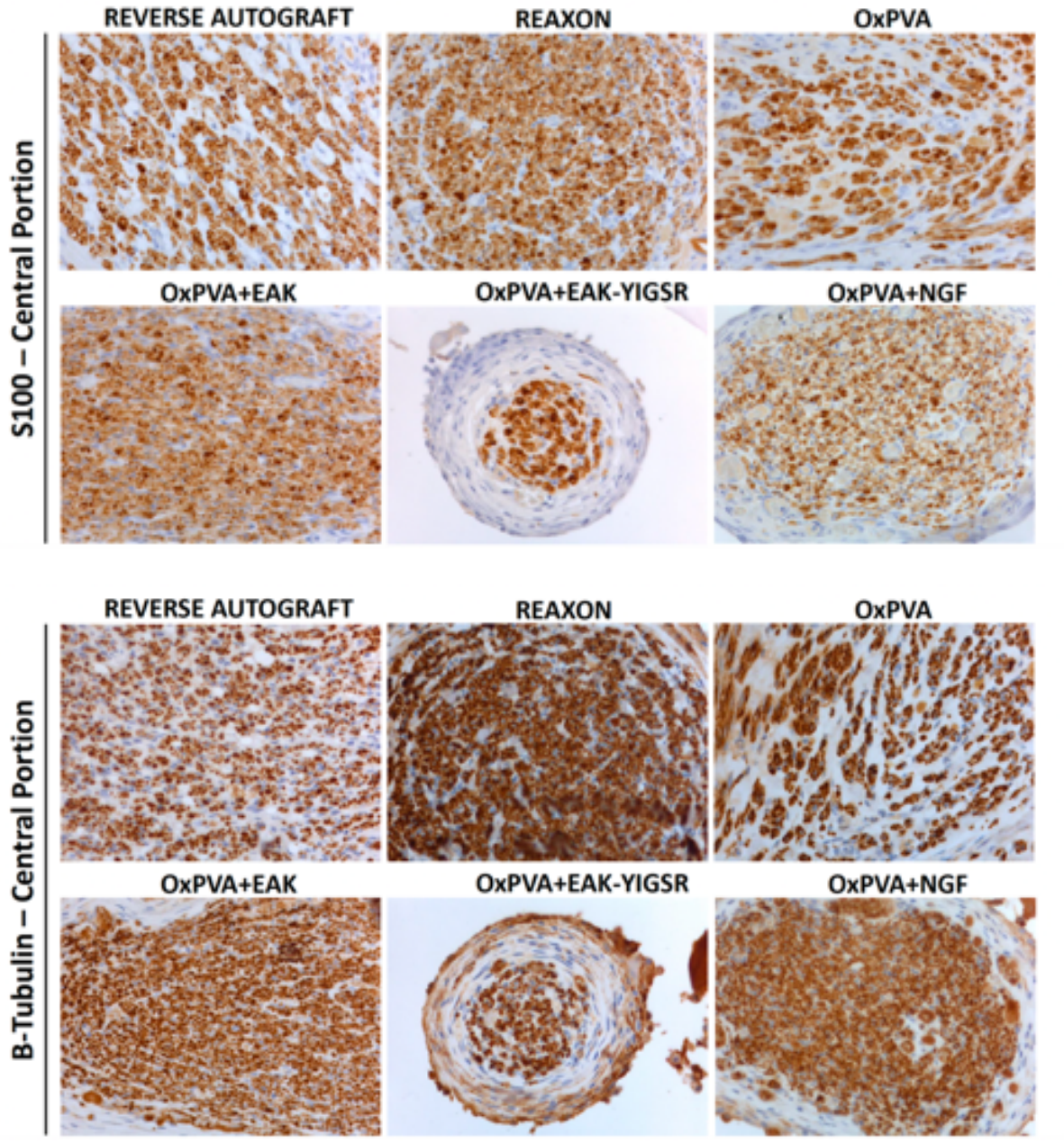

Figure 37 Immunohistochemical analysis. Anti-S100, anti-β-tubulin reactions performed on the central portion of Sprague-Dawley sciatic nerves implanted with RA, Reaxon®, OxPVA, OxPVA+EAK, OxPVA+EAK-YIGSR and OxPVA+NGF. Analysis occurred 6 weeks from surgery (40x magnification).

7.9.5 Morphometry

Morphometric analysis was carried on semithin Toluidine Blue stained section of central portions of each sample (Fig. 38). Total cross-sections, fascicular area, axons density, total axons number and myelin sheath area were acquired.

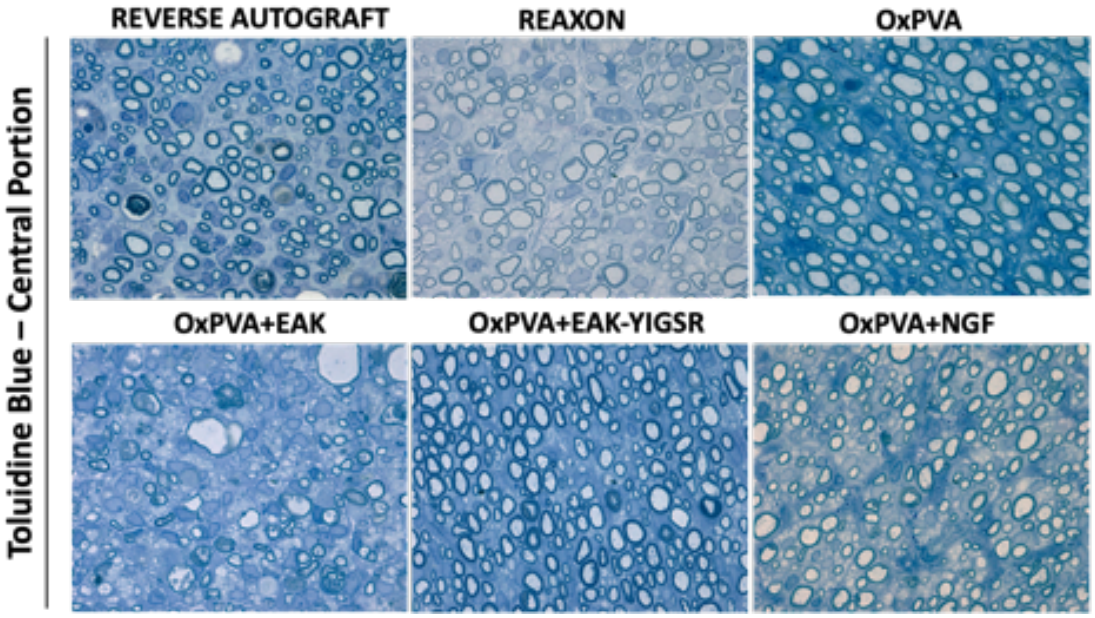

Figure 38 Toluidine Blue Stain of repaired sciatic nerves at 6-weeks after surgery. High power field of the central portion of nerve conduits (100x Magnification).

Morphometric data of the repaired sciatic nerves are presented in Fig. 39 being expressed as mean value ± SD. The measurements of the total cross-section areas at the central stump showed significant difference between RA (1120487,750±31599,549 μm^2) and OxPVA group (164280,750±1344,456 μm^2; $p < 0.0005$) and between RA (1120487,750± 31599,549 μm^2; $p<0.05$) and OxPVA+EAK group (189997,564±960,893 μm^2) and between OxPVA+EAK (189997,564±960,893μm^2; $p<0.05$) and OxPVA+NGF (268185,00±885,476 μm^2); no statistical difference was found between Reaxon® and all others experimental groups.

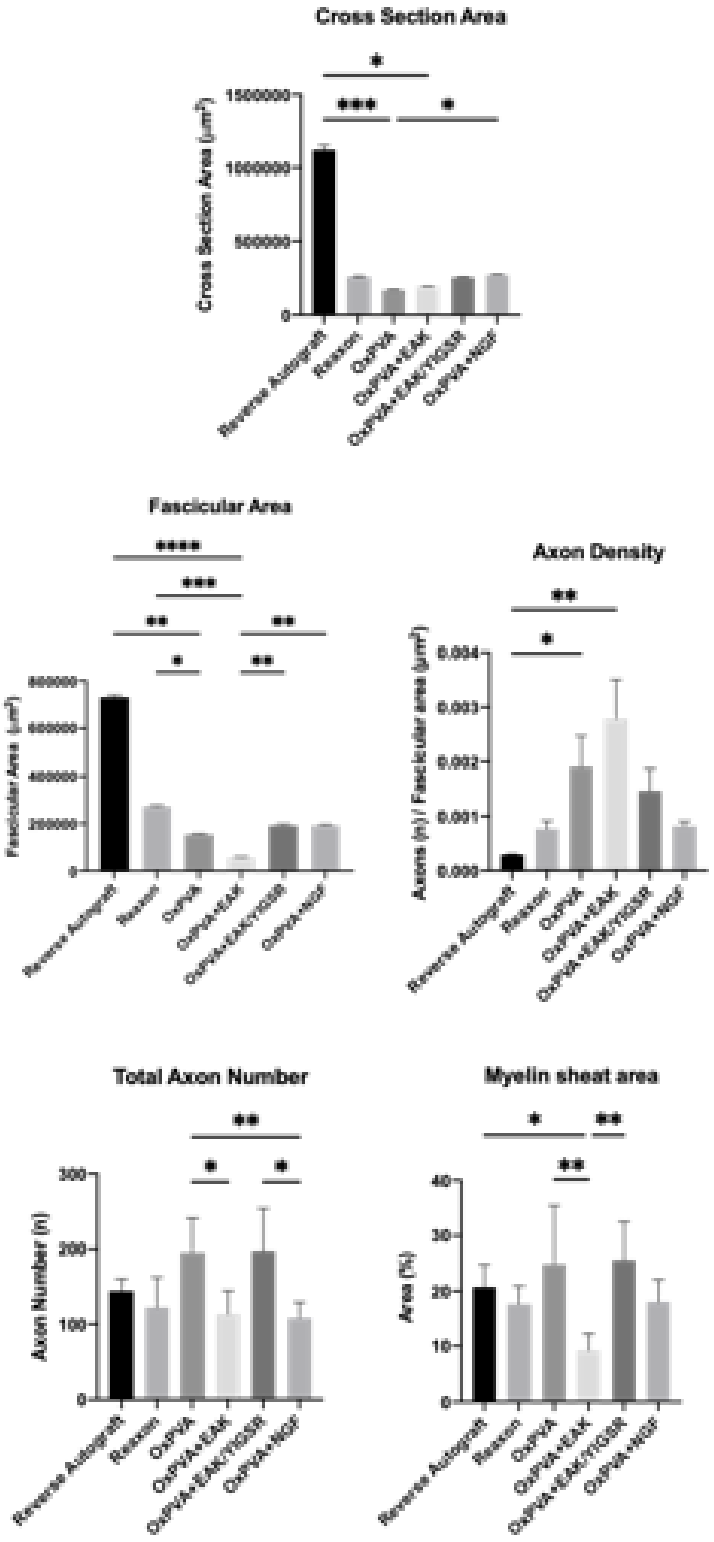

Figure 39 Histograms show mean total cross-section nerve area (µm^2), fascicular area (µm^2), axon density, total axon number and myelin sheath area (%) of the central portions of sciatic nerves implanted with RA (control group), Reaxon® (commercial product) and OxPVA-based nerve conduits (experimental groups). Statistical analyses were performed by the Kruskal-Wallis test and Dunn's multiple comparison test. Results are expressed as mean values ± SD (*$p < 0.05$; **$p \leq 0.005$; ***$p < 0.0005$; ****$p<0,0001$).

Considering fascicular area (i.e. only fasci, without the connective tissue sheath around), RA group guaranteed for higher mean values compared to all experimental groups (730908,200± 9995,622 μm^2); besides no significant difference was found between Reaxon® and OxPVA+EAK-YIGSR and between Reaxon® and OxPVA+NGF.

Axon density was significantly higher for OxPVA+EAK (1118,345± 5,46 axons/mm^2; $p \leq 0.005$) compared to RA (177,31±2,06 axons/mm^2); conversely no significant difference was found among all other groups. Except for the control group, Reaxon® showed the lowest values of axon density between the other groups.

Total number of axons was also determined, and a significant difference was encountered between OxPVA (195.83±45.18; $p<0.05$) and OxPVA+EAK (113.4±30.88) and between OxPVA (195.83±45.18; $p \leq 0.005$) versus OxPVA+NGF (108.17±21.20); conversely, no significant difference was observed between Reaxon® and all other groups.

Myelin sheath area measurements showed significant difference between OxPVA (27.14±1.0%; $p \leq 0.005$) and OxPVA+EAK (10.25±2.22%) and between OxPVA (27.14±9.10%; $p \leq 0.005$) and OxPVA+EAK-YIGSR (28.25 ±4.11%). No significant difference was found between RA and OxPVA+EAK groups.

7.9.6 Second Harmonic Generation analyses

Second Harmonic Generation Microscopy investigation was performed at central portion of nerve guide to detect structural and inflammatory response after nerve guide implantation after 6 weeks post-surgery (Fig. 40).

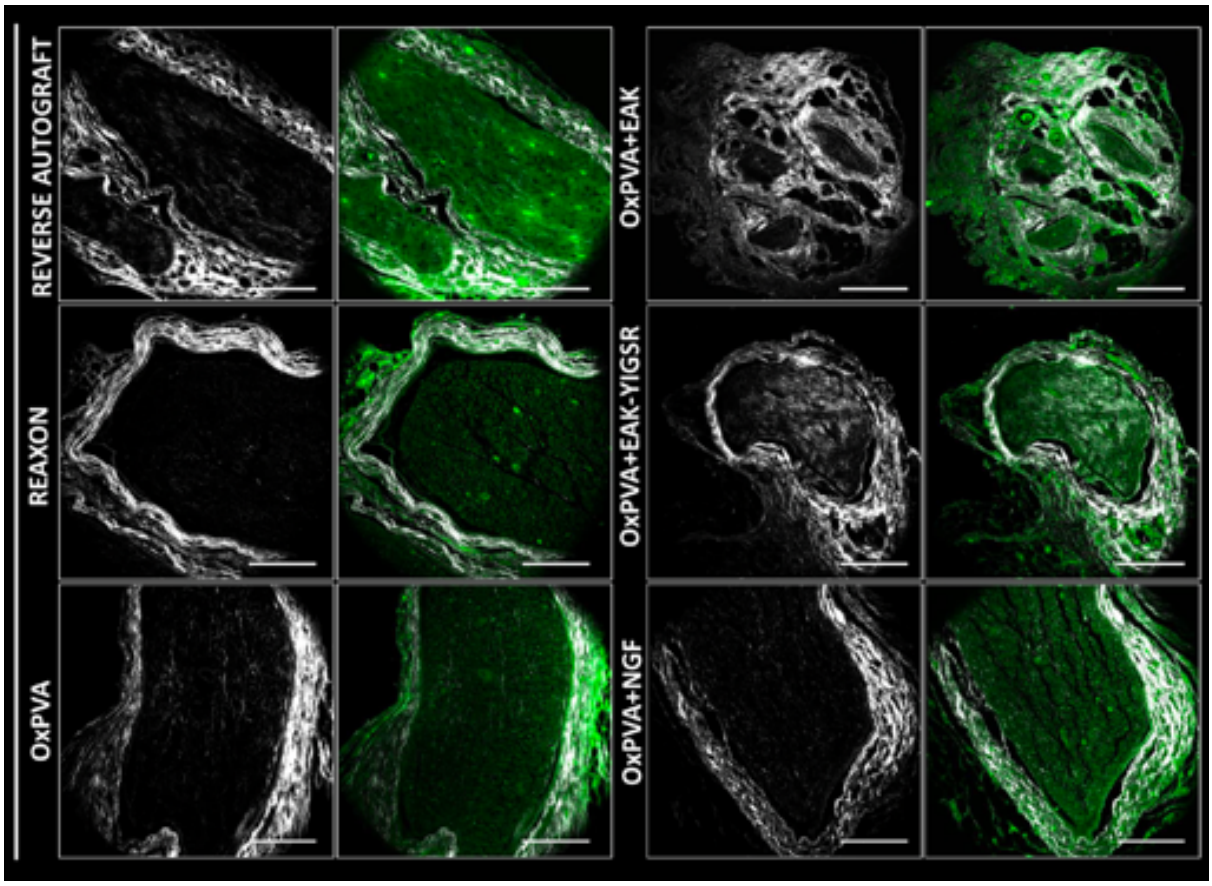

Figure 40 Second Harmonic Generation Microscopy of repaired sciatic nerves at 6 weeks after surgery. Cross-sections of the central portion of Reverse Autograft, Reaxon®, OxPVA, OxPVA+EAK, OxPVA+EAK-YIGSR and OxPVA+NGF nerve conduits explants, qualitatively evaluated by Second Harmonic Generation (SHG) microscopy (scale bars: 200 μm).

SHG Intensity analysis at 6 weeks showed OxPVA and OxPVA+YIGSR groups have statistically higher collagen levels compared to Reaxon® group, which has collagen levels quite comparable with RA group. However, SGH coherency levels showed both OxPVA and OxPVA+YIGSR groups fibers tend to be orientated predominately in one direction (anisotropic), suggesting a directional orientation of fibers coherent with a nervous regenerative process inside nerve conduits.

9. DISCUSSION

To date, surgical approaches for the treatment of peripheral nerve injuries are mainly based on neurorrhaphy or autograft in accordance with injury severity. Nevertheless, these strategies still present important shortcomings; primary suture is often not practicable due to tension between the nerve stumps, while autografts can lead to permanent co-morbidity at the donor site and limited sensorimotor functional recovery [8,26,31,63,92,95,96]. In this context, the development of new bioengineered nerve conduits or wraps appears as a newsworthy strategy to implement current clinical PNI treatment [97].

Among the variety of synthetic polymers considered in PNI repair, polyvinyl alcohol (PVA)-based ones have also been exploited. This material shows good biocompatibility, significant stability to thermal and chemical stimuli, superior tensile and flexural moduli, atoxicity and hydrophobicity, it is approved by FDA for the use as medical device (e.g., including Salubridge™ and SaluTunnel™ nerve conduits[98]). After cross-linking PVA-based conduits are not biodegradable, for this reason, on the market PVA products could lead to infections, in situ compression and consequent scarring, which have restricted efficacy and safety in clinic approaches [98–100].

Based on such considerations, we recently proposed the chemical oxidation of PVA as a new approach to obtain scaffolds showing a better overall performance compared to the native material, including biodegradability, potentially ideal for TE purposes[81]. Specifically, in this study, chemical oxidation of PVA was furtherly investigated as it was performed with $KMnO_4$ and Br_2, as distinct oxidized agents. The procedure led to the replacement of 1% or 2% of hydroxyl groups with carbonyl groups into the polymer backbone with great impact on several PVA intrinsic characteristics: swelling kinetics, protein absorption capacities, biodegradation profile. After chemical oxidation, the fabrication of tubular OxPVA_$KMnO_4$ and OxPVA_Br_2 scaffolds was successfully performed with the injection-molding technique followed by physical cross-linking by means of F-T. As for the gross appearance, OxPVA_$KMnO_4$ and OxPVA_Br_2 tubular scaffolds showed an augmented transparency if compared to the opaque PVA scaffold. This interesting feature could improve surgical operation quality, allowing to a better positioning of nerve ends inside tubular scaffolds while suturing. OxPVA_$KMnO_4$ and OxPVA_Br_2 tubular scaffolds also presented a clearly recognizable lumen with no tendency to collapse, overcoming one of the limits of vein conduits and potentially substituting muscle in vein conduits, used as nerve substitutes in clinical practice[44]. As showed by ultrastructural

characterization both OxPVA scaffolds showed increased surface rugosity, ascribable to the chemical oxidation which altered the polymer backbone and conduit wall regularity confirming injection-molding as affordable and precise manufacturing process. As previously described oxidation led to changes of physical/chemical properties of the polymer. Swelling and porosity tests showed oxidation incremented scaffold's ability to absorb molecules and increment its surface roughness, thus allowing the material to be used for drug delivery purposes. The oxidation also augmented porosity into PVA hydrogel, with the biological implication of improving the diffusion of bioactive molecules into the polymer structure. As previously reported, besides providing guidance, the controlled local delivery of therapeutic agents to the site of nerve injury results to be fundamental to accelerate the repair process [101].

OxPVA mechanical properties were modulated with physical cross-linking to obtain desirable characteristics. Both OxPVA tubular scaffolds showed good flexibility, enough to maintain the patency in response to limb flexion, while presenting adequate resistance to bear the pressure of the surrounding tissues without collapsing.

Physical cross-linking treatment avoids the use of potential toxic cross-linkers such as glutaraldehyde, granting the manufacturing of OxPVA hydrogels with low grade cytotoxicity. This was confirmed by the cytotoxicity extract test. In particular, the cytotoxicity response of SH-SY5Y and Schwann cells to OxPVA was demonstrated to be similar to the cytotoxic response of cells to known non-cytotoxic PVA. This result could be also attributed to the intensive dialysis treatment that OxPVA solutions underwent to remove $KMnO_4$ and Br_2. Furthermore, no significant morphological changes or variations in cell viability were observed in both SH-SY5Y and Schwann cell populations that were incubated with oxidized polymers-conditioned media, with a behavior similar to that of cell populations exposed to native PVA extracts, confirming biocompatibility of the oxidized polymers. Interestingly, it was also confirmed that both $KMnO_4$ and Br_2-mediated oxidation assured for increased biodegradability of scaffolds compared to the native PVA. In particular, OxPVA_Br_2 appeared to be more sensible to enzymatic degradation than OxPVA_$KMnO_4$. This experimental evidence suggests that the biodegradation profile of PVA-based conduits can be customized depending on nerve specifications (injured nerve length, diameter, anatomical position and depth), thus tuning scaffolds characteristics in order to assist the remodeling process of the regenerating nerve. With the aim to furtherly characterize the ability of OxPVA to act as functionalization platform, here we evaluated its ability in binding the neurotrophic factor CNTF.

The functionalization experiment (CNTF covalent binding) confirmed that the oxidation process implements the polymer ability to load protein molecules for drug-delivery purposes,

with similar results for OxPVA_Br_2 and OxPVA_$KMnO_4$ regarding the estimated quantity of CNTF loaded in the lumen of nerve guides. This was dictated to the chemical oxidation process, which introduced more carbonyl groups in the polymer backbone to mediate interactions with proteins and higher porosity, allowing for increased protein solution diffusion within the polymer.

Looking for easy and effective strategies to bioactivate OxPVA-derived scaffolds, OxPVA_$KMnO_4$ was mechanically incorporated with the SAP EAK, alone or conjugated to the pentapeptide YIGSR (EAK-YIGSR). In this study, the SAP EAK was used as previously demonstrating an attractive behaviour towards enteric nervous system (ENS) cells. Moreover, the SAPs can form a variety of structures allowing for various functional possibilities: when assembled, they can act as scaffolds for cell/tissue regeneration, or carriers for drug delivery[102,103]. Moreover, they can form hydrogels which are highly stable in solution (beta-sheet structures) and with great potentials: unique nanofibrous structure, intrinsic biomechanical properties and ability to ameliorate serum protein adsorption. These features are promising to prompt tissues repair; which can also furtherly optimized by the conjugation with specific peptides boosting nerve regeneration[102]. Another characteristic of the SAPs is their resistance to high temperature (90° C) [102], an important feature considering that OxPVA requires to be heated at 70° C for pouring and assure proper manipulation before cross-linking by means of F-T. Here, homogenous distribution of the SAPs (EAK and EAK-YIGSR) into OxPVA hydrogel matrix was preliminarily verified and confirmed by SHG microscopy using EAK-Rh as protein model. Intriguingly, results proved mechanical incorporation as valid, fast method to functionalize OxPVA scaffolds for tissue regeneration purposes.

In order to evaluate OxPVA regenerative potential in vivo, an approach based on lesion severity was chosen; all in vivo studies were performed using OxPVA_$KMnO_4$ (from here on, OxPVA). Firstly, OxPVA and the hemocomponent LFPm were tested for regenerative potential in comparison with a commercial product NeuraWrap™ in a rat model of PNI *without loss of substance*. After rat sciatic nerve exposure, transection and neurorrhaphy, wraps were implanted and compared for outcomes. During surgery, as expected from preliminary mechanical tests, OxPVA wraps showed good handling properties without giving rise to tears. All animals well tolerated the implant procedure, thus advocating no severe immunoreaction towards the devices. Before euthanasia (12 weeks), functional tests were performed and the SFI data suggested animals' recovery with outcomes that were slightly better for OxPVA versus the commercial product and comparable to that guaranteed by LFPm wraps. Moreover, after 12 weeks, OxPVA wraps were still recognizable in the implant site, despite appearing

thinner and more transparent. This evidence confirms material biodegradability, in accordance with previous characterization studies in vitro[75,78,80]; interestingly no tears or translocation was detected, proving exceptional mechanical strength of the material. Conversely, LFPm were completely resorbed, as no membrane residues were detectable, while NeuraWrap was still in site enveloping the surgical site. Histological examination at coaptation site showed that, in contrast to OxPVA, both LFPm and NeuraWrap™ implanted nerves display signs of coarctation (less marked in NeuraWrap™). This event is likely related to the biodegradation rate of the supports.

Despite different nature (i.e., synthetic and biological), all wraps assured for biocompatibility; in fact, only few $CD3^+$ nor $F4/80^+$ elements were recognized suggesting the absence of marked lympho-macrophagic infiltrate. Limiting inflammation at the suture site greatly influences injury repair; it allows the nerve fibers for faster crossing of neurorrhaphy site and regeneration of the early axons[103]. Sustaining this assumption, for all experimental groups, the repaired tissues were positive to markers for axons and Schwann cells (β-tubulin and S100, respectively) proving the preservation of nervous tissue[75,104]. Interestingly, homogeneous distribution of S100 positive elements proved no excessive fibroblastic response which would have compromised the proliferation of Schwann cells by creating a non-permissive environment [105,106]. This evidence was also supported by SHG microscopy images, morphometric analysis, and functional recovery assessments. According to SHG microscopy, both OxPVA and LFPm samples showed characteristics close that of NeuraWrap™ implanted nerves in terms of fibroconnective infiltrate. All the samples had characteristics referable to a PNI under recovery with the presence of collagen in the outer epineural layers and tracks of connective tissue in the fascicular area. Disproportional collagen infiltration is an important marker as it could be considered as an indicator of axonal injury[107,108].

Considering morphometric analysis, wraps based on OxPVA showed a significantly higher fascicular area versus NeuraWrap™ at proximal and distal level. This finding may be due to the mechanical protective action of the synthetic polymer, which limited coarctation of the tissue which could have affected adequate recovery after neurorrhaphy. In addition, nerves implanted with OxPVA also showed a higher total axons number at the distal stump, despite similar axon density.

OxPVA regenerative potential in vivo was then tested on a rat model of PNI with loss of substance (0.5 cm). OxPVA nerve conduits enriched with SAPs (EAK and EAK-YIGSR) and adsorbed NGF were tested for outcomes, comparing them to the commercial chitosan-based product Reaxon®, and to RA, acting as gold standard treatment. As mentioned before, the

characteristics that an ideal neuroguide should possess are flexibility, absence of lumen collapse and ease of suture. In this sense, all OxPVA-based conduits showed better overall performances compared to Reaxon® (stiffer and harder to suture), thus resulting easy to suture by the surgeon [64]. All OxPVA-based conduits also demonstrated a high size-fit ability in relation to the caliber of the nerve stump, without risk of lumen collapse. Probably this allows a better orientation of the nerve fibers during the regeneration process. In contrast, Reaxon® poor elasticity showed less adaptation to the caliber of damaged nerve stump, which may lead to not proper axonal sprouting.

Along the 6 weeks, prior to euthanasia, animal welfare was carefully monitored. In detail, to this end the trend of body weight and the occurrence of autotomy of the operated paw were considered. In fact, evident variations in animals weight suggest poor toleration of the surgical procedure. Regarding body weight, no significant differences were found at all timepoints, advising that all animals had tolerated the procedure. Evaluation of the autotomy showed no statistically significant differences among the groups (probably due to the limited number of animals considered); however, it is still appreciable that the lower values were found for the OxPVA group with results comparable to autologous nerve grafting (gold standard). The mechanism at the origin of the autotomy remains to be clarified: it is not defined whether it is a desensitization mechanism, with a picture attributable to the "phantom limb", or if the process has a painful origin [109]; the fact that OxPVA shows a lower degree of autotomy, related to the good performance of animals in the same group on functional tests, could lead to the hypothesis of desensitization, justifying the low score at the autotomy index of these animals with the early re-innervation of the affected district.

The gait analysis of the animals permitted to verify the presence of physiological nature of the march of the operated rats. The parameters analyzed were certainly affected by the autotomy of the fingers of the operated paw (as well as for the SFI scoring). Overall, considering the gait, the best results were obtained by the OxPVA+NGF and OxPVA, followed by RA, OxPVA+EAK; the OxPVA showed excellent performances, comparable that of the autologous nerve graft (gold standard).

Evaluation of the surgical site at the moment of explant confirmed the biocompatibility of the materials tested. All materials showed an integration with autologous tissue comparable between the different types of nerve conduits, in the absence of inflammatory events. All the conducts remained in place for the considered period, which proved to be sufficient for the regeneration of axonal fibers. Moreover, conduits resistance to mechanical stress ascribable to motor activity was also confirmed. Evidence of the development of proximal nerve stump

neuromas in the Reaxon® group (one out of three cases) can be traced back to the rigidity of chitosan-based neuroguide. The presence of space at the neuroguide-stump interface could have prevented the correct channeling of the regenerating fibers within the guide, thus leading to incorrect sprouting up to the genesis of neuromas. As reported in the literature, most conduits approved for clinical use do not have transparency characteristics (e.g., Neuragen®); it follows that it is impossible to appreciate the regenerating fibers through them [41]. Otherwise, the neuroguides used in this work are transparent, a feature that we have already described to be useful both in the implantation phase (i.e., to monitor the correct positioning of the stump in the guide) and explant (i.e., for a preliminary macroscopic evaluation of the outcome). Among the six types of conduits, the most transparent at explant were all the OxPVA-based ones, while the Reaxon® showed greater opacity.

Genesis of scar tissue in correspondence of the surgical site is a physiological response to implant surgery, however if too significant it can cause a limitation of functional recovery due to compression that can hinder the growth of regenerating nerve fibers [110]. During the explant phase, adhesions presence was detected in correspondence of the guides, however their appearance was compatible with the surgical procedure performed.

Immunohistochemical characterization study proved the absence of significant inflammatory events (CD3, F4/80) (furtherly confirmed by SHG analysis) and efficacy of the conduits in sustaining nerve regeneration (S100 and ß-tubulin, semithin sections stained with Toluidine Blue), at 6 weeks from surgery (a relatively short time compared to that of 12 weeks commonly considered in the literature) [75,80]. Morphometric data confirmed, as expected, that RA assured for significantly higher total cross-section area and fascicular area compared to all the other groups (RA is a transposition of an entire nerve segment). Interestingly comparable values of cross-section and fascicular area were found between functionalized OxPVA groups and Reaxon®. Finally, OxPVA+EAK-YIGSR and OxPVA nerve conduits displayed the most intersting outcomes in terms of regenerative potential, showing the higher total axons number. All OxPVA-based conduits displayed a total axons number comparable to that of RA.

10. CONCLUSIONS

In the present work, the fabrication and functionalization of 1% OxPVA-based nerve wraps and conduits was successfully performed. Collected data showed promising evidence about the possibility of using this technology to produce biocompatible and bioabsorbable devices with implemented ability to load bioactive molecules like CNTF, NGF or SAPs and to promote peripheral nerve regeneration. In vivo experiments of nerve injury without/with loss of substance showed that both wraps and conduits based on OxPVA sustain peripheral nerve repair/regeneration, in absence of inflammatory events, as showed by structural, ultrastructural, and morphometric approaches.

As for functional analysis, OxPVA-based wraps/conduits showed an outcome comparable to that of the NeuraWrap™ and Reaxon® commercial products, respectively. Moreover, considering morphometric evidences, similar or even better results were displayed by the new OxPVA-based devices (OxPVA wraps, OxPVA conduits and OxPVA+EAK-YIGSR conduits).

Intriguingly, OxPVA bioactivation by SAPs mechanical incorporation is a promising and effective strategy for next-generation conduits fabrication: different bioactive sequences may be compared for regenerative potential both alone or mixed in percentage to finely control the regenerative process. Biomaterial micropatterning together with bioactivation through peptides/growth factors may represent a valid strategy to ameliorate OxPVA-based devices performances, thus overcoming the current clinical issues in PNIs management.

11. BIBLIOGRAPHY

1. Grant, G. A., Goodkin, R. & Kliot, M. Evaluation and Surgical Management of Peripheral Nerve Problems. **44**, (1999).

2. Siemionow, M. & Brzezicki, G. *Chapter 8 Current Techniques and Concepts in Peripheral Nerve Repair*. *International Review of Neurobiology* vol. 87 (Elsevier Inc., 2009).

3. Muheremu, A. & Ao, Q. Past, Present, and Future of Nerve Conduits in the Treatment of Peripheral Nerve Injury. *BioMed Research International* vol. 2015 (2015).

4. Trumble, T. E. Peripheral nerve injury: pathophysiology and repair. *Trauma* **4**, 1047–1055 (2000).

5. An, S. *et al.* Motor function recovery during peripheral nerve multiple regeneration. 415–423 (2015) doi:10.1002/term.

6. Gutierrez, A. & England, J. D. Peripheral nerve injury. *Neuromuscular Disorders in Clinical Practice* **9781461465**, 863–869 (2014).

7. Chen, L. -E *et al.* The functional recovery of peripheral nerves following defined acute crush injuries. *Journal of Orthopaedic Research* **10**, 657–664 (1992).

8. Scheib, J. & Hoke, A. Advances in peripheral nerve regeneration. *Nature reviews. Neurology* **9**, 668–676 (2013).

9. Martini, F., Timmons, M., Tallitsch, R. & Ober, W. Human anatomy. (2006).

10. Felten, D. L., O'Banion, M. K. & Maida, M. S. Netter's Atlas of Neuroscience (Third Edition. *Netter's Atlas of Neuroscience* 247–287 (2016).

11. Pinho, A. C., Fonseca, A. C., Serra, A. C., Santos, J. D. & Coelho, J. F. J. Peripheral Nerve Regeneration: Current Status and New Strategies Using Polymeric Materials. *Advanced Healthcare Materials* **5**, 2732–2744 (2016).

12. M, S. & G, B. Chapter 8: Current techniques and concepts in peripheral nerve repair. *International review of neurobiology* **87**, 141–172 (2009).

13. Adani, Roberto., Sénès, F. M. & Società italiana di microchirurgia. Diagnosi e trattamento delle lesioni traumatiche dei nervi periferici : raccomandazioni della Società italiana di microchirurgia. (2020).

14. Experiments on the section of the glossopharyngeal and hypoglossal nerves of the frog, and observations of the alterations produced thereby in the structure of their primitive fibres. *Abstracts of the Papers Communicated to the Royal Society of London* **5**, 924–925 (1851).

15. Faroni, A., Mobasseri, S., … P. K.-A. drug delivery & 2015, undefined. Peripheral nerve regeneration: experimental strategies and future perspectives. *Elsevier*.

16. Gordon, T. & English, A. W. Strategies to promote peripheral nerve regeneration: Electrical stimulation and/or exercise. *European Journal of Neuroscience* **43**, 336–350 (2016).

17. Muheremu, A. & Ao, Q. Past, Present, and Future of Nerve Conduits in the Treatment of Peripheral Nerve Injury. *BioMed Research International* **2015**, (2015).

18. Grinsell, D. & Keating, C. P. Peripheral nerve reconstruction after injury: a review of clinical and experimental therapies. *BioMed research international* **2014**, 698256 (2014).

19. Watson, J., Gonzalez, M., Romero, A. & Kerns, J. Neuromas of the Hand and Upper Extremity. *YJHSU* **35**, 499–510 (2010).

20. Seddon, H. Surgical disorders of the peripheral nerves. in *Surgical disorders of the peripheral nerves* xi–332 (1972).

21. Sunderland, S. & Williams, H. B. Nerve injuries and their repair: a critical appraisal. (1992).

22. Seddon, H. J. Three types of nerve injury. *Brain* **66**, 237–288 (1943).

23. syndrome, S. M.-C. tunnel & 1988, undefined. Surgery of the peripheral nerve. *ci.nii.ac.jp*.

24. Clark, W. L., Trumble, T. E., Swiontkowski, M. F. & Tencer, A. F. Nerve tension and blood flow in a rat model of immediate and delayed repairs. *Journal of Hand Surgery* **17**, 677–687 (1992).

25. Sghirlanzoni, A., Lauria, G. & Pareyson, D. Malattie dei nervi periferici. *Terapia delle malattie neurologiche* 439–461 (2009) doi:10.1007/978-88-470-1120-5_35.

26. Beris, A., Gkiatas, I., Gelalis, I., Papadopoulos, D. & Kostas-Agnantis, I. Current concepts in peripheral nerve surgery. *European Journal of Orthopaedic Surgery and Traumatology* **29**, 263–269 (2019).

27. I, D., R, F. & ML, I. Innovative treatment of peripheral nerve injuries: combined reconstructive concepts. *Annals of plastic surgery* **68**, 180–187 (2012).

28. WZ, R. & SE, M. Management of nerve gaps: autografts, allografts, nerve transfers, and end-to-side neurorrhaphy. *Experimental neurology* **223**, 77–85 (2010).

29. Grinsell, D., Keating, C. P., Grinsell, D. & Keating, C. P. Peripheral Nerve Reconstruction after Injury: A Review of Clinical and Experimental Therapies. *BioMed Research International* **2014**, 1–13 (2014).

30. Nerve Graft — Paralysis Center. https://www.paralysiscenter.org/nerve-graft.

31. Griffin, J. W., Hogan, M. v, Chhabra, A. B. & Deal, D. N. Peripheral nerve repair and reconstruction. *The Journal of bone and joint surgery. American volume* **95**, 2144–2151 (2013).

32. Nectow, A. R., Marra, K. G. & Kaplan, D. L. Biomaterials for the development of peripheral nerve guidance conduits. *Tissue engineering. Part B, Reviews* **18**, 40–50 (2012).

33. Arslantunali, D., Dursun, T., Yucel, D., Hasirci, N. & Hasirci, V. Peripheral nerve conduits: Technology update. *Medical Devices: Evidence and Research* **7**, 405–424 (2014).

34. Nahabedian, M. Y. Michigan Manual of Plastic Surgery. *Annals of Surgery* **243**, 567 (2006).

35. LF, D. *et al.* Nerve Transfers-A Paradigm Shift in the Reconstructive Ladder. *Plastic and reconstructive surgery. Global open* **7**, e2290 (2019).

36. Melbourne TetraHand: Restoring Hands for Living. https://www.tetrahand.com.au/.

37. Konofaos, P. & ver Halen, J. P. Nerve repair by means of tubulization: Past, present, future. *Journal of Reconstructive Microsurgery* **29**, 149–163 (2013).

38. S, K., XF, Z. & D, B. FDA approved guidance conduits and wraps for peripheral nerve injury: a review of materials and efficacy. *Injury* **43**, 553–572 (2012).

39. R, L. & JP, V. Tissue engineering. *Science (New York, N.Y.)* **260**, 920–926 (1993).

40. Ikada, Y. Challenges in tissue engineering. *Journal of The Royal Society Interface* **3**, 589–601 (2006).

41. Battiston, B., Geuna, S., Ferrero, M. & Tos, P. Nerve repair by means of tubulization: Literature review and personal clinical experience comparing biological and synthetic conduits for sensory nerve repair. *Microsurgery* **25**, 258–267 (2005).

42. McFetridge, P. S., Daniel, J. W., Bodamyali, T., Horrocks, M. & Chaudhuri, J. B. Preparation of porcine carotid arteries for vascular tissue engineering applications. *Journal of Biomedical Materials Research - Part A* **70**, 224–234 (2004).

43. Tang, J. B. Vein conduits with interposition of nerve tissue for peripheral nerve defects. *Journal of Reconstructive Microsurgery* **11**, 21–26 (1995).

44. Sabongi, R. G., Fernandes, M. & dos Santos, J. B. G. Peripheral nerve regeneration with conduits: use of vein tubes. *Neural regeneration research* **10**, 529–533 (2015).

45. Calcagnotto, G.-N. & Braga Silva, J. La réparation de pertes de substance des nerves digitaux avec la technique de la greffe veineuse plus interposition de tissu nerveux. Étude prospective et randomisée. *Chirurgie de la Main* **25**, 126–130 (2006).

46. Stahl, S. & Goldberg, J. A. The use of vein grafts in upper extremity nerve surgery. *European journal of plastic surgery* **22**, 255–259 (1999).

47. Stahl, S. & Goldberg, J. A. The use of vein grafts in upper extremity nerve surgery. *European Journal of Plastic Surgery* **22**, 255–259 (1999).

48. ME, M. *et al.* Facial Nerve Repair by Muscle-Vein Conduit in Rats: Functional Recovery and Muscle Reinnervation. *Tissue engineering. Part A* **27**, 351–361 (2021).

49. Ramli, K. *et al.* Efficacy of Human Cell-Seeded Muscle-Stuffed Vein Conduit in Rat Sciatic Nerve Repair. *Tissue engineering. Part A* **25**, 1438–1455 (2019).

50. Marcoccio, I. & Vigasio, A. Muscle-in-vein nerve guide for secondary reconstruction in digital nerve lesions. *The Journal of hand surgery* **35**, 1418–1426 (2010).

51. Minini, A. & Megaro, A. Muscle in vein conduits: Our experience. *Acta Biomedica* **92**, (2021).

52. S, H., A, B. & R, S. Peripheral Nerve Conduit: Materials and Structures. *ACS chemical neuroscience* **10**, 3349–3365 (2019).

53. Lundborg, G. & Rosén, B. Hand function after nerve repair. *Acta Physiologica* **189**, 207–217 (2007).

54. Lundborg, G., Dahlin, L. B. & Danielsen, N. Ulnar nerve repair by the silicone chamber technique. *Scandinavian Journal of Plastic and Reconstructive Surgery and Hand Surgery* **25**, 79–82 (1991).

55. Lundborg, G., Rosén, B., Dahlin, L., Danielsen, N. & Holmberg, J. Tubular versus conventional repair of median and ulnar nerves in the human forearm: early results from a prospective, randomized, clinical study. *The Journal of hand surgery* **22**, 99–106 (1997).

56. Pitta, M., Wolford, L., Mehra, P., maxillofacial, J. H.-J. of oral and & 2001, undefined. Use of Gore-Tex tubing as a conduit for inferior alveolar and lingual nerve repair: experience with 6 cases. *Elsevier*.

57. S, S. & Z, S. Reconstruction of upper-extremity peripheral-nerve injuries with ePTFE conduits. *Journal of reconstructive microsurgery* **14**, 227–232 (1998).

58. A, M. & Q, A. Past, Present, and Future of Nerve Conduits in the Treatment of Peripheral Nerve Injury. *BioMed research international* **2015**, (2015).

59. Marquardt, L. M. & Sakiyama-Elbert, S. E. Engineering peripheral nerve repair. *Current Opinion in Biotechnology* **24**, 887–892 (2013).

60. Hasırcı, N., Şahin, D. A. & Usal, T. D. Peripheral nerve conduits: Technology update. (2014).

61. Pabari, A., Lloyd-Hughes, H., Seifalian, A. M. & Mosahebi, A. Nerve conduits for peripheral nerve surgery. *Plastic and Reconstructive Surgery* **133**, 1420–1430 (2014).

62. Houshyar, S., Bhattacharyya, A. & Shanks, R. Peripheral Nerve Conduit: Materials and Structures. *ACS chemical neuroscience* **10**, 3349–3365 (2019).

63. R, L. *et al.* Peripheral nerve injuries treatment: a systematic review. *Cell biochemistry and biophysics* **68**, 449–454 (2014).

64. Kehoe, S., Zhang, X. F. & Boyd, D. FDA approved guidance conduits and wraps for peripheral nerve injury: A review of materials and efficacy. *Injury* **43**, 553–572 (2012).

65. Houshyar, S., Bhattacharyya, A. & Shanks, R. Peripheral Nerve Conduit: Materials and Structures. *ACS Chemical Neuroscience* **10**, 3349–3365 (2019).

66. Hospodiuk, M., Dey, M., Sosnoski, D. & Ozbolat, I. T. The bioink: A comprehensive review on bioprintable materials. *Biotechnology advances* **35**, 217–239 (2017).

67. Jiang, Z. *et al.* Extrusion 3D Printing of Polymeric Materials with Advanced Properties. *Advanced Science* vol. 7 2001379 (2020).

68. H, M., R, S., M, Y., T, O. & H, S. A polylactic acid non-woven nerve conduit for facial nerve regeneration in rats. *Journal of tissue engineering and regenerative medicine* **8**, 454–462 (2014).

69. Kehoe, S., Zhang, X. F. & Boyd, D. FDA approved guidance conduits and wraps for peripheral nerve injury: A review of materials and efficacy. *Injury* **43**, 553–572 (2012).

70. Aghajanian, S., Taghi Doulabi, A., Akhbari, M. & Shams, A. Facial nerve regeneration using silicone conduits filled with ammonia-functionalized graphene oxide and frankincense-embedded hydrogel. *Inflammation and Regeneration* **41**, (2021).

71. Qian, Y. *et al.* An integrated multi-layer 3D-fabrication of PDA/RGD coated graphene loaded PCL nanoscaffold for peripheral nerve restoration. *Nature Communications* **9**, (2018).

72. Guo, H., Lv, R. & Bai, S. Recent advances on 3D printing graphene-based composites. *Nano Materials Science* **1**, 101–115 (2019).

73. Zhu, W., Harris, B. T. & Zhang, L. G. Gelatin methacrylamide hydrogel with graphene nanoplatelets for neural cell-laden 3D bioprinting. *Proceedings of the Annual International Conference of the IEEE Engineering in Medicine and Biology Society, EMBS* **2016-Octob**, 4185–4188 (2016).

74. Aghajanian, S., Taghi Doulabi, A., Akhbari, M. & Shams, A. Facial nerve regeneration using silicone conduits filled with ammonia-functionalized graphene oxide and frankincense-embedded hydrogel. *Inflammation and regeneration* **41**, 13 (2021).

75. Stocco, E. *et al.* Partially oxidized polyvinyl alcohol conduitfor peripheral nerve regeneration. *Scientific Reports* **8**, 1–14 (2018).

76. Barbon, S. *et al.* Halogen-mediated partial oxidation of polyvinyl alcohol for tissue engineering purposes. *International Journal of Molecular Sciences* **21**, (2020).

77. Porzionato, A. *et al.* Development of Oxidized Polyvinyl Alcohol-Based Nerve Conduits Coupled with the Ciliary Neurotrophic Factor. *Materials (Basel, Switzerland)* **12**, (2019).

78. Stocco, E. *et al.* Partially oxidized polyvinyl alcohol as a promising material for tissue engineering. *Journal of Tissue Engineering and Regenerative Medicine* **11**, 2060–2070 (2017).

79. Barbon, S. *et al.* Biofabrication of a novel leukocyte-fibrin-platelet membrane as a cells and growth factors delivery platform for tissue engineering applications. *Journal of tissue engineering and regenerative medicine* **12**, 1891–1906 (2018).

80. Porzionato, A. *et al.* Development of oxidized polyvinyl alcohol-based nerve conduits coupled with the ciliary neurotrophic factor. *Materials* **12**, (2019).

81. Gupta, N. V. & Shivakumar, H. G. Investigation of Swelling Behavior and Mechanical Properties of a pH-Sensitive Superporous Hydrogel Composite. *Iranian journal of pharmaceutical research : IJPR* **11**, 481–493 (2012).

82. E, D. *et al.* Mitochondrial alarmins released by degenerating motor axon terminals activate perisynaptic Schwann cells. *Proceedings of the National Academy of Sciences of the United States of America* **112**, E497–E505 (2015).

83. S, N. *et al.* Hydrogen peroxide is a neuronal alarmin that triggers specific RNAs, local translation of Annexin A2, and cytoskeletal remodeling in Schwann cells. *RNA (New York, N.Y.)* **24**, 915–925 (2018).

84. Marin, Ștefania *et al.* Collagen-Polyvinyl Alcohol-Indomethacin Biohybrid Matrices as Wound Dressings. *Pharmaceutics* vol. 10 (2018).

85. P, B. *et al.* 3D Synthetic Peptide-based Architectures for the Engineering of the Enteric Nervous System. *Scientific reports* **9**, (2019).

86. S, B. *et al.* Biofabrication of a novel leukocyte-fibrin-platelet membrane as a cells and growth factors delivery platform for tissue engineering applications. *Journal of tissue engineering and regenerative medicine* **12**, 1891–1906 (2018).

87. JR, B., SE, M. & DA, H. Functional evaluation of complete sciatic, peroneal, and posterior tibial nerve lesions in the rat. *Plastic and reconstructive surgery* **83**, 129–136 (1989).

88. PD, W. *et al.* Autotomy following peripheral nerve lesions: experimental anaesthesia dolorosa. *Pain* **7**, 103–113 (1979).

89. Von Frey Hairs, Semmes-Weinstein set of monofilaments. https://www.ugobasile.com/products/catalogue/pain-and-inflammation/item/52-37450-275-von-frey-hairs.

90. Campana, G. & Rimondini, R. Mechanical nociception measurement in mice and rats with automated Von Frey equipment. *Methods in Molecular Biology* **1230**, 229–231 (2015).

91. Saleh, M., Muneshige, H., sciences, Y. I.-L. & 1998, undefined. Effects of neurotropin on hyperalgesia and allodynia in mononeuropathic rats. *Elsevier*.

92. Ijkema-Paassen, J., Jansen, K., Gramsbergen, A. & Meek, M. F. Transection of peripheral nerves, bridging strategies and effect evaluation. *Biomaterials* **25**, 1583–1592 (2004).

93. J, P. *et al.* Reduction of extraneural scarring by ADCON-T/N after surgical intervention. *Neurosurgery* **38**, 976–984 (1996).

94. Dornseifer, U. *et al.* Surgical therapy of peripheral nerve lesions: Current status and new perspectives. *Zentralblatt fur Neurochirurgie* **68**, 101–110 (2007).

95. Radić, B., Radić, P. & Duraković, D. Peripheral nerve injury in sports. *Acta Clinica Croatica* **57**, 561–569 (2018).

96. Wang, M. L., Rivlin, M., Graham, J. G. & Beredjiklian, P. K. Peripheral nerve injury, scarring, and recovery. *Connective tissue research* **60**, 3–9 (2019).

97. Faroni, A., Mobasseri, S. A., Kingham, P. J. & Reid, A. J. Peripheral nerve regeneration: Experimental strategies and future perspectives. *Advanced Drug Delivery Reviews* **82**, 160–167 (2015).

98. J, D., H, C., L, Q., X, Y. & X, J. Biomimetic neural scaffolds: a crucial step towards optimal peripheral nerve regeneration. *Biomaterials science* **6**, 1299–1311 (2018).

99. Gaudin, R. *et al.* Approaches to peripheral nerve repair: Generations of biomaterial conduits yielding to replacing autologous nerve grafts in craniomaxillofacial surgery. *BioMed Research International* **2016**, (2016).

100. Bliley, J. M. & Marra, K. G. Polymeric Biomaterials as Tissue Scaffolds. *Stem Cell Biology and Tissue Engineering in Dental Sciences* 149–161 (2015) doi:10.1016/B978-0-12-397157-9.00013-8.

101. P, L. *et al.* Novel drug delivering conduit for peripheral nerve regeneration. *Journal of neural engineering* **14**, (2017).

102. Brun, P. *et al.* 3D Synthetic Peptide-based Architectures for the Engineering of the Enteric Nervous System OPEN. doi:10.1038/s41598-019-42071-7.

103. Sarhane, K. A. *et al.* Macroporous nanofiber wraps promote axonal regeneration and functional recovery in nerve repair by limiting fibrosis. (2019) doi:10.1016/j.actbio.2019.02.034.

104. S, M., T, O., N, T., Y, S. & T, H. Cavernous nerve regeneration by biodegradable alginate gel sponge sheet placement without sutures. *Urology* **68**, 1366–1371 (2006).

105. SS, K. *et al.* Use of human amniotic membrane wrap in reducing perineural adhesions in a rabbit model of ulnar nerve neurorrhaphy. *The Journal of hand surgery, European volume* **35**, 214–219 (2010).

106. PD, K. *et al.* Collagen nerve protector in rat sciatic nerve repair: A morphometric and histological analysis. *Microsurgery* **30**, 392–396 (2010).

107. PJ, J., P, N., DA, H. & SE, M. Nerve endoneurial microstructure facilitates uniform distribution of regenerative fibers: a post hoc comparison of midgraft nerve fiber densities. *Journal of reconstructive microsurgery* **27**, 83–90 (2011).

108. G, K., B, H. & N, S. Chapter 19: The role of collagen in peripheral nerve repair. *International review of neurobiology* **87**, 363–379 (2009).

109. Weber, R. A., Proctor, W. H., Warner, M. R. & Verheyden, C. N. Autotomy and the sciatic functional index. *Microsurgery* **14**, 323–327 (1993).

110. K, S. *et al.* Protective effect of biodegradable nerve conduit against peripheral nerve adhesion after neurolysis. *Journal of neurosurgery* **129**, 815–824 (2018).

111. Stocco, E. *et al.* Bio-activated oxidized polyvinyl alcohol towards next-genera-2 tion nerve conduits development 3. *Polymers* **13**, (2021).

Scientific Contributions

Porzionato, A. et al. Development of Oxidized Polyvinyl Alcohol-Based Nerve Conduits Coupled with the Ciliary Neurotrophic Factor. Materials, 2019, 12.

Stocco, E. et al. A. Bio-activated oxidized polyvinyl alcohol towards next-generation nerve conduits development. Polymers, 2021.

Stocco, E. et al. Meniscal substitutes by 3D printing technologies: Current advances and future perspectives. Journal of Tissue Engineering, 2021. (under revision).

Emmi, A. et al. 3D Reconstruction of the Morpho-Functional Topography of the Human Vagal Trigone. Frontiers in Neuroanatomy, 2021 vol. 15 20.

Attendance at conferences and seminars

Oxidized polyvinyl alcohol-based nerve conduits for peripheral nerve regeneration in severe injury: a comparative pre-clinical study. Stocco E, Barbon, *De Rose E*, Faccio D, Petrelli L, Rambaldo A, Sandrin D, Dettin M, Macchi V, Tiengo C, De Caro R, Porzionato A. 74° Congresso nazionale SIAI 2021 || 24-25 SETTEMBRE 2021 - ORAL PRESENTATION